1982

Reduced order modelling in multimachine power systems

Carlos Grande-Moran
Iowa State University

INFORMATION TO USERS

This reproduction was made from a copy of a document sent to us for microfilming. While the most advanced technology has been used to photograph and reproduce this document, the quality of the reproduction is heavily dependent upon the quality of the material submitted.

The following explanation of techniques is provided to help clarify markings or notations which may appear on this reproduction.

1. The sign or "target" for pages apparently lacking from the document photographed is "Missing Page(s)". If it was possible to obtain the missing page(s) or section, they are spliced into the film along with adjacent pages. This may have necessitated cutting through an image and duplicating adjacent pages to assure complete continuity.

2. When an image on the film is obliterated with a round black mark, it is an indication of either blurred copy because of movement during exposure, duplicate copy, or copyrighted materials that should not have been filmed. For blurred pages, a good image of the page can be found in the adjacent frame. If copyrighted materials were deleted, a target note will appear listing the pages in the adjacent frame.

3. When a map, drawing or chart, etc., is part of the material being photographed, a definite method of "sectioning" the material has been followed. It is customary to begin filming at the upper left hand corner of a large sheet and to continue from left to right in equal sections with small overlaps. If necessary, sectioning is continued again—beginning below the first row and continuing on until complete.

4. For illustrations that cannot be satisfactorily reproduced by xerographic means, photographic prints can be purchased at additional cost and inserted into your xerographic copy. These prints are available upon request from the Dissertations Customer Services Department.

5. Some pages in any document may have indistinct print. In all cases the best available copy has been filmed.

University Microfilms International
300 N. Zeeb Road
Ann Arbor, MI 48106

Grande-Moran, Carlos

REDUCED ORDER MODELLING IN MULTIMACHINE POWER SYSTEMS

Iowa State University PH.D. 1982

Reduced order modelling in multimachine power systems

by

Carlos Grande-Moran

A Dissertation Submitted to the
Graduate Faculty in Partial Fulfillment of the
Requirements for the Degree of
DOCTOR OF PHILOSOPHY

Major: Electrical Engineering

Approved:

Signature was redacted for privacy.

In Charge of Major Work

Signature was redacted for privacy.

For the Major Department

Signature was redacted for privacy.

For the Graduate College

Iowa State University
Ames, Iowa

1982

TABLE OF CONTENTS

LIST OF PRINCIPAL SYMBOLS

G_{ij}	real part of the ij^{th} element of the reduced admittance matrix (p.u.)
B_{ij}	imaginary part of the ij^{th} element of the reduced admittance matrix (p.u.)
E	magnitude of internal voltage of a synchronous machine back of transient impedance (p.u.)
δ	rotor angle of a synchronous machine with respect to a synchronously rotating reference frame (electrical radians)
δ_{ij}	$(\delta_i-\delta_j)$ relative rotor angle
$\delta°$	rotor angle at an operating point (electrical radians)
E''_N	voltage behind subtransient impedance (p.u.)
E''_D, E''_Q	D and Q axes components of E''_N (p.u.)
E''_d, E''_q	d and q axes components of E''_m (p.u.)
E'_d, E'_q	d and q axes components of E'_m (p.u.)
E_{F_D}	field voltage (p.u.)
Im	machine current (p.u.)
I_D, I_Q	D and Q axes components of Im (p.u.)
I_d, I_q	d and q axes components of Im (p.u.)
V_t	machine terminal voltage (p.u.)
V_D, V_Q	D and Q axes components of V_t (p.u.)
V_d, V_q	d and q axes components of V_t (p.u.)
V_{REF}	reference voltage (p.u.)
x_ℓ	armature leakage reactance (p.u.)

x_d, x_q	d and q axes synchronous reactances (p.u.)
x'_d, x'_q	d and q axes transient reactances (p.u.)
x''_d, x''_q	d and q axes subtransient reactances (p.u.)
$x_{f\ell}$	leakage reactance of field winding (p.u.)
$x_{Q\ell}$	leakage reactance of q-axis damper winding (p.u.)
$x_{D\ell}$	leakage reactance of d-axis damper winding (p.u.)
T'_{do}, T'_{qo}	d and q axes open circuit transient time constants (seconds)
T''_{do}, T''_{qo}	d and q axes open circuit subtransient time constants (seconds)
r_F	field winding resistance (p.u.)
P_e	electrical power output of asynchronous machine (p.u.)
Q_e	reactive power output of asynchronous machine at internal bus (p.u.)
P_m	mechanical power input of asynchronous machine (p.u.)
P_a	accelerating power of generator at $t = 0^+$
H	inertia constant of generator (seconds)
ω	angular velocity (electrical radians/seconds)
ω_R	synchronous velocity (electrical radians/seconds)
P_{m_0}	mechanical power input due to setting action of valve (p.u.)
K_A, K_F, K_R, K_E	gains in regulator-exciter system (p.u.)
T_A, T_F, T_R	time constants in regulator subsystem (seconds)
T_E	exciter time constant (seconds)
K, F	gains in turbine-governor system (p.u.)

τ_1, τ_2	governor time constants (seconds)
τ_3, τ_5	turbine time constants (seconds)

Other symbols are explained as and when they are introduced.

1. OVERVIEW OF THE PROBLEM AND OBJECTIVES

1.1 Introduction

Present day power systems are large in size and highly interconnected so that simulation of their dynamic behavior becomes costly in terms of computer time. Two contributing factors are:

i) high dimensionality of the models.
ii) numerical stiffness of system equations.

The problem of dimensionality arises because of the large number of generators and the need to represent the generator units (i.e., synchronous generators and their associated control units) in great detail for stability studies. The second feature, on the other hand, is a consequence of the presence in the system of equations of small and large time constants in part due to the modelling of electrical transient phenomena in the synchronous machine windings and the voltage regulator-exciter system. These time constants, then, result in system dynamic phenomena consisting of fast or short-term phenomena which disappear after a few hundredths of a second and slow or long-term phenomena which dominate the system response during most of the simulation period.

To capture the fast phenomena, a smaller integration step size must be used. Hence, the digital simulation of large scale systems is computationally expensive. This emphasizes the need for models which are of lesser order and also accurate enough from an engineering point of view. To obtain models of reduced order, we need algorithms for the selection of the best dynamic equivalent possible, i.e., a model which describes the dominant modes of the systems while keeping computational costs and

time down. A major step is the identification of those generators in the system which are coherent (two generators are said to be coherent if their relative maximum angular difference is within a specified coherency threshold). Once this has been accomplished, the next step is the determination of the dynamic equivalents which describe the combined system response of the different coherent groups.

This dissertation covers two major areas of research in dynamic equivalencing, the first dealing with the reduction of models of large dimensionality and the second with both high dimensionality and numerical stiffness of system equations. Two methods are developed to achieve order reduction in power system models. They are

i) Coherency identification of generators and their grouping using a sensitivity based slow coherency approach.
ii) A direct coherency method based on the eigenvalues and eigenvectors of the linearized system model which identifies and groups the system coherent generators.

Methods dealing with coherency identification are desirably independent of fault location so that there will be no need to store and compare generator swing curves any time a dynamic equivalent of the system is constructed for different fault locations. Thus, the methods for grouping coherent generators will be simple and efficient in terms of computer time. Moreover, the reliability of results is of prime importance so there should not be any necessity to verify results from the "base" case swing curves. Two different approaches are used in coherency identification to represent the power system model. The first divides the system into two subsystems.

i) A study subsystem where the nonlinear representation of generating unit models is done fully. Thus, various types of system disturbances can be applied at different locations in the subsystem.
ii) An external subsystem that is obtained from the linearization of the machine equations and from which a reduced order model can be obtained. Thus the reduction of the original system model is based on the reduction of the external subsystem leaving the study subsystem untouched.

The use of a linearized model for the external subsystem is justified by the following observations [38]

i) The coherent behavior of a group of generators is unaffected by changing the fault clearing time.
ii) The omission of elaborate detail in the generating units models does not appreciably affect the natural frequencies of the system. Thus, the classical synchronous machine model may be used.
iii) Since the damping coefficients which describe those torques produced by the synchronous machine damper windings, D_i, do not significantly affect the natural modes of the system, they can be neglected in the classical synchronous machine model.

The second approach considers the linearized system model[1] for the entire system with no distinction or limiting boundaries between groups of generators. It is assumed that one of the coherent groups contains the system reference generator which in some instances is the only generator the coherent group will be composed of.

With reference to the second area of research, a method based on singular perturbation techniques has been developed. Broadly, the method resolves the original system equations into slow and fast

---

[1]The assumptions used earlier for the linearization of the external subsystem are also used here.

subsystems which are solved independently using two different time scales, one for the slow subsystem using a real time scale and the other for the fast subsystem using a stretched variable which permits the capture of the fast phenomena taking place near t=0. This feature yields savings in computer time due to the use of a larger step size in the numerical integration of the fast subsystem and an order reduction in the system model as compared to the small step size (i.e., larger number of iterations) used in conventional integration algorithms to capture the fast phenomena of the system response.

A brief historical overview of those methods found in the literature dealing with the above topics follows.

1.2 Historical Overview of Methods for Constructing Reduced Order Models

The methods for constructing reduced order models for dynamic and transient stability studies may be broadly classified into four groups:

i) Equivalents based on distribution factors [6,44].

ii) Equivalents based on modal analysis [2,12,13,14,15,18,23, 29,34,48,50,51,52,53].

iii) Equivalents based on coherency analysis [1,7,24,25,35,37, 38,39,44,45].

iv) Equivalents based on singular perturbation techniques [5,9,30,33,54,54,56].

The first method attempting to obtain a reduced order model from a large power system was proposed by Brown and co-authors [6]. This method, based on early work done with network analyzers, used a set of distribution factors to obtain equivalent loads and generation for the external subsystem, leaving the study subsystem untouched. Results

provided by the method lacked accuracy and reliability since the method was devised on an heuristic basis and was limited by the state of the art computation available at the time.

In 1970, a method based on modal analysis was proposed by Elangovan and Kuppurajulu [18]. This method was motivated by work done on the simplification of large linear systems by Davison and Chidambara [12,13,14]. The method represents the system transient response by using two different reduced models, each of them for a different time period, one where the slow response prevails and the other where the fast response prevails. Moreover, this algorithm presupposes first obtaining the linearized version of the system equations about a specified equilibrium point and then using a previous knowledge of the approximate time behavior of the state variables in order to construct a reduced model. The major shortcoming of the method is the requirement for a prior knowledge of the approximate time behavior of the state variables. Otherwise, the results are quite satisfactory from an engineering viewpoint.

Almost simultaneously with the foregoing work, a method based on coherency analysis was proposed by Chang and Adibi [7]. This method used the classical model for synchronous machines and constant admittances for loads. In addition, the system is divided into study and external subsystems with the entire system operating near a steady-state equilibrium point. The generators are modeled as time varying current sources in parallel with transient reactances. The principal objective of the method is to cluster into groups those generators which swing

together, so that only those nodes pertaining to the study subsystem and the reference generator of each coherent group are retained. The remainder of the generating and load buses are eliminated by means of simple algebraic manipulation of the system load-flow equations. Finally, the simulation of the power system is carried out by using the reduced order model. The only drawback of the method is that the new system variables do not correspond to the power system variables and thus we cannot use the algorithm as part of conventional stability programs.

Two years later, in 1973, a method based on pattern recognition was proposed by Lee and Schweppe [24]. The method uses the concepts of electrical distance (based on network transfer admittances) and a reflection distance which is designed to measure the dynamical effect of a generator on the stability of the study system. The prime objective of the algorithm is to obtain a set of generators distributed among three concentric circles with the inner circle being assigned to the study subsystem. The middle circle is formed by those generators which are deemed important to the stability of the inner circle generators and the outer circle is composed of generators which are to be incorporated in an equivalent. The two electromechanical distances are used to calculate a set of coherency measures that eventually determine the groups of coherent generators in the outer circle.

Another method based on modal analysis was proposed in 1975 by Van Ness and co-workers [51,52]. It requires the computation of the system eigen space obtained from the linearization of the equations for the

entire system. The reduced order model is formed by selecting the most dominant modes, i.e., those modes close to the s-plane origin, from the system matrix eigenvalues. The accuracy of the desired order reduction is improved by minimizing the difference between the eigenvectors of the original model and the eigenvectors of the desired reduced order model. The principal application for which the method was devised was in the tuning and design of the synchronous machine control units under small size perturbation (i.e., dynamic stability). No attempt was made to cluster groups of coherent generators to reduce the order of the power system. The major concern was the reduction of the control unit models associated with each of the synchronous generators.

More recently, in 1978, a linear simulation method based on a coherency approach was proposed by Podmore [37] and Podmore and Germond [38]. The method has had considerable acceptance and uses simplified swing curves to identify the coherent groups of generators based on the maximum angular excursion between generators under transient conditions. The algorithm requires the storage and comparison of the swing curves obtained from the linearized model as the fault is shifted throughout the system. This is its major shortcoming because of the great deal of computer time and memory used in processing all this information. The technique also makes use of the concept of study and external subsystems and the coherency equivalent is only obtained for those generators belonging to the external system.

A year later, a coherency identification technique based on modal analysis was proposed by Adgoankar [1] and Pai and Adgoankar [35]. The technique uses a linear model of the system from which the system eigen

structure is computed. The linearized ordinary differential equations are then cast into two separate state-space matrix equations, one for the faulted period and the other for the post-fault period. A closed solution for the preceding system of equations is obtained by using a modal response for linear systems developed by Desoer [15] in the late fifties. In the absence of significant deviations of the rotor angles from their steady-state values during the fault and post-fault periods, the solution of the post-fault system equations is used to compute a set of coherency measures which, in conjunction with a transitive recognition rule used in the linear simulation method, determine the groups of coherent generators in the external system. The transistive rule can be briefly stated as follows, if generator "a" is coherent with generator "b" and "b" happens to be coherent with a generator "c", then "a" is coherent with "c". One of the features which makes this method very attractive for coherency identification is that it does not resort to storage and comparison of swing curves for different fault locations. Instead, it makes use of the set of coherency measures, a coherency criterion (i.e., two generators are said to be coherent if their maximum relative angular excursion is less than a specified coherency threshold, ε, which ranges between 3° and 5°) and a similarity transformation which allows the permutation of the reference generator in the study subsystem when a change is made in its boundary.

More recently, three different methods, the first using a probabilistically based coherency approach, the second based on singular perturbation techniques and the third based on a slow coherency approach,

were proposed by Schlueter and co-authors [45], Avramovic [5] and others [9,30,53,54,55] respectively.

The first method, a RMS coherency based approach, uses a linearized model of the entire system which is cast into a state-space form with the input vector expressed in terms of the incremental mechanical power inputs and the injected power at load buses. These inputs are used to model various types of system disturbances, such as load shedding, generation loss and electrical faults. Then a random input vector as well as a covariance matrix is defined so that different fault locations and magnitudes of the perturbations can be accounted for. A set of RMS coherency measures based on the linearized system model and the probabilistic representation of disturbances is used to identify the groups of coherent generators. This is done in conjunction with a commutative recognition rule, i.e., every member of a coherent group must be pairwise coherent one to another. Since the method is probabilistic in nature, the equivalents obtained are constructed only once and can be used for any disturbance that might occur in the system during the transient conditions.

The method based on singular perturbation techniques, on the other hand, decomposes the linearized system equations into slow and fast subsystems by appropriately identifying the slow and fast variables present in the generator unit model and then casting them into a singular perturbed form, that is, into two sets of linear ordinary differential equations, one containing the slow variables and the other the fast ones. The solution of such subsystems is done by means of asymptotic expansions of the slow and fast variables and the use of two different time scales,

one using the "real" time variable t and the other a stretched variable τ which stretches out those times near t=0. The time scale decomposition yields a great deal of savings in computer time because a larger integration step size can be used in obtaining both subsystem responses. Moreover, the physical significance of the original system variables is not lost in the reduction process.

The third method, based on slow coherency, also uses a linearized version of the entire system. It requires the computation of the slow eigen structure of the system matrix which is used in determining the reference generators of the coherent groups, in number equal to the dimension of the slow eigen space. The selection of these reference generators is done by means of a Gaussian type elimination on a matrix whose columns consist of the basis vectors of the slow eigen space. After this procedure has been concluded, the assignation of those generators not considered as references to coherent groups is accomplished. While the method seems to be independent of fault location in most cases, as claimed by the author, the many cases worked in this dissertation indicate that this is true only if the size of system generation is much bigger than the fault size.

Finally, a modal method called selective modal analysis, the most recent contribution to model order reduction (1981), has been proposed by Perez-Arriaga, et al. [34]. This algorithm uses a zero-input type model obtained from the linearized system model and requires the computation of the system eigen structure. This eigen structure is then divided into sets of "relevant" and "less relevant" modes. The principal

application in power systems is in the solution of the stiff differential equations resulting from the modelling of the generating units.

The following section contains a brief discussion of methods from which the underlying concepts used in this dissertation are obtained.

1.3 State of the Art in Reduced Order Modelling

Several methods which serve as background for this dissertation are now reviewed briefly.

1.3.1 Linear simulation method [37,38,39]

The linear simulation method determines the groups of coherent generators by comparing the swing curves obtained from the simplified linear model of the entire system but uses the concept of external and study subsystems for the dynamic aggregation of the machines in the external subsystems. The effect of a bus fault on the system is approximated by the response of the unfaulted system and a step input equal to the accelerating power at $t=0^+$ for the duration of the fault.

The dynamical equations for the $i^{\underline{th}}$ generator in a system of n generators are given by

$$\frac{2H_i}{\omega_R}\frac{d}{dt}(\Delta\omega_i) = \Delta Pm_i - \Delta Pe_i - D_i\Delta\omega_i \qquad (1.1a)$$

$$\frac{d}{dt}(\Delta\delta_i) = \Delta\omega_i \qquad i=1,2,3,\ldots,n. \qquad (1.1b)$$

where

H_i is the machine inertia constant in seconds.

$\Delta\omega_i$ is the speed deviation in electrical radians/seconds.

$\Delta\delta_i$ is the rotor angle deviation in electrical radians.

D_i is the damping constants in seconds.

ΔPm_i is the change in mechanical input in p.u.

ΔPe_i is the change in electrical output power in p.u.

The network equations in polar form are linearized with the real power equations decoupled from the reactive power equations to obtain

$$\begin{bmatrix} \Delta \underline{P}_G \\ - - \\ \Delta \underline{P}_L \end{bmatrix} = \left[\begin{array}{c|c} [\frac{\partial P_G}{\partial \delta}] & [\frac{\partial P_G}{\partial \theta}] \\ \hline [\frac{\partial P_L}{\partial \delta}] & [\frac{\partial P_L}{\partial \theta}] \end{array}\right] \begin{bmatrix} \Delta \underline{\delta} \\ - - \\ \Delta \underline{\theta} \end{bmatrix} \tag{1.2}$$

where

$\Delta \underline{P}_G$ is a vector containing the change in electrical output powers at generation buses.

$\Delta \underline{P}_L$ is a vector containing the change in electrical powers at load buses.

$\Delta \underline{\delta}$ is a vector containing the angle deviations at generation buses.

$\Delta \underline{\theta}$ is a vector containing the angle deviations at load buses.

The partial derivatives in (1.2) are computed using the voltages and angles at the pre-fault steady-state operating point. Other types of disturbances can be simulated by introducing step changes in ΔP_{L_i}, ΔPm_i or ΔP_{G_i}, i.e., loss of load, mechanical input or generation can be simulated.

A trapezoidal integration technique is applied to obtain a time domain solution of the linearized swing equations. The groups of coherent generators are determined by clustering the approximate swing

curves from the linear simulation using a transistive recognition rule. The modelling of several disturbances proposed in the method has been successfully tested in power systems of different sizes, giving in every case reliable results for typical fault clearing times. However, the simulation has to be repeated for every change in fault location, needing in every case the storage and comparison of the swing curves to obtain the groups of coherent generators.

1.3.2 Slow coherency method [5]

The linearized model of the power system about a post-fault equilibrium point with zero damping is cast in the matrix form

$$\Delta\ddot{\underline{\delta}} = \bar{\underline{A}}\,\Delta\underline{\delta} \tag{1.3}$$

where $\Delta\underline{\delta}$ is an n-dimensional vector.

Disturbances are modeled as initial conditions at the fault clearing time. For structural changes due to loss of lines, the post-fault [Y] matrix is modified appropriately. Slow coherency for r-decomposable systems, i.e., those systems that can be decomposed into r area groupings based on the r "slowest" eigenvalues of $\bar{\underline{A}}$, is defined as follows: Machines i and j are said to be slowly coherent if their rotor angle differences $(\Delta\delta_i - \Delta\delta_j)$ do not contain any motion due to the r "slowest" modes. Mathematically, this is expressed in matrix form by

$$\Delta\underline{\delta}_F - \underline{L}_g \Delta\underline{\delta}_R = \underline{z} \tag{1.4}$$

where $\Delta\underline{\delta}_R$ is a r-dimensional vector composed of all reference generators of the r coherent groups, $\Delta\underline{\delta}_F$ is a (n-r)-dimensional vector consisting of the remaining generators, $\underline{L}_g$ is a grouping matrix whose entries are ones

and zeros, associating the references generators in $\Delta\underline{\delta}_R$ with the remaining generators in $\Delta\underline{\delta}_F$ and $\underline{z}$ in an r-dimensional vector which describes the fast intra-group oscillations.

The following algorithm has been designed to identify the entries of $\Delta\underline{\delta}_R$, $\Delta\underline{\delta}_F$ and $\underline{L}_g$.

i) Select the r slowest modes of $\underline{\bar{A}}$.

ii) Construct an n×r matrix $\underline{V}$, whose columns are the eigenvectors of the r slowest modes of $\underline{\bar{A}}$.

iii) Perform a Gaussian elimination on $\underline{V}$ to find the set of group-reference generators. The procedure results in partitioning matrix $\underline{V}$ into a r×r matrix $\underline{V}_1$ and a (n-r)×r matrix $\underline{V}_2$ whose row indices are related to the numbers assigned to generators for identification.

iv) Determine a matrix $\underline{Ld}$ using the result of step (iii) as follows

$$\underline{Ld} = \underline{V}_2\underline{V}_1^{-1} \tag{1.5}$$

v) By approximating the largest positive entry in each row of $\underline{Ld}$ as one and setting all other entries to zero, the grouping matrix $\underline{L}_g$ is obtained.

vi) The matrix $\underline{L}_g$ is then used to assign the follower generators in $\Delta\underline{\delta}_F$ to the coherent areas having as references the generators in $\Delta\underline{\delta}_R$.

One of the salient features of the method is that it does not resort to the storage and comparison of swing curves to obtain the groups of coherent generators. In addition, if the power system is robust, the coherency configuration obtained by this method is independent of the fault location.

1.3.3 Root-mean-square coherency method [45]

A simplified, linearized model of an n-machine system is used in this method in the matrix form,

$$\dot{\underline{x}}(t) = \underline{\underline{A}}\underline{x}(t) + \underline{\underline{B}}\underline{u}(t) \tag{1.6}$$

where the (2n-2)-dimensional vector $\underline{x}$ and the (n+k)-dimensional input vector $\underline{u}$ are defined as

$$\underline{x} = [\Delta\hat{\underline{\delta}} \quad \Delta\hat{\underline{\omega}}]^T \quad \text{and} \quad \underline{u} = [\Delta\underline{P}_m \quad \Delta\underline{P}_L]^T$$

The system consists of n generators and k load buses and the state variables $\Delta\hat{\delta}_i$ and $\Delta\hat{\omega}_i$, for the $i^{\underline{th}}$ machine, are referred to the system reference generator, numbered as n. A classical model is used to represent the system generators.

A set of coherence coefficients based on a statistical representation of the system disturbances and the maximum angular excursion experienced by any pair of machines within the power system is computed. The evaluation of the coherency coefficients between any pair of generators is facilitated by constructing a square, (n-1)-dimensional, symmetric matrix, $\hat{\underline{S}}_x$, given by

$$\hat{\underline{S}}_x = \lim_{T\to\infty} \frac{1}{T^n} E\{\int_0^T \Delta\hat{\underline{\delta}}(t)\Delta\hat{\underline{\delta}}^T(t)dt\} \tag{1.7}$$

so that the coherency measures are then defined as

$$C_{ij} = \sqrt{\hat{S}_{x_{ii}} - 2\hat{S}_{x_{ij}} + \hat{S}_{x_{jj}}} \; ; \quad \begin{matrix} i=1,2,\ldots,(n-2) \\ j=i+1,\ldots,(n-2) \end{matrix} \tag{1.8}$$

$$C_{in} = \sqrt{\hat{S}_{x_{ii}}} \; ; \quad i=1,2,\ldots,n-1 \tag{1.9}$$

It has been found that for step disturbances, the matrix $\hat{\underline{S}}_x$ is an explicit function of the system parameters, i.e., the machine inertias and synchronizing power coefficients, making the method insensitive to type or location of the disturbances. Consequently, a single modal coherent equivalent can be used in multiple transient stability studies. The clustering algorithm used in the grouping of coherent generators is based on a commutative recognition rule which ensures that generators in a coherent group are all pairwise coherent.

1.3.4 Singular perturbation technique [5,30,35,55]

The singular perturbation technique uses a linearized model for a multimachine system with equations in the form

$$\dot{\underline{\omega}} = \underline{\underline{A}}\underline{\omega} + \underline{\underline{B}}\underline{u}; \quad \underline{\omega}(0) = \underline{\omega}^{\circ} \tag{1.10}$$

The method can be outlined as follows,

i) Cast equation (1.10) into a singular perturbed form, or the so-called state separable form.

ii) Obtain a solution from the equations of step (i), i.e., the solution of the slow and fast subsystems which, if performed separately and at different time scales, alleviates the stiffness problem associated with the original system equations.

The singular perturbed form of the system equations is given by

$$\begin{bmatrix} \dot{\underline{x}} \\ \hline \varepsilon\underline{y} \end{bmatrix} = \left[\begin{array}{c|c} \underline{A}_{11} & \underline{A}_{12} \\ \hline \underline{A}'_{21} & \underline{A}'_{22} \end{array}\right] \begin{bmatrix} \underline{x} \\ \hline \underline{y} \end{bmatrix} + \begin{bmatrix} \underline{B}_1\underline{u} \\ \hline \underline{B}'_2\underline{u} \end{bmatrix} ; \quad \underline{\omega}(0) = \begin{bmatrix} \underline{x}(0) \\ \hline \underline{y}(0) \end{bmatrix} \tag{1.11}$$

where $\underline{x}(t)$ is a vector describing the slow dynamics of the system and $\underline{y}(t)$ is a vector describing the fast dynamics. The parameter ε, a positive small number that accounts for small time constants, small inertias, inverses of high gains, etc., is called the "perturbation" parameter, and the vector $\underline{u}$ represents the disturbances or inputs to the system.

The solution of equations (1.11) is composed of two terms, an outer solution which describes the system response distant from t=0 and the boundary layer correction describing the system response near t=0. Mathematically, this is expressed in the form of

$$\underline{x}(t,\varepsilon) = \underline{X}(t,\varepsilon) + \varepsilon\underline{p}(\tau,\varepsilon) \tag{1.12a}$$

$$\underline{y}(t,\varepsilon) = \underline{Y}(t,\varepsilon) + \underline{q}(\tau,\varepsilon) \tag{1.12b}$$

where $\underline{X}$ and $\underline{Y}$ are the outer expansion of $\underline{x}$ and $\underline{y}$, and $\underline{p}$ and $\underline{q}$ are the boundary layer corrections to $\underline{x}$ and $\underline{y}$.

Since two different time scales are used in (1.12), two different time variables are defined,

i) a real time t for the slow phenomena.

ii) a stretched variable τ, defined as t/ε, for the fast phenomena.

As can be seen from its definition, the stretched variable τ tends to infinity as $\varepsilon \to 0$, permitting the representation of $\underline{X}$, $\underline{Y}$, $\underline{p}$ and $\underline{q}$ by means of the following asymptotic expansions [30]

$$\underline{X}(t,\varepsilon) \sim \sum_{j=0}^{\infty} \underline{X}_j(t)\varepsilon^j \tag{1.13a}$$

$$\underline{Y}(t,\varepsilon) \sim \sum_{j=0}^{\infty} \underline{Y}_j(t)\varepsilon^j \tag{1.13b}$$

$$\underline{p}(\tau,\varepsilon) \sim \sum_{j=0}^{\infty} \underline{p}_j(\tau)\varepsilon^j \tag{1.13c}$$

$$\underline{q}(\tau,\varepsilon) \sim \sum_{j=0}^{\infty} \underline{q}_j(\tau)\varepsilon^j \tag{1.13d}$$

Thus, the solution of (1.12) using the first order approximation of $(\underline{X},\underline{Y})$ and $(\underline{p},\underline{q})$, i.e., the first two terms of the asymptotic expansions, to $\underline{x}$ and $\underline{y}$ is given by

$$\underline{x}(t,\varepsilon) = \underline{X}_0(t) + \varepsilon[\underline{X}_1(t) + \underline{p}_0(\tau)] + \underline{0}(\varepsilon^2) \tag{1.14a}$$

$$\underline{y}(t,\varepsilon) = \underline{Y}_0(t) + \underline{q}_0(\tau) + \varepsilon[\underline{Y}_1(t) + \underline{q}_1(\tau)] + \underline{0}(\varepsilon^2) \tag{1.14b}$$

where $\underline{X}_0$, $\underline{Y}_0$ and $\underline{q}_0$ form the zero order approximations to $\underline{x}(t)$ and $\underline{y}(t)$ which are obtained when ε is set to zero in equations (1.11) and by solving for $\underline{q}_0(\tau)$ in the equation

$$\frac{d\underline{q}_0(\tau)}{d\tau} = \underline{A}'_{22}\, \underline{q}_0(\tau); \quad \underline{q}_0(\tau) = \underline{y}(0) - \underline{Y}_0(0) \tag{1.15}$$

The solution $(\underline{X}_0,\underline{Y}_0)$ describes the quasi-steady states of the system. The first order approximation is obtained by substituting the asymptotic expansion into the perturbed form equations (1.11) and equating coefficients of like powers of ε on both sides of the equations.

In terms of computer time, the zero order approximation looks very attractive for dynamic simulation of multimachine power systems because

of the time scale separation which allows the use of larger integration step size. Moreover, the physical identities of the original state variables are retained in the reduced order model allowing the use of these models with conventional stability programs.

1.4 Scope and Outline of the Dissertation

With the preceding background of previous work in the areas of coherency identification and model reduction for power system stability studies, the principal objectives pursued by this research and a summary of it are now presented.

The principal objectives the research leading to this dissertation were

i) The development of efficient and reliable coherency recognition criteria which do not require simulation and comparison of swing curves and which are based on the eigen structure of the system matrix $\underline{A}$.

ii) The establishment of efficient criteria by which the decomposition of the full scale system model into coherent groups or areas will facilitate the selection of the appropriate dynamic equivalent replacing the set of coherent generators.

iii) The demonstration of the importance and future role of reduced order modelling techniques in transient and dynamic stability studies.

A summary of the dissertation is as follows. Chapter 2 is concerned with the mathematical modelling of power systems as used in coherency analysis. The nonlinear generator swing equations as well as the load flow equations interconnecting the system generators, are stated here. The assumptions of linearity, classical model representation for generating units and the modelling of electrical disturbances are also stated in this chapter. The state-space representation

$$\dot{\underline{x}} = \underline{\underline{A}}\underline{x} + \underline{\underline{B}}\underline{u}, \ \underline{x}(0)$$

of the linearized model is developed. Moreover, the relationships between eigenvalues, eigenvectors and reciprocal eigenvectors of the system matrices $\underline{\underline{A}}$ and $\bar{\underline{\underline{A}}}$ are discussed as well as the effect of the injected reactive power, Q_{e_i}, on the system modes.

Chapter 3 deals with the sensitivity based slow coherency method, starting with a brief review of the slow coherency method and its use in identifying coherent groups of generators and following with a short discussion on underlying features concerning the identification of the model variables with fast and slow oscillations of the full scale model. Modifications in the procedures for the identification of coherent group-reference machines are described. These modifications are based on a sensitivity matrix, $\bar{\underline{S}}$, whose entries provide information concerning the sensitivity of the slowest system eigenvalues to small variations in generator inertias. An algorithm to select the reference generators is also described and two numerical examples are used to validate this approach.

Chapter 4 introduces a direct method based on a RMS coherency measure. One of the n generators is chosen as a system reference. It is usually the machine with the largest inertia unless a different selection is required because of the change of fault location. Salient features of the most used grouping algorithms in coherency identification, transistive and commutative recognition rules, are introduced and discussed. Finally, numerical examples of practical power systems are used to illustrate the method.

In Chapter 5, a method based on singular perturbation theory for the reduction and simulation of power systems in dynamic stability studies is presented. The modelling of generating units and their associated controls is presented and derived. Also, important features of the technique and motivation behind the application of the technique to the problem of dynamic stability are stated. Lastly, a numerical example is presented to illustrate the salient features of the method as used in the reduction of the order of power system models.

Chapter 6 includes a summary and conclusions reached together with some suggestions and comments concerning future research.

Two appendices contain the system data for the New England, Modified Iowa and SWC Systems and the synchronous machine hybrid model with the exciter-voltage regulator and governor-turbine system models are provided.

Finally, a bibliography contains most of the pertinent references related to the subjects on Coherency Analysis and Reduced Order Modelling.

2. MATHEMATICAL MODELLING FOR COHERENCY ANALYSIS

2.1 Introduction

A review of the existing methods for coherency analysis has been presented in Section 1.3. It was also pointed out that there exists a need for more reliable and direct methods which reduce the computational work involved in the dynamic simulation of power systems. In this chapter, the mathematical formulation forming the basis for such direct methods is discussed. We begin with the nonlinear swing equations for the synchronous generator based on its classical model and the nonlinear algebraic load-flow equations of the network. These equations are then linearized around a steady-state operating point, which in most cases is selected as the pre-fault operating point and will be referred to as the base case. Next a state space model of the form $\dot{\underline{x}} = \underline{\underline{A}}\underline{x} + \underline{\underline{B}}\underline{u}$, for $t > 0$, is developed. In view of the particular structure of the $\underline{\underline{A}}$ matrix, the eigen structure (i.e., eigenvalues and their associated eigenvectors) analysis of this matrix exhibits interesting properties which are discussed. A numerical example of a three machine system is used to illustrate these properties.

2.2 The Nonlinear Model

Under the usual assumptions of a constant voltage behind transient reactance (this point being referred to as an internal node), constant mechanical power input, negligible damping constants and network representation at the internal nodes (after converting loads into constant

admittances), the multimachine power system results in the following set of second order nonlinear differential equations [1,3,31]

$$\frac{2H_i}{\omega_R}\frac{d^2\delta_i}{dt^2} = Pm_i - Pe_i \tag{2.1a}$$

where

$$Pe_i = \sum_{j=1}^{n} |E_i||E_j||Y_{ij}|\cos(\theta_{ij}-\delta_{ij}) \quad i=1,2,3,\ldots,n \tag{2.1b}$$

The above variables are defined for the $i^{\underline{th}}$ generator as follows:

δ_i is the rotor angle, in electrical radians, with respect to the synchronous rotating reference frame.

ω_R is the system synchronous speed in electrical radians/seconds.

H_i is the machine inertia constant in seconds.

Pm_i is the mechanical power input in p.u.

Pe_i is the electrical power output in p.u.

$|E_i|$ is the magnitude of the machine internal node voltage in p.u.

$|Y_{ij}|$ is the magnitude of the transfer admittance between the internal nodes i and j in p.u.

θ_{ij} is the argument of the transfer admittance Y_{ij}.

δ_{ij} is the rotor angular difference, $(\delta_i-\delta_j)$, in electrical radians.

The above equation can be cast in the state space form by defining the rotor angle δ_i and angular speeds ω_i (i=1,2,...,n) as state variables and using the auxiliary equation

$$\frac{d}{dt}\delta_i = \omega_i - \omega_R \tag{2.2}$$

to relate the rotor angle δ_i to the rotor angular speed ω_i.

Although it is not needed now, it is noted for later use that the injected reactive power at the internal nodes is given by

$$Qe_i = -\sum_{j=1}^{n} |E_i||E_j||Y_{ij}|\sin(\theta_{ij}-\delta_{ij}) \qquad i=1,2,3,\ldots,n \qquad (2.3)$$

2.3 The Linearized Model

The use of a linearized model in coherency identification is justified by the following observations.

i) The coherent behavior of a set of generators is not altered by changing the fault clearing time [32]. This statement is justified from the observation that in conventional transient stability studies the groups of coherent generators remain unchanged as the fault clearing time is increased.

ii) The omission of elaborate detail in the generating unit models, such as the exciter-voltage regulator and governor-turbine systems, does affect the damping of the swing curves but not the system natural frequencies which in turn play a dominant role in determining the coherent behavior of generators [32]. Therefore, the classical model is used to represent the synchronous machine.

iii) Since the small damping constants, D_i, do not have a significant effect on the frequencies of the oscillatory modes [40], they may be neglected.

Defining $\underline{u} = [Pm_1 Pm_2 \ldots Pm_n]^T$ and $\underline{x} = [\delta_1 \delta_2 \ldots \delta_n \,|\, \omega_1 \omega_2 \ldots \omega_n]^T$, we can construct the 2n set of differential equations as

$$\dot{\underline{x}} = \underline{f}(\underline{x},\underline{u}) \qquad (2.4)$$

where the above 2n-dimensional equations consist of

$$f_i(\underline{x},\underline{u}) = \omega_i - \omega_R \qquad (2.5a)$$

$$f_{n+i}(\underline{x},\underline{u}) = \frac{\omega_R}{2H_i}(Pm_i - Pe_i) \qquad i=1,2,3,\ldots,n \qquad (2.5b)$$

The linearization of equations (2.5) is done about some specified equilibrium point which represents a steady-state operating condition (e.g., the pre-fault state) of the system. If such a point is labeled as $(\underline{x}_e, \underline{u}_e)$ then, by expanding equations (2.5) about $(\underline{x}_e, \underline{u}_e)$ in a Taylor series and neglecting the second and higher degree terms, the following set of differential equations in the state space form and in terms of the perturbed variables $\underline{x}$ and $\underline{u}$ (i.e., $\underline{x} = \underline{x}_e + \underline{x}$ and $\underline{u} = \underline{u}_e + \underline{u}$) is obtained.

$$\dot{\underline{x}} = \underline{A}\underline{x} + \underline{B}\underline{u} \tag{2.6}$$

where

$$\underline{x} = [\Delta\delta_1 \Delta\delta_2 \ldots . \Delta\delta_n \,\vdots\, \Delta\omega_1 \Delta\omega_2 \ldots . \Delta\omega_n]^T = [\Delta\underline{\delta}^T \,\vdots\, \Delta\underline{\omega}^T]^T \tag{2.7}$$

and

$$\underline{u} = [\Delta Pm_1 \Delta Pm_2 \ldots . \Delta Pm_n]^T = [\Delta \underline{P}_m^T]^T \tag{2.8}$$

The above choice of state variables leads to the following expressions for matrices $\underline{A}$ and $\underline{B}$.

$$\underline{A} = \begin{array}{c} \\ n \\ n \end{array} \begin{array}{c} \begin{array}{cc} n & n \end{array} \\ \left[\begin{array}{c|c} \underline{0} & \underline{I}_n \\ \hline \underline{\bar{A}} & \underline{0} \end{array}\right] \end{array} \tag{2.9}$$

$$B = \begin{array}{c} \\ n \\ n \end{array} \begin{array}{c} \begin{array}{c} n \end{array} \\ \left[\begin{array}{c} \underline{0} \\ \hline \underline{\bar{B}} \end{array}\right] \end{array} \tag{2.10}$$

Matrix $\underline{I}_n$ is the square identity matrix of order n and matrices $\bar{\underline{A}}$ and $\bar{\underline{B}}$ are given by

$$\bar{\underline{A}} = \begin{matrix} \\ n \end{matrix} \overset{\overset{n}{\downarrow}}{\begin{bmatrix} -(\omega_R/2H_1)\left(\frac{\partial Pe_1}{\partial \delta_1}\right) & \cdots & -(\omega_R/2H_1)\left(\frac{\partial Pe_1}{\partial \delta_n}\right) \\ \vdots & & \\ -(\omega_R/2H_n)\left(\frac{\partial Pe_n}{\partial \delta_1}\right) & \cdots & -(\omega_R/2H_n)\left(\frac{\partial Pe_n}{\partial \delta_n}\right) \end{bmatrix}}\Bigg|_{(\underline{x}_e,\underline{u}_e)} \tag{2.11}$$

and

$$\bar{\underline{B}} = \begin{matrix} \\ n \end{matrix} \overset{\overset{n}{\downarrow}}{\begin{bmatrix} (\omega_R/2H_1) & 0 & \cdots & 0 \\ 0 & (\omega_R/2H_2) & \cdots & 0 \\ \vdots & \vdots & & \vdots \\ 0 & 0 & \cdots & (\omega_R/2H_n) \end{bmatrix}} \tag{2.12}$$

where the partial derivatives $\left(\frac{\partial Pe_i}{\partial \delta_j}\right)$ are defined as

$$\frac{\partial Pe_i}{\partial \delta_j} = \begin{cases} -|E_i||E_j||Y_{ij}|\sin(\theta_{ij}-\delta_{ij})\big|_{(\underline{x}_e,\underline{u}_e)} & \text{if } i\neq j \\ \sum\limits_{\substack{k=1 \\ k\neq i}}^{n} |E_i||E_k||Y_{ik}|\sin(\theta_{ik}-\delta_{ik})\big|_{(\underline{x}_e,\underline{u}_e)} & \text{if } i=j \end{cases} \tag{2.13}$$

The above results permit the representation of equations (2.5) in the perturbed form as

$$\frac{d}{dt}\Delta\delta_i = \Delta\omega_i \tag{2.14a}$$

$$\Delta\dot{\omega}_i = \frac{\omega_R}{2H_i}\left[\Delta Pm_i - \sum_{j=1}^{n} \frac{\partial Pe_i}{\partial \delta_j}\Big|_{(\underline{x}_e,\underline{u}_e)}\Delta\delta_j\right] \quad i=1,2,3,..n \tag{2.14b}$$

The off-diagonal entries of $\underline{\bar{A}}$, after an algebraic manipulation, define the synchronizing power coefficient as

$$Ps_{ij} = \frac{\partial Pe_i}{\partial \delta_j} = -\left(\frac{2H_i}{\omega_R}\right)\bar{a}_{ij} \tag{2.14c}$$

between nodes i and j which describes the "strength of the forces" keeping machine i in synchronism with machine j.

2.4 Modes of Oscillation and Eigen Structure of the System Matrices $\underline{A}$ and $\underline{\bar{A}}$.

The modes of oscillation of a dynamical system are revealed by the zero-input equivalent system, i.e., a dynamical system whose input vector $\underline{u}$ is the null vector $\underline{0}$. Mathematically, this is expressed as

$$\dot{\underline{x}} = \underline{A}\underline{x} \tag{2.15}$$

where $\underline{A}$ is as given in detail in equation (2.11).

Some well-known properties of the matrices $\underline{A}$ and $\underline{\bar{A}}$ [1,5,32] are given below.

i) In the absence of damping, the eigenvalues of $\underline{\bar{A}}$ are all real and nonpositive. This statement is true only if the operating point is stable; however, we have no interest in nonstable operating points.

ii) The rank of $\underline{\bar{A}}$ is (n-1).

iii) $\bar{\underline{A}}$ has a zero eigenvalue.

iv) The eigenvalues of $\underline{A}$ are the square roots of the eigenvalues of $\bar{\underline{A}}$.

v) The zero eigenvalue of $\bar{\underline{A}}$ has a non-zero associated eigenvector whose entries are all identical.

A method for computing the eigen structure of $\underline{A}$ from that of $\bar{\underline{A}}$ is now developed using the above properties. Let the eigenvalues and associated eigenvectors of $\bar{\underline{A}}$ be $\bar{\lambda}_i$ and $\underline{x}_i$ respectively, and the eigenvalues and eigenvectors of $\underline{A}$ be λ_i and $\underline{\alpha}_i$. The following equations then hold.

$$\bar{\underline{A}}\underline{x}_i = \bar{\lambda}_i\underline{x}_i \qquad i=1,2,3,\ldots,n \tag{2.16a}$$

$$\underline{A}\underline{\alpha}_i = \lambda_i\underline{\alpha}_i \qquad i=1,2,3,\ldots,2n \tag{2.16b}$$

Let $\underline{\alpha}_i$ be partitioned as

$$\underline{\alpha}_i = [\underline{\alpha}_i^{1T} \,;\, \underline{\alpha}_i^{2T}]^T \qquad i=1,2,3,\ldots,2n \tag{2.17}$$

and equation (2.16b) becomes

$$\left[\begin{array}{c:c} \underline{0} & \underline{I}_n \\ \hdashline \bar{\underline{A}} & \underline{0} \end{array}\right]\left[\begin{array}{c} \underline{\alpha}_i^1 \\ \hdashline \underline{\alpha}_i^2 \end{array}\right] = \lambda_i \left[\begin{array}{c} \underline{\alpha}_i^1 \\ \hdashline \underline{\alpha}_i^2 \end{array}\right] \tag{2.18}$$

with the result that

$$\underline{\alpha}_i^2 = \lambda_i\underline{\alpha}_i^1 \tag{2.19a}$$

$$\bar{\underline{A}}\underline{\alpha}_i^1 = \lambda_i\underline{\alpha}_i^2 \qquad i=1,2,\ldots,2n \tag{2.19b}$$

Substituting equation (2.19a) into equation (2.19b), we obtain

$$\bar{\underline{A}}\underline{\alpha}_i^1 = (\lambda_i)^2\underline{\alpha}_i^1 \qquad i=1,2,3,\ldots,2n \tag{2.20}$$

From equation (2.20) it can be seen that there are 2n $\underline{\alpha}_i^1$ occurring in identical pairs because the eigenvalues λ_i's (i=1,2,...,2n) appear in imaginary conjugate pairs and generate n distinct values of $(\lambda_i)^2$ (assuming no repeated eigenvalues). Using property iv which states that

$$(\lambda_i)^2 = \bar{\lambda}_i \qquad i=1,2,\ldots,n \tag{2.21}$$

and comparing equation (2.20) with equation (2.16a), it is evident that

$$\underline{\alpha}_i^1 = \underline{x}_i \qquad i=1,2,\ldots,n \tag{2.22}$$

where the $\underline{x}_i$ are the eigenvectors of $\bar{\underline{A}}$.

Using the above results, the eigenvectors $\underline{\alpha}_i$ and $\underline{\alpha}_i^*$, associated with λ_i and λ_i^*, respectively, are

$$\begin{aligned}
\underline{\alpha}_i &= [\underline{x}_i^T \,|\, +j\sqrt{|\bar{\lambda}_i|}\;\; \underline{x}_i^T]^T = [\underline{x}_i^T \,|\, \underline{0}^T]^T + j[\underline{0}^T \,|\, \sqrt{|\bar{\lambda}_i|}\;\underline{x}_i^T]^T \\
\underline{\alpha}_i^* &= [\underline{x}_i^T \,|\, -j\sqrt{|\bar{\lambda}_i|}\;\; \underline{x}_i^T]^T = [\underline{x}_i^T \,|\, \underline{0}^T]^T - j[\underline{0}^T \,|\, \sqrt{|\bar{\lambda}_i|}\;\underline{x}_i^T]^T \\
&\qquad\qquad\qquad\qquad\qquad\qquad\qquad\qquad\qquad\qquad i=1,2,3,\ldots n
\end{aligned} \tag{2.23}$$

Similarly, the eigenvalues and eigenvectors of $\underline{A}^T$ can be computed from those of $\bar{\underline{A}}^T$. The eigenvectors of $\underline{A}^T$ and $\bar{\underline{A}}^T$ constitute the reciprocal basis vectors of $\underline{A}$ and $\bar{\underline{A}}$ respectively. Now, let the eigenvalues and associated eigenvectors of $\bar{\underline{A}}^T$ be $\bar{\lambda}_i$ and $\underline{\omega}_i$ and those of $\underline{A}^T$ be λ_i and β_i.

It is noted in passing that the eigenvalues of a matrix and those of its transpose are identical. The following equations then hold for $\bar{\underline{A}}^T$

$$\bar{\underline{A}}^T \underline{\omega}_i = \bar{\lambda}_i \underline{\omega}_i \qquad i=1,2,3,\ldots,n \tag{2.24}$$

and for the matrix $\underline{A}^T$ the set of reciprocal basis vectors is obtained by means of the following matrix equation [17].

$$\underline{A}^T \underline{\beta}_i = \lambda_i^* \underline{\beta}_i \qquad i=1,2,3,\ldots,2n \tag{2.25}$$

The set of vectors $\{\underline{\beta}_i,\ i=1,2,\ldots,2n\}$ constitutes the reciprocal basis vectors of the set of vectors $\{\underline{\alpha}_i,\ i=1,2,3,\ldots,2n\}$ lying in the 2n-dimensional conjugate linear vector space of the $\underline{\alpha}_i$'s. Let β_i be partitioned as

$$\underline{\beta}_i = \left[\underline{\beta}_i^{1T} \,\vdots\, \underline{\beta}_i^{2T}\right]^T \qquad i=1,2,\ldots,2n$$

and equation (2.25) becomes

$$\left[\begin{array}{c:c} \underline{0} & \bar{\underline{A}}^T \\ \hdashline \underline{I}_n & \underline{0} \end{array}\right] \left[\begin{array}{c} \underline{\beta}_i^1 \\ \hdashline \underline{\beta}_i^2 \end{array}\right] = \lambda_i^* \left[\begin{array}{c} \underline{\beta}_i^1 \\ \hdashline \underline{\beta}_i^2 \end{array}\right] \tag{2.26}$$

Consequently,

$$\bar{\underline{A}}^T \underline{\beta}_i^2 = \lambda_i^* \underline{\beta}_i^1 \tag{2.27a}$$

and

$$\underline{\beta}_i^1 = \lambda_i^* \underline{\beta}_i^2 \tag{2.27b}$$

Substituting (2.27b) into (2.27a),

$$\underline{\bar{A}}^T \underline{\beta}_i^2 = (\lambda_i^*)^2 \, \underline{\beta}_i^2 \qquad i=1,2,3,\ldots,2n \tag{2.28}$$

Because of reasoning similar to that used in equation (2.20) and the fact that

$$(\lambda_i^*)^2 = \bar{\lambda}_i \qquad i=1,2,3,\ldots,n \tag{2.29}$$

and comparing equation (2.28) with equation (2.24), it is evident that

$$\underline{\beta}_i^2 = \underline{\omega}_i \qquad i=1,2,3,\ldots,n \tag{2.30}$$

Thus, using the above results, the eigenvectors of $\underline{A}^T$ are expressed in terms of those of $\underline{\bar{A}}^T$ as follows:

$$\begin{aligned} \underline{\beta}_i &= [-j\sqrt{|\bar{\lambda}_i|}\ \underline{\omega}_i^T \,|\, \underline{\omega}_i^T]^T = [\underline{0}^T \,|\, \underline{\omega}_i^T]^T - j[\sqrt{|\bar{\lambda}_i|}\ \underline{\omega}_i^T \,|\, \underline{0}^T]^T \\ \underline{\beta}_i^* &= [j\sqrt{|\bar{\lambda}_i|}\ \underline{\omega}_i^T \,|\, \underline{\omega}_i^T]^T = [\underline{0}^T \,|\, \underline{\omega}_i^T]^T + j[\sqrt{|\bar{\lambda}_i|}\ \underline{\omega}_i^T \,|\, \underline{0}^T]^T \\ & \qquad\qquad\qquad\qquad\qquad\qquad\qquad\qquad i=1,2,3,\ldots,n \end{aligned} \tag{2.31}$$

These relationships between the eigen structures of the matrices $\underline{A}$ and $\underline{\bar{A}}$ and those of $\underline{A}^T$ and $\underline{\bar{A}}^T$ are useful in the determination of a sensitivity matrix and the time response of linear systems as will be shown in Chapters 3 and 4.

2.5 Numerical Examples

Before considering the problem of identifying the coherent generators, we now illustrate the above theory using a three machine power system [4]. A single line diagram of the system is shown in Fig. 2.1 and the complete system data are provided in Appendix A.

The data for the steady-state operating point used to compute the system matrix $\underline{A}$ are given in Table 2.1. The fault applied to the system is a three-phase fault near bus 7 at the end of line 5-7. The fault is cleared in five cycles by opening and then reclosing line 5-7. This implies that the pre-fault state is identical to the post-fault state as long as the loading conditions are maintained. Furthermore, lines 2-7, 4-3 and 9-1 include the synchronous transient reactance x'd and hence buses 1, 2 and 3 are internal nodes. In addition, [Y]pre-fault = [Y]post-fault.

Table 2.1 Power System Initial Conditions

	Generated Power (p.u.)			Voltage $\bar{E}_i$	
Bus	P_{G_i}	Q_{G_i}	Q_{e_i}	Magnitude (p.u.)	Angle (Degrees)
1	0.85	-0.109	-0.0169	1.017	13.175
2	1.63	0.067	0.3696	1.0502	19.732
3	0.716	0.27	0.3032	1.057	2.272
					MVA BASE: 100

The matrices $\bar{\underline{A}}$ and $\underline{A}$ were computed from the system data and initial conditions using equations (2.13) and (2.9), with the result that

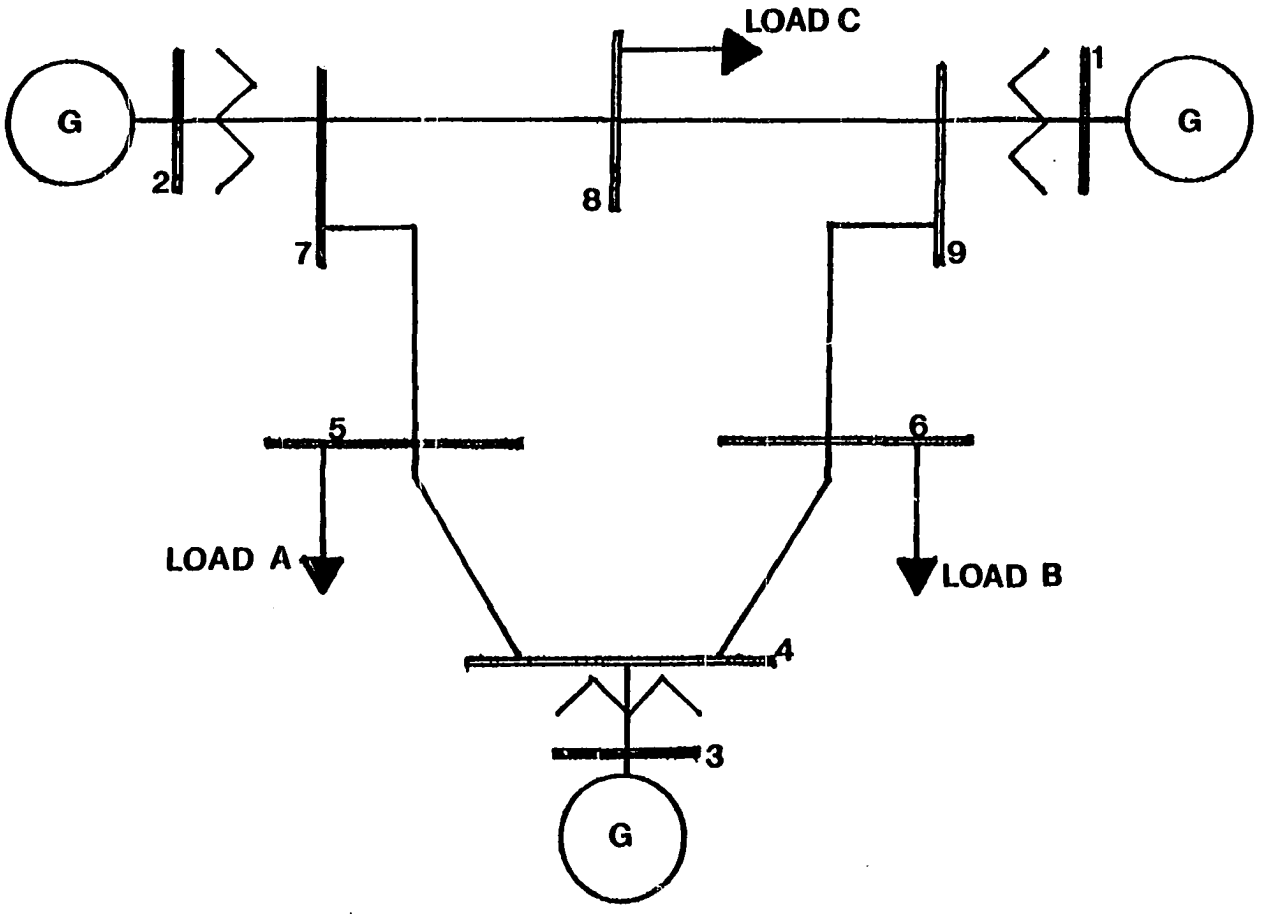

Fig. 2.1 The nine-bus power system line diagram
(The WSCC system)

$$\bar{\underline{A}} = \begin{bmatrix} -152.2617 & 73.9229 & 78.3387 \\ 33.2374 & -77.5909 & 44.3535 \\ 10.6555 & 13.5321 & -24.1876 \end{bmatrix}$$

$$\underline{A} = \begin{bmatrix} 0.0 & 0.0 & 0.0 & 1.0 & 0.0 & 0.0 \\ 0.0 & 0.0 & 0.0 & 0.0 & 1.0 & 0.0 \\ 0.0 & 0.0 & 0.0 & 0.0 & 0.0 & 1.0 \\ -152.2616 & 73.9229 & 78.3387 & 0.0 & 0.0 & 0.0 \\ 33.2374 & -77.5909 & 44.3535 & 0.0 & 0.0 & 0.0 \\ 10.6555 & 13.5321 & -24.1876 & 0.0 & 0.0 & 0.0 \end{bmatrix}$$

The eigenvalues and their associated eigenvectors for matrices $\bar{\underline{A}}$ and $\bar{\underline{A}}^T$ were computed using the program EIGEN[1]. The eigenvectors of $\underline{A}$ and $\underline{A}^T$ were obtained by the use of equations (2.23) and (2.31). For the sake of brevity, only a subset of the total set of eigenvectors are given here.

The eigenvalues of $\bar{\underline{A}}$ and $\bar{\underline{A}}^T$ are

$$\bar{\lambda}_1 = -178.52 \qquad \bar{\lambda}_2 = 0.0 \qquad \bar{\lambda}_3 = -75.5192$$

---

[1]EIGEN is a library program subroutine available at the ISU VAX system to compute the eigenvalues and associated eigenvectors of a real matrix.

Using the above results, the eigenvalues of $\underline{A}$ and $\underline{A}^T$ are

$$\lambda_1 = j13.3611 \qquad \lambda_1^* = -j13.3611$$

$$\lambda_2 = 0.0 \qquad \lambda_2^* = 0.0$$

$$\lambda_3 = j8.6902 \qquad \lambda_3^* = -j8.6902$$

The eigenvectors of $\bar{\underline{A}}$ and $\bar{\underline{A}}^T$ are

$$\underline{x}_1 = [-0.9541 \quad 0.2967 \quad 0.0399]^T \qquad \underline{\omega}_1 = [-0.7973 \quad 0.5509 \quad 0.2464]^T$$

$$\underline{x}_2 = [0.618 \quad 0.618 \quad 0.618]^T \qquad \underline{\omega}_2 = [0.1352 \quad 0.3017 \quad 0.9911]^T$$

$$\underline{x}_3 = [-0.5723 \quad -0.9992 \quad 0.3822]^T \qquad \underline{\omega}_3 = [-0.1926 \quad -0.7452 \quad 0.9378]^T$$

In order to show that the set of vectors $\underline{\omega}$ are indeed a reciprocal basis to the set of vectors $\underline{x}$, we take the dot product between pairs of vectors in the two sets, observing that

$$\langle \underline{\omega}_i, \underline{x}_i \rangle = \langle \underline{x}_i, \underline{\omega}_i \rangle \neq 0$$

and

$$\langle \underline{\omega}_j, \underline{x}_i \rangle = \langle \underline{x}_i, \underline{\omega}_j \rangle = 0 \qquad \text{for all } i \neq j$$

A subset of two eigenvectors and reciprocal basis vectors of $\underline{A}$ and $\underline{A}^T$ is given below.

$$\underline{\alpha}_i = [-0.9541 \quad 0.2967 \quad 0.0399 \quad 0.0 \quad 0.0 \quad 0.0]^T$$
$$+ j[0.0 \quad 0.0 \quad 0.0 \quad -12.748 \quad 3.964 \quad 0.533]^T$$

$$\underline{\alpha}_1^* = [-0.9541 \quad 0.2967 \quad 0.0399 \quad 0.0 \quad 0.0 \quad 0.0]^T$$
$$- j[0.0 \quad 0.0 \quad 0.0 \quad -12.748 \quad 3.964 \quad 0.533]^T$$

and

$$\underline{\beta}_1 = [0.0 \quad 0.0 \quad 0.0 \quad -0.7973 \quad 0.5509 \quad 0.2464]^T$$
$$- j[-10.653 \quad 7.361 \quad 3.292 \quad 0.0 \quad 0.0 \quad 0.0]^T$$
$$\underline{\beta}_1^* = [0.0 \quad 0.0 \quad 0.0 \quad -0.7973 \quad 0.5509 \quad 0.2464]^T$$
$$+ j[-10.653 \quad 7.361 \quad 3.292 \quad 0.0 \quad 0.0 \quad 0.0]^T$$

It is also important to note that the rank of matrix $\underline{\bar{A}}$ is no more than two. This is because the sum of columns of $\underline{\bar{A}}$ is equal to zero (i.e., they are linearly dependent). As a result, it is usual to find in dynamic and transient stability algorithms that one of the system generators is chosen as a reference, reducing the number of state variables to (2n-2). That is, the rotor angle and angular speed of each of the (n-1) generators are referred to the angle and speed δ_n and ω_n respectively. This statement is valid only for uniform damping (i.e., $D_i/2H_i$ is the same for all i). In the event that damping is not uniform, the reduction in the number of state variables is by one. In this case, we can refer only the (n-1) machine rotor angles, δ_i's, to the reference generator angle δ_n. The direct coherency method developed in Chapter 4 will make use of the first condition so that the dimension of the vector space is (2n-2) instead of 2n.

In order to show the effect of the elimination of the zero eigenvalues of $\underline{\bar{A}}$ and $\underline{A}$, the reduced matrices $\underline{\bar{A}}_1$ and $\underline{A}_1$ (i.e., those $\underline{\bar{A}}$ and $\underline{A}$ matrices whose ranks are (n-1) and (2n-2) respectively) along with their eigenvalues and eigenvectors are now determined. The reduced matrix $\underline{A}_1$ is

$$\underline{A}_1 = \begin{bmatrix} -91.1231 & 22.5819 \\ 60.3908 & -162.917 \end{bmatrix}$$

with its eigenvalues being

$$\bar{\lambda}_1 = -75.52 \qquad \bar{\lambda}_2 = -178.50$$

and the associated eigenvectors of $\underline{\bar{A}}_1$ and $\underline{\bar{A}}_1^T$ are

$$\underline{x}_1 = [0.8227 \quad 0.5685]^T \qquad \underline{\omega}_1 = [0.9682 \quad 0.2502]^T$$

$$\underline{x}_2 = [-0.2665 \quad 1.03]^T \qquad \underline{\omega}_2 = [-0.6056 \quad 0.8764]^T$$

The reduced matrix $\underline{A}_1$ is

$$\underline{A}_1 = \begin{bmatrix} 0.0 & 0.0 & 1.0 & 0.0 \\ 0.0 & 0.0 & 0.0 & 0.0 \\ -91.1231 & 22.5819 & 0.0 & 0.0 \\ 60.3908 & -162.917 & 0.0 & 0.0 \end{bmatrix}$$

with its eigenvalues being

$$\lambda_1 = j8.69 \qquad \lambda_1^* = -j8.69$$

$$\lambda_2 = j13.36 \qquad \lambda_2^* = -j13.36$$

and the associated eigenvectors of $\underline{A}_1$ and $\underline{A}_1^T$ being

$$\underline{\alpha}_1 = [0.8227 \quad 0.5685 \quad 0.0 \quad 0.0]^T + j[0.0 \quad 0.0 \quad 7.149 \quad 4.94]^T$$

$$\underline{\alpha}_2 = \underline{\alpha}_1^*$$

$$\underline{\alpha}_3 = [-0.2665 \quad 1.03 \quad 0.0 \quad 0.0]^T + j[0.0 \quad 0.0 \quad -3.56 \quad 13.76]^T$$

$$\underline{\alpha}_4 = \underline{\alpha}_3^*$$

$$\underline{\beta}_1 = [0.0 \quad 0.0 \quad 0.9682 \quad 0.2502]^T - j[8.414 \quad 2.174 \quad 0.0 \quad 0.0]^T$$

$$\underline{\beta}_2 = \underline{\beta}_1^*$$

$$\underline{\beta}_3 = [0.0 \quad 0.0 \quad -0.6056 \quad 0.8764]^T - j[-8.091 \quad 11.709 \quad 0.0 \quad 0.0]^T$$

$$\underline{\beta}_4 = \underline{\beta}_3^*$$

It can be shown after some algebraic manipulations[1] that the diagonal and off-diagonal elements of the reduced matrix $\bar{\underline{A}}_1$ are given by

$$\bar{a}_{ii_1} = \frac{\omega_R}{2H_i}\left(B_{ii}|E_i|^2 + Q_{e_i}\right) + \frac{\omega_R}{2H_n}\left[|E_n||E_i||Yn_i|\sin(\theta_{ni}+\delta_{in})\right]\Big|_{\underline{x}_e,\underline{u}_e}$$

$$\bar{a}_{ij_1} = -\frac{\omega_R}{2H_i}\left[|E_i||E_j||Y_{ij}|\sin(\theta_{ij}-\delta_{ij})\right] + \frac{\omega_R}{2H_n}\left[|E_n||E_j||Y_{nj}|\sin(\theta_{nj}+\delta_{nj})\right]_{\underline{x}_e,\underline{u}_e}$$

where H_n is the inertia constant of the system reference generator.

---

[1] Referred to Chapter 4, Section 4.3.

Given that in usual situations $H_n >> H_i$, the reduced matrix $\bar{\underline{A}}_1$ is row dominant [54], that is, an n×n matrix $\underline{B} = (b_{ij})$ is said to be row dominant if $|b_{ii}| > \sum_{\substack{j=1 \\ i\neq j}}^{n} |b_{ij}|$ $\forall i \epsilon N$. This permits the nonzero natural modes to be estimated by use of the diagonal terms only. Since the diagonal term $\bar{a}_{ii_1}$ is given approximately by $(\omega_R/2H_i)(B_{ii}|E_i|^2+Qe_i)$, the stability of a power system whose $\bar{\underline{A}}_1$ is row dominant depends on the injected reactive power Qe_i.

In most practical systems, $B_{ii} < 0$ and the term $B_{ii}|E_i|^2$ is negative. The sign of the diagonal element of $\bar{\underline{A}}_1$ will hence depend on the injected reactive power Qe_i. Thus, if $Qe_i > |B_{ii}|E_i|^2|$ for some i, the system is unstable. On the contrary, if $Qe_i < |B_{ii}|E_i|^2|$ for all i, the system is stable.

In order to demonstrate the effect of the injected reactive power, Qe_i, on the natural modes of oscillation of $\bar{\underline{A}}_1$ (i.e., the nonzero modes of oscillation of $\bar{\underline{A}}$) the loading conditions at buses 5, 6 and 8 were modified and a new matrix $\bar{\underline{A}}_1$ and its eigen structure were computed. Table 2.2 shows the new system initial conditions. These initial conditions were obtained from a load-flow analysis in which the loads at buses 5, 6 and 8 were set at

i) Bus 5: P_L = 125MW and Q_L = 100MVAR.

ii) Bus 6: P_L = 120MW and Q_L = 80MVAR.

iii) Bus 8: P_L = 100MW and Q_L = 70MVAR.

Table 2.2 New Initial Conditions

	Generated Power (p.u.)			Voltage $\underline{E}_i$	
Bus	P_{G_i}	Q_{G_i}	Q_{e_i}	Magnitude (p.u.)	Angle (Degrees)
1	0.85	0.368	0.4511	1.1004	10.4727
2	1.63	0.555	0.6217	1.1064	17.8444
3	1.038	1.022	1.1412	1.1014	3.1593
					MVA BASE: 100

The new matrix $\bar{\underline{A}}_1$ is

$$\bar{\underline{A}}_1 = \begin{bmatrix} -89.9319 & 23.5540 \\ 63.2630 & -164.3950 \end{bmatrix}$$

The eigenvalues of $\bar{\underline{A}}_1$ are

$$\bar{\lambda}_1 = -73.5324 \qquad \bar{\lambda}_2 = -180.7944$$

and their associated eigenvectors and reciprocal basis vectors are

$$\underline{x}_1 = [-0.6093 \quad -0.8751]^T \qquad \underline{\omega}_1 = [-0.2676 \quad -1.0322]^T$$

$$\underline{x}_2 = [-0.968 \quad 0.2509]^T \qquad \underline{\omega}_2 = [-0.8207 \quad 0.5714]^T$$

Although the injected reactive powers at the internal nodes 1, 2 and 3 have been changed substantially compared to those values given in Table 2.1, the location of the nonzero eigenvalues does not show any significant change. This means that for the present case the term $B_{ii}|E_i|^2$ plays a dominant role in determining the nonzero natural modes.

CHAPTER 3. SENSITIVITY BASED SLOW COHERENCY METHOD

3.1 Introduction

Consider the matrix equation

$$\dot{\underline{x}} = \underline{A}\underline{x} \tag{3.1}$$

As discussed previously, the eigenvalues of $\underline{A}$ are $\pm\sqrt{|\bar{\lambda}_i|}$ (i=1,2,...,n), where $\bar{\lambda}_i$ are the eigenvalues of $\underline{\bar{A}}$. The implication is that the natural frequencies of oscillation are

$$0, \sqrt{|\bar{\lambda}_1|}, \sqrt{|\bar{\lambda}_2|}, \ldots, \sqrt{|\bar{\lambda}_{n-1}|}$$

expressed in electrical radians per second. In terms of the physical phenomena involved, it is useful to divide these frequencies into two subsets, the slow frequencies and the fast frequencies. This division is arbitrary and based on judgement as to its efficacy.

In power systems, observation shows that machines often tend to swing together in groups after a disturbance. This suggests that the order of a system might be reduced if full advantage can be taken of this to combine machines in dynamic equivalents.

For the purpose of a more precise discussion, a series of definitions are stated.

Definition 3.1: Two machines, i and j, are said to be coherent if

$$\Delta\delta_i(t) - \Delta\delta_j(t) = 0 \qquad t > 0 \tag{3.2}$$

where $\Delta\delta$ is the change in angle as measured from t=0, the time of the occurrence of the disturbance.

Definition 3.2: Two machines are said to be coherent with respect to the slow natural frequencies if

$$\Delta\delta_i(t) - \Delta\delta_j(t) - Z_{ij}(t) = 0 \qquad t > 0 \tag{3.3}$$

where $Z_{ij}(t)$ is a variable containing all of the contributions of the fast frequencies to the angular separation of machines i and j. This is more usually referred to as slow coherency.

Definition 3.3: A group of machines in which all pairs of machines satisfy equation (3.3) is said to be a slow coherent group or simply a coherent group in the slow frequency sense.

Definition 3.4: A system of n-machines which can be decomposed into r coherent groups of machines is said to be an r-decomposable system.

The preceding definitions are statements of ideal coherency, unattainable in physical systems (except for certain very special situations). They can be modified by rewriting equations (3.2) and (3.3) as

$$|\Delta\delta_i(t) - \Delta\delta_j(t)| \leq \varepsilon \qquad t > 0 \tag{3.4}$$

$$|\Delta\delta_i(t) - \Delta\delta_j(t) - Z_{ij}(t)| \leq \varepsilon \qquad t > 0 \tag{3.5}$$

respectively. In this case, the definitions are modified by use of near or nearly, although the modifier is often omitted in common use. A commonly accepted range of values for ε is from 3 to 5 electrical degrees although there is no agreement on a fixed range.

These definitions of near-coherency are difficult to apply without extensive examination of the system to the point of being self-defeating in terms of reduction in computation. What are generally referred to as slow coherency methods are based on the accomplishment of the following steps.

i) The natural frequencies are identified and divided into slow and fast subsets thus establishing the number of coherent groups.

ii) A reference machine is identified for each coherent group.

iii) The remaining machines are assigned to groups as followers.

In this chapter, a sensitivity based slow coherency method is proposed as a procedure for selection of the reference generators of the different coherent groups. We first review the slow coherency method proposed by Avramovic [5], then the physical implications of slow coherency are examined. Finally, a sensitivity based method of grouping is proposed and validated with practical systems.

3.2 Review of the Slow Coherency Method in the Identification of Coherent Groups

Slow coherency identifies groups of coherent generators in a power system. As a result, the groups can be replaced by an equivalent generator. Such a step is called dynamic equivalencing. The rationale behind the concept of coherency as it is known at the present time is based on the observation that machines close to the fault respond with large angular swings, whereas machines distant from the fault respond with much smaller swings which are often coherent.

Slow coherency is a member of the class of coherency methods where the selection of coherent groups of generators is based on the premise

that inter-group motions are principally excited by the system's slow eigenvalues and intra-group motions (i.e., oscillations within the group) are principally excited by the system's fast eigenvalues. A mathematical treatment of this is given in references [5] and [55].

A grouping technique designed to select the group-reference generators and their associated followers is given in reference [5] and is summarized below.

i) Decide on the r slow eigenvalues of $\underline{A}$. This is equivalent to determining the r slow natural frequencies of $\underline{A}$. This in turn determines the number of coherent groups or equivalent generators into which the system will be decomposed.

ii) Partition the rotor angle vector $\Delta\underline{\delta}(t)$ in equation (1.3) into group-reference and follower angles $\Delta\underline{\delta}_R(t)$ and $\Delta\underline{\delta}_F(t)$ respectively. The order of $\Delta\underline{\delta}_R(t)$ is r while that of $\Delta\underline{\delta}_F(t)$ is (n-r). In view of the partition of $\Delta\underline{\delta}(t)$, equation (3.3) is cast in matrix form as

$$\Delta\underline{\delta}_F(t) - \underline{Lg}\Delta\underline{\delta}_R(t) = \underline{Z}(t) \tag{3.6}$$

where the (i,j) entry of $\underline{Lg}$ is 1 if generators i and j belong to the same coherent group and 0 otherwise. The matrix $\underline{Lg}$ is called the grouping matrix.

The computation of the matrix $\underline{Lg}$ is achieved by the following procedure in reference [5].

i) Compute the eigenvectors associated with the slow spectrum of $\underline{A}$, which then forms the basis for the slow eigen space of dimension r.

ii) Form a matrix $\underline{V}$ whose columns are the set of eigenvectors computed in step i and the rows correspond to the n generators of the system. For convenience, as will be explained later, the generator with the largest inertia is labeled as n.

iii) A Gaussian elimination procedure is applied to matrix $\underline{V}$ to find the sets of r most linearly independent rows of $\underline{V}$ as follows.

a. Rows and columns of $\underline{V}$ are permuted so that the entry (1,1) of $\underline{V}$ is the largest in magnitude.

b. This entry (1,1) is then chosen as the pivot for performing the first step in the Gaussian elimination. The entry largest in magnitude is again chosen from the remaining $(n-1)\times(r-1)$ submatrix of the reduced $\underline{V}$ matrix and is used as the pivot for the next step.

c. The procedure terminates in r steps with the generators corresponding to the r rows permuted into the first position during the Gaussian elimination being chosen as the group-reference machines.

iv) As a result of step iii, matrix $\underline{V}$ is row partitioned into submatrices $\underline{V}_1$ and $\underline{V}_2$ of order $r\times r$ and $(n-r)\times r$ respectively,

$$\underline{V} = \begin{matrix} \\ r \\ (n-r) \end{matrix} \begin{matrix} r \\ \left[\begin{array}{c} \underline{V}_1 \\ \hline \underline{V}_2 \end{array}\right] \end{matrix} \tag{3.7}$$

where $\underline{V}_1$ is nonsingular. Once the above partitioning has been accomplished, the matrix $\underline{Ld}$ is computed by

$$\underline{Ld} = \underline{V}_2\underline{V}_1^{-1} \tag{3.8}$$

with $\underline{Ld}$ satisfying $\sum_{j=1}^{r} Ld_{ij} = 1$ $(i=1,2,\ldots,n)$.

The optimum selection of group-reference generators is obtained when the norm of the matrix $(\underline{Ld}-\underline{Lg})$ is a minimum; however, since the norm[1] of

---

[1]The norm of the matrices $\underline{Ld}$ and $\underline{Lg}$ is given by [5]

$$\|L\| = \max_i \sum_{j=1}^{r} |L_{ij}|, \quad i=1,2,\ldots,n.$$

any matrix $\underline{Lg}$ is one, the optimum matrix $\underline{Ld}$ is that one possessing the norm closest to one. Thus, the searching procedure is devoted to find the matrix $\underline{Ld}$ with the norm closest to one rather than finding the $\underline{Ld}$ which minimizes $\|\underline{Lg}-\underline{Ld}\|$.

In the class of r-near decomposable systems, typical of realistic power systems, we can find the matrix $\underline{Lg}$ approximating the matrix $\underline{Ld}$ by setting the largest nonnegative entry in each row of $\underline{Ld}$ to 1 and setting the remainder of the entries to zero provided that a correct selection of group-reference generators has been made. Physically, the (n-r) rowsof $\underline{Lg}$ are identified with the follower generators and the r columns are associated with the group-reference generators.

The follower generators are assigned to the different group-reference generators by checking the columns of $\underline{Lg}$ in which the nonzero entries appear. For example, if the 1 in row two is found in column three, then the follower generator associated with row two is assigned to the group-reference generator associated with column three. Given that there is only one nonzero entry per row, a follower generator is associated with only one of the r slow natural frequencies. If, in forming $\underline{Lg}$ from $\underline{Ld}$, there are two positive entries with almost identical values in a row, the selection of the coherent area to which the machine belongs is largely a matter of judgement.

The modification described in section 3.4 consists of identifying the group-reference generators for the coherent groups by using sensitivity coefficients defined by the partial derivatives $(\frac{\partial \lambda_i}{\partial H_j})$ as

approximated by small variations in H_j. This replaces the Gaussian elimination by a search procedure applied to a sensitivity matrix $\underline{\bar{S}}$ to determine the group-reference machines.

3.3 Physical Significance of Slow Coherency in terms of the Slow and Fast Dynamics of a group of Coherent Generators

Slow coherency is based on the proper separation of natural frequencies into slow and fast subsets. Although the actual time response is given by a weighted linear combination of all the natural frequencies, the generator swing curves in realistic power systems show tendencies for groups of generators to swing together at one of the several slow natural frequencies after a fault occurring either within or without the system. Thus, if one could identify a machine with one of the slow natural frequencies, then it would be a group-reference generator for a coherent group. The foregoing premise along with the following assumptions were used to develop the slow coherence method described in reference [5].

i) The system is r-near decomposable, so that the number of coherent groups is equal to the r slow eigenvalues of $\underline{\bar{A}}$.

ii) There exists a similarity transformation $\underline{T}$ which allows the partition of the system state variables into slow and fast variables so that

$$\underline{Z} = \underline{T}\,\Delta\underline{\delta} \tag{3.9}$$

Assuming that the above assumptions hold, the original set of equations

$$\Delta\ddot{\underline{\delta}}(t) = \underline{\bar{A}}\,\Delta\underline{\delta}(t);\ \Delta\underline{\delta}(0) = \Delta\dot{\underline{\delta}}(0) = \underline{0} \qquad t > 0 \tag{3.10}$$

can be expressed, according to reference [55], in a new coordinate system $\underline{Z}_1$, $\underline{Z}_2$ through a transformation matrix $\underline{T}$, equation (3.9), as follows

$$\begin{bmatrix} \underline{Z}_1 \\ \hline \underline{Z}_2 \end{bmatrix} = \left[\begin{array}{c|c} \underline{Hg}^{-1}\underline{H}_R & \underline{Hg}^{-1}\underline{L}^T\underline{H}_F \\ \hline -\underline{L} & \underline{I} \end{array}\right] \begin{bmatrix} \Delta\underline{\delta}_R \\ \hline \Delta\underline{\delta}_F \end{bmatrix} \tag{3.11}$$

In equation (3.11), $\underline{H}_R$ and $\underline{H}_F$ are diagonal matrices whose main diagonal entries are the inertia constants of the group-reference and follower generators respectively, and $\underline{Hg}$ is a matrix defined as

$$\underline{Hg} = \underline{H}_R + L^T\underline{H}_F\underline{L} \tag{3.12}$$

If the system is r-near decomposable, then $\underline{L} \triangleq \underline{Lg}$ and $\underline{Z}_1$ and $\underline{Z}_2$ are slow and fast variables. Thus,

$$\underline{Z}_2 \triangleq \Delta\underline{\delta}_F - \underline{Lg}\ \Delta\underline{\delta}_R \tag{3.13}$$

gives the incremental angular difference between the group-reference generators and their respective follower generators, thus describing the fast oscillations within a group. The slow variables $\underline{Z}_1$, on the other hand, satisfy the matrix equation

$$\underline{Hg}\underline{Z}_1 \triangleq \underline{H}_R\ \Delta\underline{\delta}_R + \underline{Lg}^T\underline{H}_F\ \Delta\underline{\delta}_F \tag{3.14}$$

Here, $\underline{Hg}$ is a diagonal matrix with the k^{th} entry being

$$Hg_K = \sum_{j\varepsilon \text{ area } K} H_j \tag{3.15}$$

so that the k^{th} row in equation (3.14) is given by

$$(\Sigma H_j)\ Z_{1k} \triangleq H_K \Delta\delta_K + \sum_{j\in \text{area } K} H_j \Delta\delta_j \qquad (3.16)$$

yielding the final result

$$Z_{1k} \triangleq \sum_{j\in \text{area } K} H_j \Delta\delta_j / \sum_{j\in \text{area } K} H_j \qquad k=1,2,\ldots,r \qquad (3.17)$$

Interpretively, Z_{1K} represents the motion of the center of inertia of area K.

3.4 Modification of the Slow Coherency Approach by use of Sensitivity

3.4.1 The sensitivity Matrix

A sensitivity matrix $\bar{S} = [\bar{S}_{ij}]$ is introduced as a means by which group-reference generators can be identified. The identification procedure is based on the computation of sensitivity coefficients of the dominant eigenvalues (i.e., slow natural frequencies) with respect to a generator parameter, which in the present case is the inertia constant H_j. In general, as shown in reference [19], the sensitivity with respect to a parameter α of any mode λ_i of a matrix $\underline{P}$ is

$$\frac{\partial\lambda_i}{\partial\alpha} = \frac{<\frac{\partial[P]}{\partial\alpha} t_1, \underline{Z}_i>}{<\underline{t}_i, \underline{Z}_i>} \qquad (3.18)$$

where $\underline{t}_i$ and $\underline{Z}_i$ are the characteristic and reciprocal basis vectors associated with λ_i.

In view of equation (3.18), the sensitivity coefficients S_{ij} of the eigenvalues λ_i of $\underline{A}$ are computed from the expression,

$$S_{ij} = \frac{\partial \lambda_i}{\partial H_j} = \frac{<\frac{\partial [\underline{A}]}{\partial H_j} \underline{\alpha}_i, \underline{\beta}_i>}{<\underline{\alpha}_i, \underline{\beta}_i>} \qquad \begin{matrix} i=1,2,\ldots,r \\ j=1,2,\ldots,n \end{matrix} \tag{3.19}$$

Since λ_i of $\underline{A}$ is equal to $j\omega_i$, S_{ij} will also be imaginary and determines $\frac{\partial \omega_i}{\partial H_j} = -jS_{ij}$ without explicitly determining the sensitivities of the conjugate eigenvalues.

Because of the relationship between λ_i and $\bar{\lambda}_i$ (i.e., the eigenvalues of $\underline{A}$ and $\bar{\underline{A}}$ respectively) is such that

$$\bar{\lambda}_i = \lambda_i^2 = -\omega_i^2$$

it follows that

$$-2\omega_i \frac{\partial \omega_i}{\partial H_j} = \frac{\partial \bar{\lambda}_i}{\partial H_j} = \bar{S}_{ij} = \frac{<\frac{\partial [\bar{\underline{A}}]}{\partial H_j} \underline{x}_i, \underline{\omega}_i>}{<\underline{x}_i, \underline{\omega}_i>} \tag{3.20}$$

and hence

$$S_{ij} = \frac{1}{2\lambda_i} \bar{S}_{ij} \tag{3.21}$$

where $\bar{S}_{ij}$ is the (i,j) entry of the sensitivity matrix $\bar{\underline{S}}$.

The matrix $\bar{\underline{S}} = [\bar{S}_{ij}]$ consists of (r-1) rows and n columns which are identified with the nonzero slow eigenvalues of $\bar{\underline{A}}$ and the system generators respectively. The row corresponding to the zero eigenvalue, λ_1, has been deleted because the $\bar{S}_{ij}$ elements for this eigenvalue are all zero. To show that this statement is true, one needs to show that the vector $\frac{\partial [\bar{\underline{A}}]}{\partial H_j} \underline{x}_1$ is equal to the null vector. Let the matrix $\frac{\partial [\bar{\underline{A}}]}{\partial H_j}$ be given by

$$\left(\frac{\partial[\bar{\underline{A}}]}{\partial H_j}\right)_{ik} = \begin{cases} 0 & \text{if} \quad i \neq j \\ -\dfrac{\omega_R}{2H_j^2}|E_j||E_k||Y_{jk}|\sin(\theta_{jk}-\delta_{jk})\big|_{(\underline{x}_e,\underline{u}_e)} & j \neq k, i=j \\ \dfrac{\omega_R}{2H_j^2}\sum\limits_{\substack{\ell=1 \\ \ell\neq j}}^{n}|E_j||E_\ell||Y_{j\ell}|\sin(\theta_{j\ell}-\delta_{j\ell})\big|_{(\underline{x}_e,\underline{u}_e)} & j=k;\ i=j \end{cases} \tag{3.22}$$

It is seen from the above result that

$$\left(\frac{\partial[\bar{\underline{A}}]}{\partial H_j}\right)_{ii} = -\sum_{\substack{j=1 \\ j\neq i}}^{n}\left(\frac{\partial[\bar{\underline{A}}]}{\partial H_j}\right)_{ij} \tag{3.23}$$

which along with the vector associated with the zero eigenvalue, $\underline{x}_1 = [\alpha,\alpha,\ldots,\alpha]^T$ (due to property iii in section 2.3), produces the desired result

$$\frac{\partial[\bar{\underline{A}}]}{\partial H_j}\,\underline{x}_1 = \underline{0}$$

Hence, the structure of $\bar{\underline{S}}$ is

$$\bar{\underline{S}} = \text{eigenv.} \begin{bmatrix} \longleftarrow \text{machines} \longrightarrow \\ \bar{S}_{21} & \bar{S}_{22} & \cdots & \bar{S}_{2n} \\ \bar{S}_{31} & \bar{S}_{32} & \cdots & \bar{S}_{3n} \\ \vdots & & & \\ \bar{S}_{r1} & \bar{S}_{r2} & \cdots & \bar{S}_{rn} \end{bmatrix} \tag{3.24}$$

By this means, we can work with the n-dimensional vector space of $\bar{\underline{A}}$ instead of the 2n-dimensional space of $\underline{A}$ with a consequent reduction in computation.

It is noted that the order in which the rows of $\bar{\underline{S}}$ are numbered is arbitrary. Furthermore, the factor $(1/2\lambda_i)$ common to all entries belonging to a row i need not be considered in the process of identifying the group-reference generators. The assignment of generators to eigenvalues is done using only the relative magnitudes of the different elements $\bar{S}_{ij}$ of a row, making the use of this factor unnecessary in the computational process. Consequently, savings in computation are obtained.

3.4.2 Algorithm for recognition of group-reference generators

With all entries in $\bar{\underline{S}}$ being determined by equation (3.20), the procedure for selecting the group-reference generators is as follows.

i) The generator with the largest inertia is chosen as the system reference generator and labeled as machine n in the list of system generators. Since its speed is very close to the aggregate speed of the system, we automatically choose it as the group-reference generator associated with the zero eigenvalue.

ii) Search $\bar{\underline{S}}$ to select the sensitivity coefficient with the largest magnitude. This identifies the machine which produces the biggest effect on a slow eigenvalue of $\bar{\underline{A}}$, and since there are not two coherent areas having the same group-reference generator, the row and column are deleted from $\bar{\underline{S}}$. This identifies the second group-reference generator.

iii) The largest element in magnitude is again selected from the reduced $(r-2)\times(n-1)$ matrix $\bar{\underline{S}}$ and the procedure is repeated, until all group-reference generators have been identified.

The next section presents two numerical examples based on the 10-machine New England System and the 17-machine Modified Iowa System.

3.5 Numerical Examples

We now demonstrate the use of the sensitivity coefficients in the determination of the group reference and follower generators by numerical examples. For this purpose, two systems are used, the New England System and the Modified Iowa System. These were chosen because of their different degrees of complexity and the availability of information concerning their characteristics.

3.5.1 The New England system

A line diagram of the system is shown in Fig. 3.1. Likewise, the system matrix $\underline{\bar{A}}$, its spectrum, and the characteristic and reciprocal basis vectors associated with the slow eigenvalues for the operating point given in Appendix A are shown in Tables 3.1, 3.2 and 3.3, respectively.

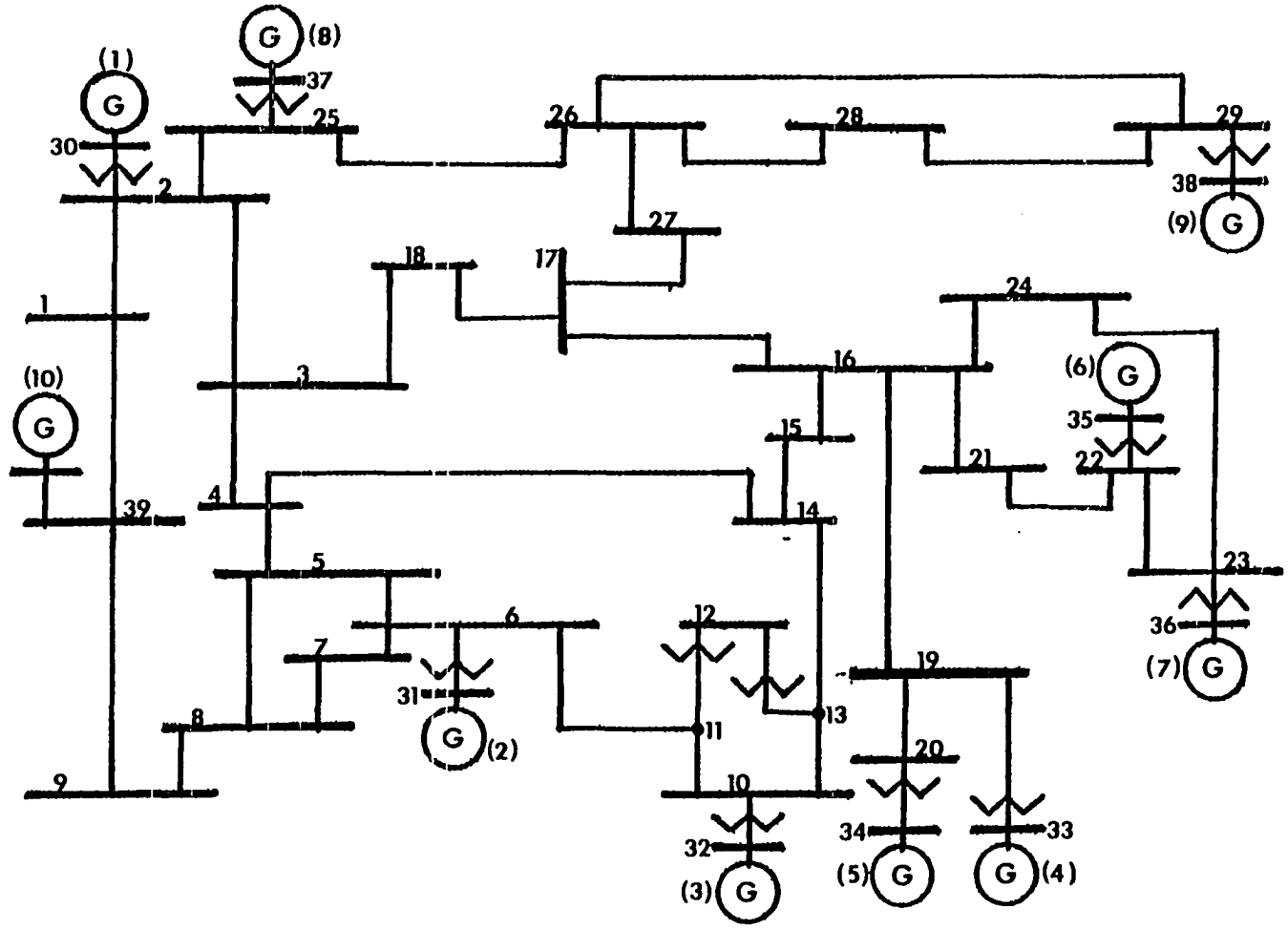

Fig. 3.1 The New England system line diagram

Table 3.1 New England System Matrix $\underline{\bar{A}}$

Unit	1	2	3	4	5	6	7	8	9	10
1	-71.3339	4.8721	6.0463	5.6478	1.9214	5.7338	4.6739	13.8418	7.8109	20.7858
2	4.8727	-49.5920	13.2190	4.0200	1.2561	4.1679	3.4143	3.2962	2.9787	12.3622
3	5.1745	11.1578	-49.0818	4.7717	1.5055	4.9363	4.0409	3.5060	3.2846	10.7046
4	6.0770	4.4417	6.2359	-69.0129	13.3959	12.6382	10.3291	4.5117	5.6781	5.7054
5	2.3613	1.7289	2.4274	15.4720	-37.7563	4.9210	4.1566	1.8424	2.2725	2.5742
6	4.8891	3.6246	5.0990	10.0789	3.2551	-63.3609	22.3401	3.8961	4.8189	5.3591
7	5.1752	3.8614	5.4357	10.7533	3.7239	29.4241	-73.6433	4.1596	5.1561	5.6506
8	22.4889	4.2117	5.3108	5.2630	1.8061	5.6985	4.6558	-77.6433	11.2526	16.9540
9	6.4318	2.0246	2.6908	3.5185	1.1605	4.0681	3.3388	6.8908	-34.8532	4.7293
10	1.9193	1.1038	1.1550	0.6004	0.2122	0.5983	0.4863	0.8429	0.5534	-7.4715

Table 3.2 Eigenvalues of $\underline{\bar{A}}$

Eigenvalue Number	Eigenvalue
1	0.0
2	-15.3388
3	-35.4377
4	-40.2564
5	-49.4722
6	-61.5391
7	-64.8203
8	-79.5347
9	-92.5014
10	-94.5193

Table 3.3 Characteristic and Reciprocal Basis Vectors Associated with the Slow Modes of $\bar{\underline{A}}$

	Gen.[a]	1	2	3	4	5	6	7	8	9	10
i) Characteristic Vectors of $\bar{\underline{A}}$	1	0.3162	0.3162	0.3162	0.3162	0.3162	0.3162	0.3162	0.3162	0.3162	0.3162
	2	-0.2883	-0.3669	-0.4083	-0.6139	-0.8072	-0.6004	-0.5945	-0.3327	-0.5914	0.4121
	3	0.0991	0.0619	0.0514	-0.2114	-0.7983	-0.0688	-0.0691	-0.1429	0.6025	-0.0143
	4	0.0417	0.5613	0.5168	-0.0487	-0.5101	0.1067	0.0989	0.0003	-0.4807	-0.0305
	5	-0.0368	0.3861	0.2876	-0.1159	0.4257	-0.5484	-0.5065	-0.0334	0.1904	-0.0050

	Gen.[a]	1	2	3	4	5	6	7	8	9	10
ii) Reciprocal Basis Vectors	1	0.0902	0.0860	0.1023	0.0802	0.0608	0.1005	0.0766	0.0604	0.1148	0.9644
	2	0.1147	0.1329	0.1744	0.1955	0.2202	0.2477	0.1864	0.1013	0.2989	-1.6719
	3	0.1268	0.0516	0.0514	-0.1811	-0.5983	-0.0646	-0.0482	0.1149	0.7698	-0.2223
	4	0.0241	0.5009	0.5454	-0.0353	-0.0326	-0.1071	0.0764	-0.0085	-0.5655	-0.2921
	5	-0.0301	0.3813	0.3360	-0.1075	0.3394	-0.6237	-0.4375	-0.0198	0.2306	-0.0688

[a]Gen. stands for generator.

[b]Eigen. stands for eigenvalue.

Generally, the slow or dominant eigenvalues are selected by judging how distant the eigenvalues of $\bar{\underline{A}}$ are located from the origin, so that the farther they are from the origin the more confident we are that those eigenvalues belong to the fast subsystem. Given that such selection is largely a matter of judgment, a compromise between the dynamical equivalent sought and the number of coherent areas into which the system will be partitioned must be established before any separation of eigenvalues is made. In cases where there is not a definite demarcation between the slow and fast subsystems, the slow modes should be selected with utmost care. Finally, because of the lack of specific guides for selection of the slow subsystem one must rely, in the worst of situations, on a knowledge of the composition and operation of the power system. In the case of this system, the slow eigenvalues selected from Table 3.2 are $\bar{\lambda}_1 = 0.0$, $\bar{\lambda}_2 = -15.3388$, $\bar{\lambda}_3 = -35.4377$, $\bar{\lambda}_4 = -40.2564$, and $\bar{\lambda}_5 = -49.4722$.

Once the slow set of eigenvalues has been selected, the computation of the sentivity matrix $\bar{\underline{S}}$ follows, with the results presented in Table 3.4.

By applying the procedure described to select the reference generators to be associated with the slow eigenvalues to the above matrix, the following results were obtained.

i) Machine 10 is first associated with the zero eigenvalue ($\bar{\lambda}_1$).

ii) Machine 5 is associated with the eigenvalue $\bar{\lambda}_3$.

iii) Machine 6 is associated with the eigenvalue $\bar{\lambda}_4$.

Table 3.4 Sensitivity Matrix $\underline{\underline{S}}$

Eigen.[b] \ Gen.[a]	1	2	3	4	5	6	7	8	9	10
2	0.00748	0.01529	0.01890	0.03989	0.06496	0.04061	0.03989	0.01318	0.04869	0.01309
3	0.01034	0.00365	0.00255	0.04629	0.63516	0.00441	0.00437	0.02338	0.46476	0.00022
4	0.00129	0.23762	0.13201	0.02131	0.27173	0.48058	0.41037	0.00133	0.06223	0.00003
5	0.00093	0.35837	0.30412	0.00232	0.26715	0.01269	0.01106	-0.00001	0.30433	0.00069

[a]Gen. stands for generators.

[b]Eigen. stands for eigenvalue.

iv) Machine 2 is associated with the eigenvalue $\bar{\lambda}_5$.

v) Machine 9 is associated with the eigenvalue $\bar{\lambda}_2$.

To show that the results obtained with the sensitivity based method are the same as those obtained with the Gaussian elimination, used in reference [5], we first determine the matrix $\underline{V}$ as

$$\underline{V} = \left[\begin{array}{c:c:c:c} & & & \\ \underline{x}_1 & \underline{x}_2 & \cdots & \underline{x}_5 \\ & & & \end{array}\right]$$

where $\underline{x}_1$ through $\underline{x}_5$ are the characteristic vectors associated with the slow eigenvalues. The Gaussian elimination previously described results in identifying machines 5, 9, 2, 6 and 10 in that order. Although the order of appearance is different from that one obtained with the sensitivity based approach, the final result is the same for both methods.

The $\underline{L}d$ matrix is computed using $\underline{L}d = \underline{V}_2\underline{V}_1^{-1}$ with the following result.

	Group-Ref.	2	6	5	9	10
$\underline{L}d =$ Followers	1	0.219564	<u>0.302267</u>	0.01577	0.203388	0.259011
	3	<u>0.902074</u>	0.112172	-0.000325	0.004519	-0.01844
	4	0.117306	<u>0.529413</u>	0.275376	0.06266	0.01524
	7	0.018315	<u>0.951513</u>	0.014469	0.011274	0.004428
	8	0.200534	<u>0.301482</u>	0.010228	0.269769	0.217787

By setting the largest positive entry in each row of $\underline{L}d$ to 1 and the remainder to zero, the grouping matrix $\underline{L}g$ is constructed.

$$\underline{L}g = \begin{array}{c} \\ 1 \\ 3 \\ 4 \\ 7 \\ 8 \end{array} \begin{array}{c} \begin{array}{ccccc} 2 & 6 & 5 & 9 & 10 \end{array} \\ \begin{bmatrix} 0 & 1 & 0 & 0 & 0 \\ 1 & 0 & 0 & 0 & 0 \\ 0 & 1 & 0 & 0 & 0 \\ 0 & 1 & 0 & 0 & 0 \\ 0 & 1 & 0 & 0 & 0 \end{bmatrix} \end{array}$$

The coherent groups obtained from the above matrix are:

Group 1: 2,3

Group 2: 6,1,4,7,8

Group 3: 5

Group 4: 9

Group 5: 10

These results agree with those obtained in reference [38] by using a clustering algorithm in conjunction with swing curves obtained from a set of linearized swing equations. Similar results were also obtained when the Philadelphia Electric Company stability program was used. With regard to these results, it is significant that the coherent group (1,8,4,6,7) did not show a strong coupling among generators. In fact, when 3ϕ-faults (with no line switching) were applied at some of the system buses, generators 1 and 8 formed a coherent group with generators 4, 6 and 7 forming in some cases the group (4,6,7) and in others the groups (4) and (6,7).

3.5.2 The Modified Iowa system (MIS)

The second numerical example uses the Modified Iowa System that is composed of 17 generators, 163 buses and 304 lines. For the sake of brevity, the information presented here consists only of tables showing the system matrix $\underline{\bar{A}}$ in Table 3.5, its eigenvalues in Table 3.6, its characteristic and reciprocal basis vectors in Table 3.7, and the sensitivity matrix in Table 3.8. The Modified Iowa System is shown in Fig. 3.2. In Tables 3.5 and 3.7, each row contains 17 entries and should be read across both pages, returning to the left for the second line giving the additional six entries.

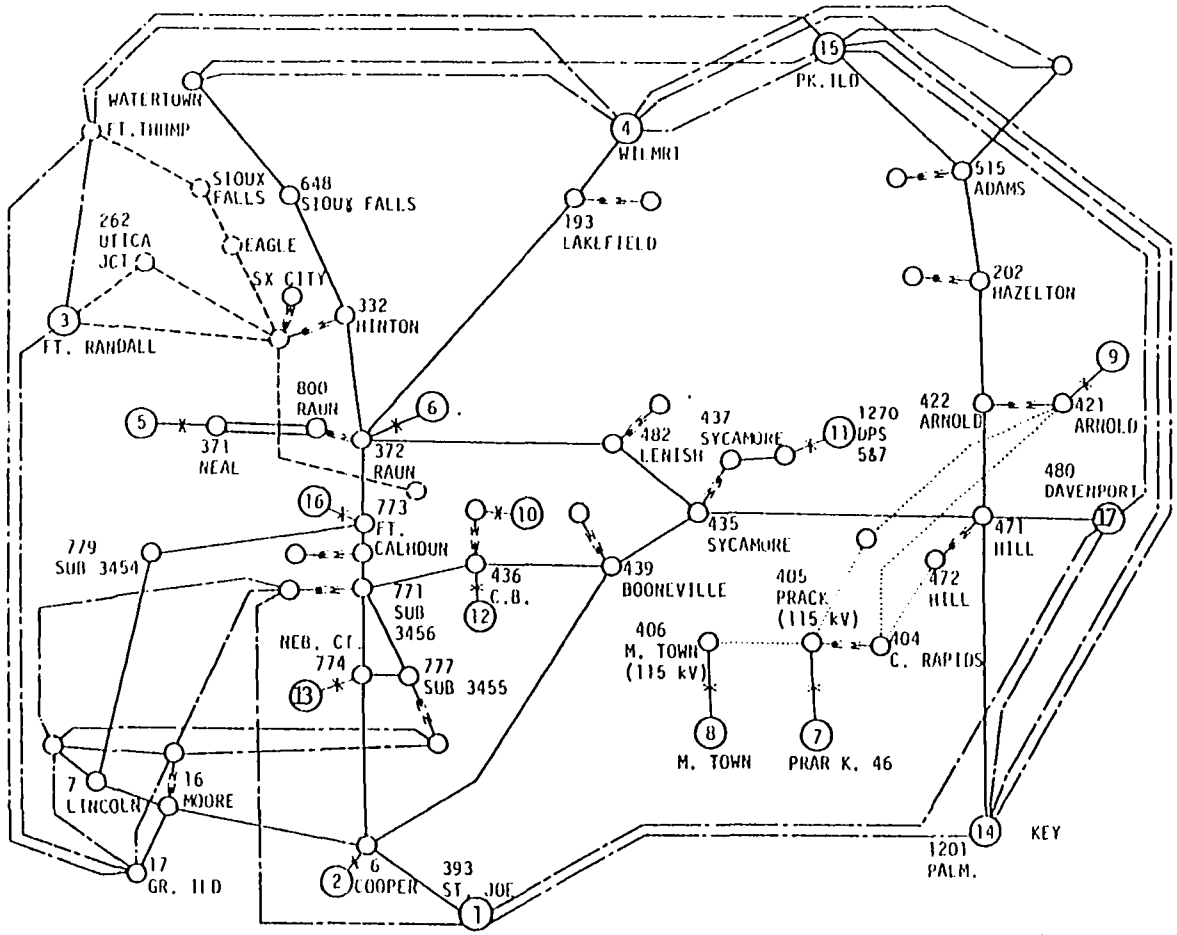

Fig. 3.2 The Modified Iowa Power System Map

0.1985	0.1927	0.5408	1.0980	1.2588
0.1630	0.1357	0.5647	1.5859	1.3046
0.1166	0.1401	0.3555	0.4169	0.5152
0.3386	0.2288	1.2542	0.2969	0.5624
0.4097	0.5536	1.1849	1.4102	1.8582
0.4670	0.5043	1.5106	2.0169	2.5508
-125.3585	4.9542	30.4018	0.3513	1.9481
12.8429	-140.4331	16.1066	1.0171	6.7598
6.2360	1.2184	-64.1355	1.3076	0.9449
0.3684	0.3690	7.7125	-142.7039	3.0551
1.1684	1.5133	3.0052	1.6465	-88.3391
0.4517	0.4180	1.4695	7.7477	3.5940
0.2416	0.2116	0.8176	3.2881	1.9139
0.4803	0.1789	1.4332	0.1265	0.4949
0.7528	0.2978	3.0890	0.1781	0.4464
0.1642	0.1590	0.5436	2.1628	1.1667
1.5332	0.4028	4.1168	0.1697	0.8248

Table 3.6 Eigenvalues of $\bar{\underline{A}}$

Eigenvalue Number	Eigenvalue
1	0.0
2	-23.9431
3	-36.8363
4	-47.5154
5	-51.1631
6	-66.2822
7	-71.0928
8	-86.9622
9	-88.7942
10	-99.6181
11	-117.4137
12	-125.9464
13	-140.4208
14	-144.0751
15	-151.1898
16	-160.8264
17	-164.4341

0.2425	0.2425	0.2425	0.2425	0.2425
0.1796	0.0359	0.1802	-0.1781	-0.0738
0.1572	0.0495	0.2185	-0.2732	-0.1629
0.0906	0.0871	0.1664	0.1648	0.1296
-0.3875	-0.2359	-0.5665	-0.1710	-0.1918
-0.4753	-0.2494	-1.2236	-0.0867	-0.0417
0.0132	-0.0444	0.0441	-0.1572	-0.1522
-0.0193	-0.0071	-0.0945	-0.0167	-0.0316
0.0116	0.0014	-0.0094	0.0538	-0.0059
-0.0161	-0.0025	-0.1060	0.0220	0.0240
-0.0072	-0.0024	-0.0659	-0.0104	-0.0150
-0.0206	-0.0045	-0.1473	-0.0071	-0.0151
0.0646	0.0125	0.8170	0.0102	0.0070
0.0011	-0.0010	0.0098	-0.0153	-0.0193

Table 3.8 Sensitivity Matrix $\underline{\underline{S}}$

Eigenvalues	Generators 1	2	3	4	5	6	7	8	9
2	0.0001	0.0112	0.0741	0.0223	0.0249	0.0195	0.0078	0.0005	0.0081
3	0.0895	0.1402	0.0032	0.0640	0.0077	0.0119	0.0161	0.0020	0.0330
4	0.0092	0.0335	0.3761	0.0543	0.0019	0.0096	0.0046	0.0037	0.0174
5	0.0020	0.0120	0.0049	0.0293	0.0045	0.0039	0.0725	0.0241	0.1704
6	0.0000	0.0005	0.0013	0.0053	0.0004	0.0006	0.2360	0.0599	1.7265
7	0.2429	0.0454	0.0049	0.0020	0.1165	0.0836	0.0001	0.0011	0.0009

Eigenvalues	Generators 10	11	12	13	14	15	16	17
2	0.0083	0.0010	0.0097	0.0109	0.0321	0.0173	0.0215	0.0262
3	0.0508	0.0146	0.0557	0.0935	0.0010	0.0742	0.0945	0.0114
4	0.0161	0.0081	0.0135	0.0214	0.0152	0.0502	0.0360	0.0007
5	0.0147	0.0155	0.0082	0.0098	0.1025	0.0266	0.0286	0.0871
6	0.0090	0.0013	0.0001	0.0003	0.0052	0.0029	0.0039	0.0568
7	0.0303	0.0164	0.0276	0.0011	0.0137	0.0053	1.2451	0.0010

The slow eigenvalues of $\bar{\underline{A}}$ chosen from Table 3.6 are $\bar{\lambda}_1 = 0.0$, $\bar{\lambda}_2 = -23.9431$, $\bar{\lambda}_3 = -36.8263$, $\bar{\lambda}_4 = -47.5154$, $\bar{\lambda}_5 = -51.1631$, $\bar{\lambda}_6 = -66.2822$, and $\bar{\lambda}_7 = -71.0928$. Following the procedure outlined in section 3.4.2, the group-reference generators were assigned as follows.

i) Machine 17 is first associated with $\bar{\lambda}_1$.

ii) Machine 9 is associated with $\bar{\lambda}_6$.

iii) Machine 16 is associated with $\bar{\lambda}_7$.

iv) Machine 3 is associated with $\bar{\lambda}_4$.

v) Machine 2 is associated with $\bar{\lambda}_3$.

vi) Machine 14 is associated with $\bar{\lambda}_5$.

The assignment of the eigenvalue $\bar{\lambda}_2$ is not obvious because the magnitudes of the coefficients $\bar{S}_{24} = 0.0224$ and $\bar{S}_{25} = 0.0249$ are almost identical. This means that the effect produced by these generators on $\bar{\lambda}_2$ is not as significant as to conclude which of these two machines can be selected as reference. Thus, in order to identify the last group-reference generator, two $\underline{L}d$ matrices, one having generator 4 as a column, and one having generator 5 as a column were computed. The $\underline{L}d$ matrix with the smallest norm was selected, identifying the last group-reference as 4. Hence, the group-reference generators are 9, 16, 3, 2, 14, 4 and 17.

As a check, the Gaussian elimination step in reference [5] was executed with the above. The $\underline{L}d$ matrix for such reference generator is

$\underline{Ld}$ =

	2	3	4	9	14	16
1	1.04238	-0.01124	-0.00686	-0.01022	0.28683	-0.27796
5	0.15861	0.18902	0.24782	0.01811	-0.00734	0.36722
6	0.24141	0.11579	0.25917	0.01822	0.00258	0.32958
7	0.02415	0.00577	0.08494	0.46207	0.03846	0.02322
8	0.12915	0.04455	0.14983	0.26353	0.06528	0.09435
10	-0.15658	0.08534	0.58386	0.17127	-0.15018	0.19015
11	0.33164	0.03267	0.07553	0.0883	0.05403	0.23441
12	0.50603	0.05661	0.07039	0.02075	0.04973	0.26150
13	0.70998	0.03152	0.03008	0.0099	0.03387	0.1737
15	-0.01772	-0.00355	0.98440	0.0182	0.01387	-0.03775

The above matrix gives rise to the following grouping matrix.

$\underline{Lg}$ =

	2	3	4	9	14	16	17
1	1	0	0	0	0	0	0
5	0	0	0	0	0	1	0
6	0	0	0	0	0	1	0
7	0	0	0	1	0	0	0
8	0	0	0	1	0	0	0
10	0	0	1	0	0	0	0
11	1	0	0	0	0	0	0
12	1	0	0	0	0	0	0
13	1	0	0	0	0	0	0
15	0	0	1	0	0	0	0

The coherent groups are

Group 1: 2,1,11,12,13

Group 2: 3

Group 3: 4,10,15

Group 4: 9,7,8

Group 5: 14

Group 6: 16,5,6

Group 7: 17

Comparison of these groups with the map of the Modified Iowa System shown in Fig. 3.2 exhibits some geographical correlation with the grouping. Alsok the grouping obtained here is supported by swing curves obtained with the Philadelphia Electric Company stability program when faults are placed at buses with a fault capacity rather small as compared with the total system generation. The groups determined with the stability program do differ. Inspection of Fig. 3.2 shows that machines 10 and 12 are close together, both geographically and electrically, and might reasonably be expected to appear in the same group, precisely the result given by the stability program. While the sensitivity based method of selecting group-reference machines reported here yields results consistent with this, the application of the method of [5] to assign follower machines places machines 10 and 12 in different groups. The reason for this inconsistency are not immediately apparent and a need for further investigation and experience is indicated. As with all approximate methods, a cautionary attitude in the general application of the method is in order until understanding and confidence are gained.

4. DIRECT METHOD OF COHERENCY IDENTIFICATION

4.1 Introduction

The sensitivity based slow coherency method discussed in the previous chapter has a limitation in that it does not take the fault location into consideration. It is intuitively clear that the fault location has a major effect on the accelerating powers experienced by the various machines during the fault and thus on the coherency of machines. Hence, there is a need for a direct method of identification of coherent groups for different fault locations. Such a method should result in a measure or index which is readily computed and interpreted. To accomplish this, we need a mathematical model to represent the system under both faulted and unfaulted conditions. To this end, we consider three conditions, or time intervals, as follows:

i) The prefault condition for $t < 0$.
ii) The faulted condition for $0 \leq t \leq t_{cl}$.
iii) The post-fault condition for $t_{cl} \leq t < \infty$.

While our ultimate interest is in the post-fault condition, the others are required to provide initial values of variables. These initial values will reflect the effects of the fault location.

The system is in equilibrium in the prefault state. This establishes a set of machine voltages and angles (back of transient reactance), electrical power outputs and mechanical power inputs equal to the electrical power inputs. This operating point can be used to write the linearized state equations

$$\dot{\underline{x}} = \underline{A}_1 \underline{x} \tag{4.1}$$

These equations differ from those in Chapter 2 in that the n^{th} equation (n corresponding to the machine with the largest inertia) is subtracted from the first (n-1) equations in each of the two sets of n equations. Thus, the rotor angles and speeds are referred to those of the n^{th} or reference machine resulting in 2(n-1) equations. It is noted that the matrix $\underline{A}_1$ incorporates the admittance matrix of the unfaulted network.

When a fault occurs at t=0, the result is a change in the electrical network and consequently in the admittance matrix. This results in a condition at $t=0^+$ in which the machine voltages and angles are the same as in the prefault condition but the electrical power outputs are different as a result of the change in the electrical network. Consequently, each machine experiences an accelerating power equal to the difference in the mechanical power input and the new electrical power output. This accelerating power is considered to be constant throughout the faulted period as is indicated conceptually in Fig. 4.1. Several possibilities for modelling the system during the faulted period are as follows:

i) Use the voltages, angles and electrical power outputs at $t=0^+$ together with the admittance matrix of the faulted network to write the equations

$$\dot{\underline{x}} = \underline{A}_1\underline{x} + \underline{B}\underline{u};\ \underline{x}(0) = \underline{0} \qquad (0 \leq t \leq t_{cl}) \tag{4.2}$$

where $\underline{u}$ is an input vector consisting of the accelerating powers. This approach incorporates the electrical characteristics of the faulted network and will require a new matrix $\underline{A}_1$ for each fault location.

ii) Consider each machine to experience a constant acceleration, as determined by its accelerating power and inertia, throughout the faulted period. This approach neglects the machine

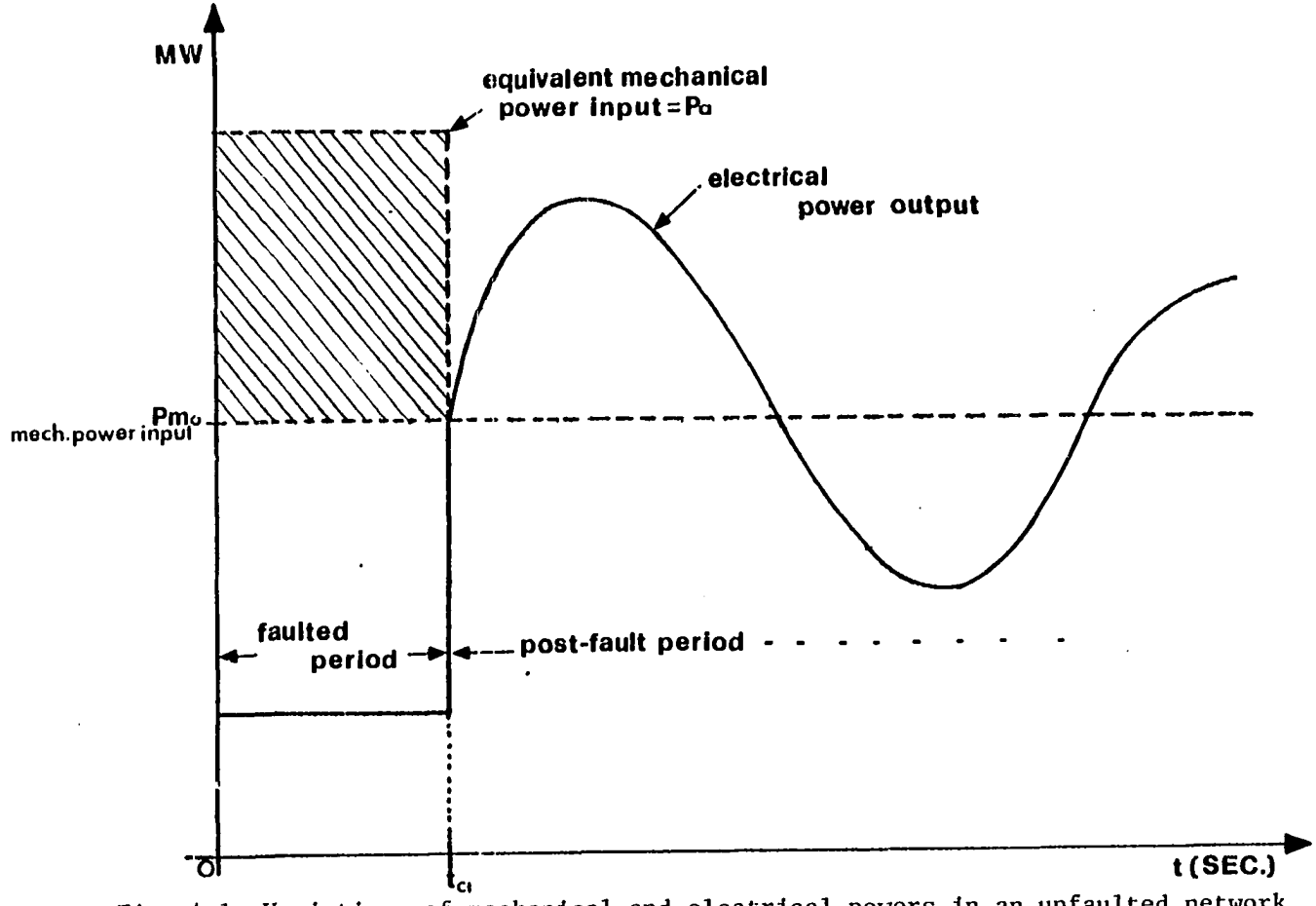

Fig. 4.1 Variations of mechanical and electrical powers in an unfaulted network to reproduce same accelerating power as in a faulted network

interactions as influenced by the electrical network but results in a very simple method of determining machine velocities and angles at $t = t_{cl}$.

iii) Use the matrix $\underline{A}_1$ as determined for the prefault condition in equation (4.2). This approach does in some sense incorporate the machine interactions.

The models described in (i) and (ii) above have the advantages of accuracy and simplicity respectively; however, they have the stated shortcomings. The model in (iii) was chosen as a suitable compromise between accuracy and simplicity. Equation (4.2) can then be used to determine the state $\underline{x}_p = \underline{x}(t_{cl})$, the initial conditions for the post-fault period.

In the post-fault period, the prefault network is restored since only three phase faults with no line switching are considered and, if a stable system is assumed, the equilibrium condition is the same as for the prefault period. Thus, the post-fault system can be described by

$$\dot{\underline{x}} = \underline{A}_1\underline{x};\ \underline{x}_p = \underline{x}(t_{cl}) \qquad (t \geq t_{cl}) \tag{4.3}$$

The matrix $\underline{A}_1$ is again that for the prefault condition as in equation (4.1) and thus only one matrix $\underline{A}_1$ is required throughout.

With the modelling of the power system established, the next step is to define a coherency index which will enable us to identify coherent groups in the system. A coherency index based on the root-mean-square value of the angular rotor excursion $\Delta\delta_{in}$ is proposed. It is possible to find the closed form solution to equations (4.2) and (4.3) as

$$\underline{x}(t) = \int_o^t e^{[\underline{A}_1](t-\tau)}\,\underline{\underline{B}}\underline{u}(\tau)d\tau \qquad (0 \leq t \leq t_{cl}) \tag{4.4}$$

and

$$\underline{x}(t) = e^{[\underline{A}_1](t-t_{c1})}\underline{x}(t_{c1}) \qquad (t \geq t_{c1}) \tag{4.5}$$

where the matrix $e^{[\underline{A}_1](t-t_{c1})}$ can be computed by making use of the characteristic and reciprocal basis vectors of $\underline{A}_1$ [15]. One can express equation (4.5) as

$$\underline{x}(t) = \underline{\underline{T}}\underline{\Omega}(t) \tag{4.6}$$

In the above equation, the 2(n-1)-dimensional vector $\underline{\Omega}(t)$ consists of terms of the kind $\cos\omega_i t$ and $\sin\omega_i t$ (i=1,2,...,n-1) in which the ω_i's, when rounded, can be expressed as integer multiples of a fundamental frequency ω_f. Thus, $\underline{x}(t)$ is periodic, permitting a coherency index based on maximum or root-mean-square values of the rotor angles.

Once the coherency indices have been computed, the next task is the determination of coherent groups for a particular fault location. To accomplish this task, a commutative recognition rule proposed in reference [45] is used. Two numerical examples are presented at the end of the chapter to validate the proposed method.

These matters will be considered in detail in the following sections. The result is a root-mean-square coherency measure, similar to that recently proposed in the literature [45], but arrived at in a completely different fashion.

4.2 Development of Coherency Indices

4.2.1 The linearized power system model

In the absence of damping, the 2(n-1) state-space equations, as derived from the 2n equations in Chapter 2, become

$$\frac{d}{dt}(\Delta\delta_{in}) = \Delta\omega_{in} \qquad (i=1,2,3,\ldots n-1) \tag{4.7}$$

$$\frac{d}{dt}(\Delta\omega_{in}) = [\frac{\omega_R}{2H_i}\Delta P_{m_i} - \frac{\omega_R}{2H_n}\Delta P_{m_n}] - [\frac{\omega_R}{2H_i}\Delta P_{e_i} - \frac{\omega_R}{2H_n}\Delta P_{e_n}]$$

$$(i=1,2,\ldots,n-1) \tag{4.8}$$

If we define

$$f_i = {}_R[\frac{1}{2H_i}\Delta P_{e_i} - \frac{1}{2H_n}\Delta P_{e_n}] \quad (i=1,2,\ldots,n-1)$$

then equation (4.2) can be rewritten as

$$\frac{d}{dt}(\Delta\omega_{in}) = \sum_{k=1}^{n-1} \frac{\partial f_i}{\partial \delta_{kn}}\Big|_{\underline{x}(0)} \Delta\delta_{kn} + \omega_R[\frac{1}{2H_i}\Delta P_{m_i} - \frac{1}{2H_n}\Delta P_{m_n}]$$

$$(i=1,2,\ldots,n-1) \tag{4.9}$$

where

$$\Delta\delta_{in} = \Delta\delta_i - \Delta\delta_n$$
$$\Delta\omega_{in} = \Delta\omega_i - \Delta\omega_n \qquad (i=1,2,\ldots,n-1)$$

The partial derivatives in equation (4.9) are, for $i \neq k$,

$$\frac{\partial f_i}{\partial \delta_{kn}} = -\frac{\omega_R}{2H_i}[|E_i||E_k||Y_{ik}|\sin(\theta_{ik}-\delta^o_{ik})$$

$$+ \frac{\omega_R}{2H_n}[|E_n||E_k||Y_{nk}|\sin(\theta_{nj}+\delta^o_{kn})] \tag{4.10}$$

and, for i=k,

$$\frac{\partial f_i}{\partial \delta_{kn}} = \frac{\omega_R}{2H_i}\left[\sum_{k=1}^{n} |E_i||E_k||Y_{ik}|\sin(\theta_{ik}-\delta_{ik}^{o})\right]$$

$$+ \frac{\omega_R}{2H_n}\left[|E_n||E_i||Y_{ni}|\sin(\theta_{ni}+\delta_{nj}^{o})\right]$$

$$= \frac{\omega_R}{2H_i}\left[B_{ii}|E_i|^2 + Q_{ei}^{o}\right] + \frac{\omega_R}{2H_n}\left[|E_n||E_i||Y_{ni}|\sin(\theta_{ni}+\delta_{in}^{o})\right]$$

$$(i=1,2,\ldots,n-1) \qquad (4.11)$$

where the "o" superscript represents the prefault state. Equations (4.2) and (4.3) can be combined as

$$\dot{\underline{x}} = \underline{A}_1\underline{x} + \underline{B}\underline{u} \qquad (4.12)$$

or, in more detail, as

$$\begin{bmatrix} \Delta\dot{\delta}_{in} \\ \vdots \\ \Delta\dot{\delta}_{n-1,n} \\ \hline \Delta\dot{\omega}_{1n} \\ \vdots \\ \Delta\dot{\omega}_{n-1,n} \end{bmatrix} \begin{matrix} \\ \\ (n-1) \\ \\ = \\ \\ (n-1) \\ \\ \end{matrix} \begin{bmatrix} & \overset{(n-1)}{} & \overset{(n-1)}{} \\ & & \\ & \underline{0} & \underline{I} \\ & & \\ \hline & & \\ & \bar{\underline{A}}_1 & \underline{0} \\ & & \end{bmatrix} \begin{bmatrix} \Delta\delta_{in} \\ \vdots \\ \Delta\delta_{n-1,n} \\ \hline \Delta\omega_{in} \\ \vdots \\ \Delta\omega_{n-1,n} \end{bmatrix} + \begin{bmatrix} & \overset{(n)}{} & \\ & & \\ & \underline{0} & \\ & & \\ \hline p_1' & 0 \ \ldots \ 0 & -p_n' \\ 0 & p_2' \ \ldots \ 0 & -p_n' \\ \vdots & \vdots \quad \vdots & \vdots \\ 0 & 0 \ \ldots \ p_{n-1}' & -p_n' \end{bmatrix} \begin{bmatrix} \Delta P_{m1} \\ \Delta P_{m2} \\ \vdots \\ \Delta P_{mn} \end{bmatrix}$$

(4.13)

In the above equation, the square matrix $\bar{\underline{A}}_1$ and the p_i''s of the $\underline{B}$ matrix are given by

$$\bar{\underline{A}}_1 = \left[\begin{array}{ccc} \frac{\partial f_1}{\partial \delta_{in}} & \cdots & \frac{\partial f_1}{\partial \delta_{n-1,n}} \\ \vdots & & \vdots \\ \frac{\partial f_{n-1}}{\partial \delta_{in}} & \cdots & \frac{\partial f_{n-1}}{\partial \delta_{n-1,n}} \end{array} \right] \Bigg|_{\underline{x}(0)} \tag{4.14}$$

and

$$p_i' = \frac{\omega_R}{2H_i} \qquad (i=1,2,\ldots,n) \tag{4.15}$$

4.2.2 Computation of accelerating powers

The electrical power output at t=0 (i.e., immediately before the disturbance takes place) is given by

$$P_{e_i}(0^-) = |E_i|^2 G_{ii} + \sum_{\substack{j=1 \\ i \neq j}}^{n} |E_i||E_j||Y_{ij}|\cos(\theta_{ij} - \delta_{ij}(0^-)) \tag{4.16}$$

where $|Y_{ij}|\angle\theta_{ij}$ is the (i,j) element of the prefault admittance matrix. Because the rotor angles cannot change in zero time

$$\delta_{ij}(0^+) = \delta_{ij}(0^-) = \delta_{ij}^o \quad \text{for every i and j.}$$

Moreover, the internal voltage $|E_i|$ and the mechanical input powers P_{m_i} (i=1,2,...,n) are assumed to be constant over the period $0 \leq t \leq t_{cl}$ because of the use of the classical model for synchronous machines. This leads to an accelerating power P_{acc_i} for $0 \leq t \leq t_{cl}$ given by

$$P_{acc_i} = P_{e_i}(0^-) - P_{e_i}(0^+) \qquad (i=1,2,\ldots,n) \tag{4.17}$$

where $P_{e_i}(0^+)$ is given by

$$P_{e_i}(0^+) = G_{ii}|E_i|^2 + \sum_{\substack{j=1 \\ i\neq j}}^{n} |E_i||E_j||Y_{ij}|\cos(\theta_{ij}-\delta_{ij}^o) \qquad (i=1,2,\ldots,n) \tag{4.18}$$

In equation (4.18), $|Y_{ij}|\underline{/\theta_{ij}}$ is the (i,j) element of the admittance matrix during the faulted period. After some algebraic manipulations, equation (4.17) becomes

$$P_{acc_i} = \Delta G_{ii}|E_i|^2 + \sum_{\substack{j=1 \\ i\neq j}}^{n} |E_i||E_j|(\Delta G_{ij}\cos\delta_{ij}^o + \Delta B_{ij}\sin\delta_{ij}^o) \tag{4.19}$$

where

$$\Delta G_{ii} = G_{ii}^o - G_{ii}^F$$

$$\Delta G_{ij} = G_{ij}^o - G_{ij}^F$$

$$\Delta B_{ij} = B_{ij}^o - B_{ij}^F$$

The superscripts "o" and "F" denote the prefault and faulted states respectively.

4.2.3 Modal response in linear systems

The modal response of linear systems as applied to the set of equations (4.2) and (4.3) is based on an earlier work by Desoer [15]. As described in [8], the closed form solution for the faulted period is given by

$$\underline{x}(t) = e^{[\underline{A}_1]t}\,\underline{x}(0) + \int_o^t e^{[\underline{A}_1](t-\tau)}\,\underline{\underline{B}}\underline{u}(\tau)d\tau \qquad (0 \leq t \leq t_{c1}) \tag{4.20}$$

which becomes

$$\underline{x}(t) = \int_o^t e^{[\underline{A}_1](t-\tau)}\,\underline{\underline{B}}\underline{u}(\tau)d\tau \tag{4.21}$$

because $\underline{x}(0) = \underline{0}$.

The closed form solution for the post-fault period is

$$\underline{x}(t) = e^{[\underline{A}_1](t-t_{c1})}\,\underline{x}(t_{c1}) \qquad (t \geq t_{c1}) \tag{4.22}$$

Assuming a new time reference for the interval $[t_{c1},\infty)$, such that $t' = t - t_{c1}$, equation (4.22) becomes

$$\underline{x}(t') = e^{[\underline{A}_1]t'}\,\underline{x}(0) \qquad (t' \geq 0) \tag{4.23}$$

where $\underline{x}(0) = \underline{x}(t_{c1})$ and $e^{[\underline{A}_1]t'} = \underline{I}_{n-1}$ at $t' = 0$.

The modal representation of equations (4.21) and (4.23) as suggested by [15] are

$$\underline{x}(t) = \sum_{i=1}^{2n-2} \left[\int_o^t < \underline{q}_i, \underline{\underline{B}}\underline{u}(\tau) > e^{\lambda_i(t-\tau)}\,d\tau\right]\underline{p}_i \qquad (0 \leq t \leq t_{c1}) \tag{4.24}$$

$$\underline{x}(t') = \sum_{i=1}^{2n-2} < \underline{q}_i, \underline{x}(0) > e^{\lambda_i t'}\,\underline{p}_i \qquad (t' \geq 0) \tag{4.25}$$

where $\lambda_i, \underline{p}_i$ and $\underline{q}_i$ are the i^{th} eigenvalue, eigenvector and reciprocal basis vector of $\underline{A}_1$ respectively, such that

$$\underline{A}_1 \underline{p}_i = \lambda_i \underline{p}_i \qquad (i=1,2,\ldots,n-1)$$

$$\underline{A}_1 \underline{q}_i = \lambda_i^* \underline{q}_i \qquad (i=1,2,\ldots,n-1)$$

and with the additional requirements on $\underline{p}_i$ and $\underline{q}_i$ that

$$\begin{aligned} &\langle \underline{p}_i, \underline{p}_i \rangle = 1.0 \qquad (i=1,2,\ldots,n-1) \\ &\langle \underline{p}_i, \underline{q}_j \rangle = \delta_{ij} \end{aligned} \tag{4.26}$$

where $\delta_{ij} = 0$ if $i \neq j$ and $\delta_{ij} = 1$ if $i=j$.

Since the eigenvalues of $\underline{\bar{A}}_1$ are all distinct nonpositive real numbers, the eigenvalues of $\underline{A}_1$ are all imaginary. Thus, the eigenvectors ($\underline{p}_i$'s) and reciprocal basis vectors ($\underline{q}_i$'s) are complex and those vectors can be written as[1]

$$\underline{p}_i = \underline{p}_i' + j\underline{p}_i'' \qquad (i=1,2,\ldots,2(n-1)) \tag{4.27}$$

and

$$2\underline{q}_i = \underline{q}_i' + j\underline{q}_i'' \qquad (i=1,2,\ldots,2(n-1)) \tag{4.28}$$

In the above equations, the real and imaginary components of $\underline{p}_i$ and $\underline{q}_i$ satisfy

$$\langle \underline{q}_i', \underline{p}_i' \rangle = 1.0 \quad \text{and} \quad \langle \underline{q}_i', \underline{p}_i'' \rangle = 0 \tag{4.29}$$

$$\langle \underline{q}_i'', \underline{p}_i'' \rangle = 1.0 \quad \text{and} \quad \langle \underline{q}_i'', \underline{p}_i' \rangle = 0 \qquad (i=1,2,\ldots,n-1) \tag{4.30}$$

---

[1] Refer to Chapter 2, Section 2.4. The only difference is that the minus sign shown in equation (2.31) has been absorbed by the vector $\underline{q}_i''$ in equation (4.28).

The closed form solutions for equations (4.24) and (4.25), in that order, are now developed. In equation (4.24) the vectors $\underline{q}_i$ and $\underline{\underline{B}}\underline{u}$ are time invariant. This permits us to write

$$x(t) = \sum_{i=1}^{2n-2} [\int_o^t e^{\lambda_i(t-\tau)} d\tau] <\underline{q}_i, \underline{\underline{B}}\underline{u}> \underline{p}_i \qquad (0 \leq t \leq t_{cl}) \tag{4.31}$$

Let us assume now that we have ordered the eigenvalues λ_i of $\underline{\underline{A}}_1$ such that $\lambda_i = \lambda^*_{n-1+i}$ $(i=1,2,\ldots,n-1)$. Thus, by analyzing the response due to the eigenvalues λ_1 and λ_n one can infer the complete solution for $\underline{x}(t)$ in (4.31) due to the 2(n-1) eigenvalues. The contribution of these two eigenvalues to the total modal response is

$$[\int_o^t e^{\lambda_1(t-\tau)} d\tau] <\underline{q}_1, \underline{\underline{B}}\underline{u}> \underline{p}_1 + [\int_o^t e^{\lambda_n(t-\tau)} d\tau] <\underline{q}_n, \underline{\underline{B}}\underline{u}> \underline{p}_n \tag{4.32}$$

which can be rewritten as

$$2R_e[(\int_o^t e^{\lambda_1(t-\tau)} d\tau) <\underline{q}_1, \underline{\underline{B}}\underline{u}> \underline{p}_1] \tag{4.33}$$

because $\lambda_1 = j\omega_1$ and $\lambda_n = -j\omega_1$. Further simplification of equation (4.33) leads to

$$(1/\omega_1)\sin\omega_1 t[<\underline{q}_1', \underline{\underline{B}}\underline{u}> \underline{p}_1' + <\underline{q}_1'', \underline{\underline{B}}\underline{u}> \underline{p}_1''] +$$

$$(1/\omega_1)(1-\cos\omega_1 t)[<\underline{q}_1'', \underline{\underline{B}}\underline{u}> \underline{p}_1' - <\underline{q}_1', \underline{\underline{B}}\underline{u}> \underline{p}_1''] \tag{4.34}$$

Application of the above procedure to the (n-1) pairs of eigenvalues permits us to write equation (4.31) in a more compact form as

$$\underline{x}(t) = \sum_{i=1}^{n-1} (\gamma_i'\underline{p}_i' - \gamma_i\underline{p}_i'')\left(\frac{1-\cos\omega_i t}{\omega_i}\right)$$

$$+ \sum_{i=1}^{n-1} (\gamma_i'\underline{p}_i' + \gamma_i''\underline{p}_i'')\frac{\sin\omega_i t}{\omega_i} \qquad (0 \leq t \leq t_{cl}) \tag{4.35}$$

where

$$\gamma_i' = \langle \underline{q}_i', \underline{Bu} \rangle \quad \text{and} \quad \gamma_i = \langle \underline{q}_i'', \underline{Bu} \rangle$$

Writing equation (4.35) in matrix form, we obtain

$$\underline{x}(t) = \underline{\Gamma}\underline{\omega}(t) \qquad (0 \leq t \leq t_{cl}) \tag{4.36}$$

The matrix $\underline{\Gamma}$ is

$$\underline{\Gamma} = [\underline{\Gamma}_1' \,|\, \underline{\Gamma}_1'' \,|\, \ldots \,|\, \underline{\Gamma}_i' \,|\, \underline{\Gamma}_i'' \,|\, \ldots \,|\, \Gamma_{n-1}' \,|\, \Gamma_{n-1}''] \tag{4.37}$$

where the column vectors $\underline{\Gamma}_i'$ and $\underline{\Gamma}_i''$ are given by

$$\Gamma_i' = (1/\omega_i)(\gamma_i'\underline{p}_i' - \gamma_i\underline{p}_i'') \qquad (i=1,2,\ldots,n-1)$$

and (4.38)

$$\Gamma_i'' = (1/\omega_i)(\gamma_i'\underline{p}_i' + \gamma_i''\underline{p}_i'') \qquad (i=1,2,\ldots,n-1)$$

In addition, the vector $\underline{\omega}(t)$ is defined as

$$\underline{\omega}(t) = [(1-\cos\omega_1 t) \,|\, \sin\omega_1 t \,|\, \ldots \,|\, (1-\cos\omega_{n-1} t) \,|\, \sin\omega_{n-1} t]^T \tag{4.39}$$

The principal use of equation (4.36) is for the determination of the initial conditions of the postfault state, i.e., $\underline{x}(t_{cl})$.

Following a similar procedure, the post-fault solution is expanded in terms of the eigenvectors $\underline{p}_i$ and the reciprocal basis vectors $\underline{q}_i$ and the initial condition $\underline{x}(0) = \underline{x}(t_{cl})$ to yield

$$x(t') = \sum_{i=1}^{n-1} [\ell_i' \cos\omega_i t' + \ell_i'' \cos\omega_i t'] \underline{p}_i'$$

$$+ \sum_{i=1}^{n-1} [\ell_i'' \cos\omega_i t' - \ell_i' \sin\omega_i t'] \underline{p}_i'' \qquad (t' \geq 0) \tag{4.40}$$

where the scalars ℓ_i' and ℓ_i'' are

$$\ell_i' = \langle \underline{q}_i', \underline{x}(0) \rangle \qquad (i=1,2,\ldots,n-1)$$

and $\tag{4.41}$

$$\ell_i'' = \langle \underline{q}_i'', \underline{x}(0) \rangle \qquad (i=1,2,\ldots,n-1)$$

Equation (4.40) can be written as

$$\underline{x}(t') = \underline{T}\Omega(t') \qquad (t' \geq 0) \tag{4.42}$$

where

$$\underline{T} = [\underline{T}_1' | \underline{T}_1'' | \ldots | \underline{T}_i' | \underline{T}_i'' | \ldots | \underline{T}_{n-1}' | \underline{T}_{n-1}''] \tag{4.43}$$

with

$$\underline{T}_i' = \ell_i' \underline{p}_i' + \ell_i'' \underline{p}_i'' \qquad (i=1,2,\ldots,n-1)$$

and $\tag{4.44}$

$$\underline{T}_i'' = \ell_i'' \underline{p}_i' - \ell_i' \underline{p}_i'' \qquad (i=1,2,\ldots,n-1)$$

The vector $\Omega(t')$ is given by

$$\Omega(t') = [\cos\omega_1 t' | \sin\omega_i t' | \ldots \cos\omega_i t' | \sin\omega_i t' | \ldots | \cos\omega_{n-1} t' \sin\omega_{n-1} t']^T \tag{4.45}$$

4.2.4 Derivation of the coherency indices and root-mean-square (RMS) coherency measure

For typical fault clearing times, the differences in rotor angles at $t=0^+$ and $t=t_{cl}$ are very small. Therefore, it is sufficient to examine only the post-fault response to determine the coherency among generators. To determine if two generators i and j are coherent, the angular deviation between the state variables $\Delta\delta_{in}(t)$ and $\Delta\delta_{jn}(t)$ should be examined. From equation (4.42), we have that $\Delta\delta_{in} = \langle \underline{r}_i, \underline{\Omega}(t') \rangle$ and $\Delta\delta_{nj} = \langle \underline{r}_j, \underline{\Omega}(t') \rangle$ resulting in

$$\Delta\delta_{ij} = \langle (\underline{r}_i - \underline{r}_j), \underline{\Omega}(t') \rangle \tag{4.46}$$

where $\underline{r}_i$ and $\underline{r}_j$ are the rows i and j of the first (n-1) rows of $\underline{T}$. It is noted that with the ω_i's of equation (4.46) being rational numbers, as they will be when rounded, $\Delta\delta_{ij}(t)$ is a periodic function with an average value of zero and having maximum and root-mean-square values.

A possible coherency criterion would call for

$$|\Delta\delta_{ij}| = |\Delta\delta_{in} - \Delta\delta_{nj}| \leq \varepsilon \qquad (t' [0,\infty)) \tag{4.47}$$

or

$$|\langle (\underline{r}_i - \underline{r}_j), \underline{\Omega}(t') | \leq \varepsilon \tag{4.48}$$

Perfect coherency would call for $\Delta\delta_{ij} = 0$, implying that the Euclidian norm of the vector difference $(\underline{r}_i - \underline{r}_j)$, $\|\underline{r}_i - \underline{r}_j\|$, must be equal to zero because the norm of the vector $\|\underline{\Omega}(t')\|$ is always different from zero at any time t. Perfect coherency is rarely achieved and is not a reasonable criterion. If we were to process equation (4.46) looking for the maximum

value of $|\Delta\delta_{ij}|$ to compare with some ε, this would be tantamount to the production of swing curves, the very process which we wish to avoid. We then turn our attention to possible criteria which involve only the elements of the vector $(\underline{r}_i - \underline{r}_j)$.

Equation (4.48) can be rewritten as

$$\Delta\delta_{ij} = \sum_{n=1}^{n-1} [(r_{ik}-r_{jk})^2 + (r_{i(k+1)} - r_{j(k+1)}^2]^{1/2} \cos(\omega_k t' + \phi_k) \qquad (4.49)$$

From this, it can be stated that

$$|\Delta\delta_{ij}|_{max} \leq \sum_{k=1}^{n-1} [(r_{ik}-r_{nk})^2 + (r_{i(k+1)}-r_{j(k+1)})^2]^{1/2} \qquad (4.50)$$

This is a bound which would be reached only if the frequencies, ω_k, are such that

$$\omega_k t' + \phi_k = p\pi \qquad (k=1,2,.,.,,n-1) \qquad (4.51)$$

for some t', p being some integer. Thus

$$\sum_{k=1}^{n-1} [(r_{ik}-r_{jk})^2 + (r_{i(k+1)}-r_{j(k+1)})^2]^{1/2} \leq \varepsilon \qquad (4.52)$$

is a possible criterion but not a very useful one.

The nature of the problem suggests the use of the root-mean-square value of $\Delta\delta_{ij}$ as a measure of coherency. From equation (4.49) the root-mean-square value of $\Delta\delta_{ij}$ is

$$RMS(\Delta\delta_{ij}) =$$

$$\sqrt{\frac{(r_{i1}-r_{j1})^2+(r_{i2}-r_{j2})^2+\ldots+(r_{i(2n-3)}-r_{j(2n-3)})^2+(r_{i(2n-2)}-r_{j(2n-2)})^2}{2}}$$

$$= \frac{\|\underline{r}_i - \underline{r}_j\|}{\sqrt{2}} \tag{4.53}$$

and an appropriate coherency criterion is

$$\frac{\|\underline{r}_i - \underline{r}_j\|}{\sqrt{2}} \leq \varepsilon \tag{4.54}$$

where the ε used here is a bound on the rms value of the angular deviation $\Delta\delta_{ij}$.

A normalized coherency index α_{ij} is obtained from equation (4.53) by dividing by $\|\underline{r}_k\|/\sqrt{2}$, where k is the row with the maximum norm. The coherency index is thus defined as

$$\alpha_{ij} = \frac{\|\underline{r}_i - \underline{r}_j\|/\sqrt{2}}{\|\underline{r}_k\|/\sqrt{2}} = \frac{\|\underline{r}_i - \underline{r}_j\|}{\|\underline{r}_k\|} \tag{4.55}$$

and the coherency criterion is then stated as

$$\frac{\|\underline{r}_i - \underline{r}_j\|}{\|\underline{r}_k\|} \leq \varepsilon' \tag{4.56}$$

where $\varepsilon' = \varepsilon\sqrt{2}/\|\underline{r}_k\|$.

Equation (4.56) describes a coherency measure that is easy to compute and which permits the identification of coherency between pairs of

generators without having to evaluate and compare swing curves over the time period under consideration. Furthermore, reciprocity in coherency identification assures that $\alpha_{ij} = \alpha_{ji}$ such that only $(n-1)(n-2)/2$ coherency indices are required.

4.3 Grouping Algorithms

There are two clustering algorithms for processing swing curves of generators in use. They are the transitive [38] and commutative [45] algorithm.

4.3.1 The transitive algorithm

This procedure for forming the groups of coherent generators uses a transitive process, i.e., if generator a is coherent with generator b and generator a is coherent with generator c, then generators c and b are coherent. In the grouping process, a comparison generator is established for each coherent group and all other eligible generators are compared against this generator to determine if they should be included in the same group.

The process begins by letting the generator labeled as one be the reference for the first group. The remaining generators are then processed in order to determine if they meet the coherency criterion. If so, they are assigned to the first group. The first generator failing to meet the criterion becomes the reference for the second group. All remaining generators are then examined for inclusion in the second group with the first to fail becoming the reference for the third group. The process continues until the first (n-1) generators have been assigned

to groups. The n^{th} generator or system reference generator forms a group by itself. The rationale on which the approach is based is such that a minimization of the number of computations needed to process the entire set of generators is accomplished. In fact, the number of coherency indices required (if they are computed one at a time and only as needed) is bounded below by (n-2) and above by (n-1)(n-2)/2.

4.3.2 The commutative algorithm

The commutative coherency recognition algorithm requires that a generator assigned to a coherent group be pairwise coherent with every generator in the group. Therefore, the use of a commutative rule prevents generators which are not pairwise coherent from being assigned to the same group.

The process starts by ordering the (n-1)(n-2)/2 coherency indices from the smallest to the largest in a ranking table. The determination of coherent groups by use of the ranking table commences by letting each of the (n-1) generators in the original system model represent a coherent group containing exactly one generator. The reference generator is considered a coherent group by itself with no other generators being coherent with it. The number of coherent groups is then reduced by starting at rank 1 (i.e., the first entry in the ranking table) and merging that pair of generators into a single coherent group provided that the coherency threshold is satisfied. The algorithm proceeds through successively higher ranks merging coherent groups using a commutative coherency recognition rule and ending when the specified threshold (ε') can no longer be met.

The following simple example illustrates the use of both algorithms in the search for coherent groups. Suppose there are three generators with coherency indices

$$\alpha_{12} = 0.035, \quad \alpha_{13} = 0.053, \quad \alpha_{23} = 0.095$$

and let the prespecified coherency threshold be $\varepsilon' = 0.087$. The transitive rule will give the following results.

i) If one starts processing the generators in the order 1,2,3 or 1,3,2, there is only one resulting coherent group, that is, (1,2,3). On the contrary, if we start processing the generators in the order 2,3,1 or 3,1,2, two results may be obtained, they are

   a) (1,2), (3)

   b) (1,3), (2)

ii) The commutative rule would start by first constructing the following ranking table

rank	coherency index	generator pair
1	0.035	(1,2)
2	0.053	(1,3)
3	0.095	(2,3)

It is evident from the ranking table that there is only one possible grouping, that is, (1,2), (3). This results from the fact that while α_{13} passes the coherency test, α_{23} fails. Thus, generator 3 constitutes a coherent group by itself. On the other hand, if the coherency index α_{23} was also less than the coherency threshold, ε', the resulting coherent group would be (1,2,3) since all generators in the group are pairwise coherent.

Thus the transitive rule is seen to be sensitive to labeling of generators while the commutative rule is not. For this reason, the commutative rule was chosen for use here.

4.4 Numerical Examples

We now illustrate the use of the root-mean-square (RMS) coherency approach in identifying groups of coherent generators as the fault location is shifted. The New England and Modified Iowa Systems are used to demonstrate the application of this method.

Two different fault locations for the New England System (Fig. 3.1) are used.

i) A three-phase fault on bus 29 with t_{cl} = 0.10 sec. (no line switching).

ii) A three-phase fault on bus 19 with t_{cl} = 0.10 sec. (no line switching).

To conclude, a case involving a three-phase fault on bus 435-SYCAMORE in the Modified Iowa System (Fig. 3.2) with t_{cl} = 0.10 sec. and no line switching is presented. Numerical results are listed in a tabulated form.

4.4.1 The New England system

To commence, the system matrix $\bar{\underline{A}}_1$ with generator 10 chosen as the reference is

$$\bar{\underline{A}}_1 = \begin{array}{c} \begin{array}{ccccccccc} 1 & 2 & 3 & 4 & 5 & 6 & 7 & 8 & 9 \end{array} \\ \begin{bmatrix} -73.253 & 3.768 & 4.891 & 5.047 & 1.709 & 5.135 & 4.188 & 12.999 & 7.257 \\ 2.958 & -50.696 & 12.064 & 3.419 & 1.044 & 3.569 & 2.928 & 2.453 & 2.425 \\ 3.255 & 10.054 & -50.237 & 4.171 & 1.293 & 4.338 & 3.555 & 2.663 & 2.731 \\ 4.158 & 3.338 & 5.081 & -69.613 & 13.184 & 12.039 & 9.843 & 3.669 & 5.125 \\ 0.442 & 0.625 & 1.272 & 14.872 & -37.969 & 4.323 & 3.670 & 0.999 & 1.719 \\ 2.969 & 2.521 & 3.944 & 9.479 & 3.043 & -63.959 & 21.854 & 3.053 & 4.266 \\ 3.256 & 2.758 & 4.281 & 10.153 & 3.512 & 28.826 & -73.826 & 3.317 & 4.603 \\ 20.569 & 3.108 & 4.156 & 4.665 & 1.594 & 5.100 & 4.169 & -78.486 & 10.699 \\ 4.513 & 0.921 & 1.536 & 2.918 & 0.948 & 3.469 & 2.852 & 6.048 & -35.407 \end{bmatrix} \end{array}$$

The eigenvalues of the above matrix are

-15.299, -35.456, -40.375, -49.409, -61.539, -64.818, -79.528, -92.501 and -94.519.

The associated eigenvectors are

$\underline{x}_1 = [-2.4903 \quad -2.7698 \quad -2.9170 \quad -3.6482 \quad -4.3352 \quad -3.6000 \quad -3.5791 \quad -2.6484 \quad -3.5679]^T$

$\underline{x}_2 = [-1.0967 \quad -0.7380 \quad -0.6360 \quad 1.9072 \quad 7.5843 \quad 0.5272 \quad 0.5305 \quad -1.5211 \quad -5.9670]^T$

$\underline{x}_3 = [-0.6943 \quad -5.6817 \quad -5.2551 \quad 0.1743 \quad 4.6033 \quad -1.3179 \quad 1.2427 \quad -0.2964 \quad 4.3215]^T$

$\underline{x}_4 = [-0.3181 \quad 3.9094 \quad 2.9248 \quad -1.1085 \quad 4.3053 \quad -5.4308 \quad -5.0116 \quad 0.2835 \quad 1.9531]^T$

$\underline{x}_5 = [0.2982 \quad -7.3396 \quad 6.7755 \quad -0.0019 \quad 0.0014 \quad -0.5618 \quad -0.4947 \quad 0.3026 \quad -0.1324]^T$

$$\underline{x}_6 = [-6.7734 \quad 0.5611 \quad 1.3718 \quad -0.4925 \quad -0.0026 \quad 1.5772 \quad 1.3375 \quad -7.1372 \quad 2.1508]^T$$

$$\underline{x}_7 = [0.7982 \quad 0.1952 \quad 0.3828 \quad -9.0976 \quad 2.8303 \quad 2.2442 \quad 1.5884 \quad 1.1753 \quad 0.0016]^T$$

$$\underline{x}_8 = [-5.4053 \quad -0.0454 \quad -0.0399 \quad -0.1118 \quad -0.0477 \quad -0.2958 \quad 0.0993 \quad 8.4139 \quad -0.4427]^T$$

$$\underline{x}_9 = [-0.0619 \quad -0.0274 \quad -0.0405 \quad -0.4637 \quad 0.0289 \quad -5.714 \quad 8.2219 \quad -0.0767 \quad -0.0249]^T$$

and the reciprocal basis vectors are

$$\underline{\omega}_1 = [-1.9563 \quad -2.2671 \quad -2.9749 \quad -3.3356 \quad -3.7560 \quad -4.2254 \quad -3.1799 \quad -1.7281 \quad -5.0987]^T$$

$$\underline{\omega}_2 = [1.2643 \quad 0.5147 \quad 0.5129 \quad -1.8059 \quad -5.9659 \quad -0.6441 \quad -0.4808 \quad 1.1465 \quad 7.6752]^T$$

$$\underline{\omega}_3 = [0.244 \quad 5.0629 \quad 5.5127 \quad -0.3569 \quad -3.5636 \quad 1.0827 \quad 0.7726 \quad -0.0865 \quad -5.7159]^T$$

$$\underline{\omega}_4 = [-0.2999 \quad 3.7941 \quad 3.3434 \quad -1.0694 \quad 3.3767 \quad -6.2051 \quad -4.3526 \quad -0.1973 \quad 2.2946]^T$$

$$\underline{\omega}_5 = [-0.4034 \quad 6.7642 \quad -7.3576 \quad -0.0030 \quad 0.0014 \quad 0.6237 \quad 0.4149 \quad -0.2315 \quad 0.1736]^T$$

$$\underline{\omega}_6 = [-7.9395 \quad 0.9480 \quad 1.9574 \quad -0.3008 \quad 0.2412 \quad 2.3489 \quad 1.5311 \quad -4.8702 \quad 2.9289]^T$$

$$\underline{\omega}_7 = [1.0686 \quad 0.2189 \quad 0.5022 \quad -9.0941 \quad 2.4588 \quad 2.8361 \quad 1.4675 \quad 0.6735 \quad 0.1510]^T$$

$$\underline{\omega}_8 = [-7.3033 \quad 0.1087 \quad 0.1271 \quad 0.2417 \quad -0.0283 \quad -0.0078 \quad 0.0169 \quad 6.8329 \quad -0.3844]^T$$

$$\underline{\omega}_9 = [0.1438 \quad -0.0278 \quad -0.0492 \quad -0.4044 \quad 0.0045 \quad -6.8090 \quad 7.4174 \quad -0.2414 \quad -0.0218]^T$$

The coherent groups of generators for three-phase faults on buses 29 and 19 with $t_{cl} = 0.10$ sec. are chosen using a coherency threshold of $\varepsilon = 0.087$ radians (or 5 electrical degrees). Although we are using the same absolute threshold for both cases, the normalized thresholds, ε', will be different.

4.4.1.1 Fault on bus 29 To give the reader some feel for the appearance of the vectors $\underline{r}_i$ and $\underline{r}_j$, the rows of $\underline{T}$, the first (n-1) rows of the matrix $\underline{T}$ are given. These are followed by Table 4.1 which lists the coherency indices computed from the rows of $\underline{T}$, as well as the coherent groups of generators selected by the application of the commutative rule to the coherency indices as the coherency threshold is made progressively larger.

The first (n-1) rows of $\underline{T}$ are

$$\underline{r}_1 = [0.04498 \quad 0.22703 \quad 0.01680 \quad 0.05474 \quad -0.02168 \quad -0.00109 \quad -0.00297 \quad -0.00011 \quad -0.00028 \quad -0.03088 \quad -0.07253 \quad -0.01361 \quad -0.02609 \quad 0.0 \quad 0.0]$$

$\underline{r}_2$ = [0.05003 0.25256 0.01130 0.03683 -0.05838 -0.17753
0.01337 0.03645 0.00282 0.00681 0.00256 0.00601
-0.00006 -0.00012 -0.00011 -0.00022 0.0 0.0]

$\underline{r}_3$ = [0.05269 0.26597 0.00974 0.03174 -0.05399 -0.16419
0.01000 0.02728 -0.00260 -0.00628 0.00626 0.01469
-0.00012 -0.00024 -0.0001 -0.00019 0.0 0.0]

$\underline{r}_4$ = [0.06589 0.33262 -0.02920 -0.09516 0.00179 0.00544
-0.00379 -0.01034 0.0 0.0 -0.00225 -0.00528 0.00278
0.00581 -0.00028 -0.00054 -0.00003 -0.00005]

$\underline{r}_5$ = [0.07830 0.39526 -0.11611 -0.37843 0.04729 0.14382
0.01472 0.04015 0.0 0.0 -0.00001 -0.00003 -0.00086
-0.00181 -0.00012 -0.00023 0.0 0.0]

$\underline{r}_6$ = [0.06503 0.32824 -0.00807 -0.02630 -0.01354 -0.04118
-0.01857 -0.05065 0.00022 0.00052 0.00719 0.01689
-0.00143 -0.00075 -0.000143 -0.00032 -0.00060]

$\underline{r}_7$ = [0.06465 0.32633 -0.00813 -0.02650 -0.01277 -0.03884
-0.01714 -0.04674 0.00019 0.0046 0.00610 0.01433
-0.00048 -0.00101 0.00025 0.00048 0.00046 0.00087]

$\underline{r}_8$ = [0.04783 0.24144 0.02329 0.07590 -0.00304 -0.00925
-0.00097 -0.00265 -0.00012 -0.00028 -0.03532 -0.07642
-0.00036 -0.00075 0.02119 0.0406 0.0 -0.00001]

$$\underline{r}_g = [0.06445 \quad 0.32532 \quad 0.09136 \quad 0.29774 \quad 0.04441 \quad 0.13504$$
$$0.00668 \quad 0.01821 \quad 0.00005 \quad 0.00012 \quad 0.00981 \quad 0.02303$$
$$0.0 \quad 0.0 \quad -0.00112 \quad -0.00214 \quad 0.0 \quad 0.0]$$

The vector $\underline{u}$, composed of the accelerating powers used to compute the vector $\underline{x}(t_{cl})$, is given by

$$\underline{u} = [1.314 \quad 4.2509 \quad 4.308 \quad 6.9927 \quad 4.6832 \quad 6.0318 \quad 6.5961$$
$$11.2372 \quad 44.211]^T$$

The third column in Table 4.1 shows the coherent groups that appear as the coherency threshold is made progressively larger so that it exceeds the α_{ij} in a given row. For the ε' specified, the process would terminate after 5 rows; however, it is continued for completeness until there are only two coherent groups, the system reference generator and the remaining n-1 generators. It is interesting to note that with a normalized coherency threshold of 0.2104, corresponding to an unnormalized rms threshold of 0.0873 (5 electrical degrees), the grouping obtained matches the grouping obtained in ref. [38] by detailed computation of swing curves using a maximum angular deviation of 5 electrical degrees.

Summarizing the results obtained in Table 4.1, one can say that the number of coherent groups for $\varepsilon' = 0.2104$ is six with the following generators as members of them.

Group 1: (1,8)
Group 2: (2,3)
Group 3: (4,6,7)
Group 4: 5
Group 5: 9
Group 6: 10

Table 4.1 Three-phase fault on bus 29, New England System: coherency threshold $\varepsilon' = 0.2104$ $\|\underline{r}_k\| = 0.5864$ k=5

Coherency Indices α_{ij}	Pair (i,j)	Coherent Groups of Generators
0.01113	(6,7)	1, 2, 3, 4, 5, (6,7), 8, 9
0.04817	(2,3)	1, (2,3), 4, 5, (6,7), 8, 9
0.13808	(1,8)	(1,8), (2,3), 4, 5, (6,7), 9
0.16525	(4,7)	"
0.17145	(4,6)	(1,8), (2,3), (4,6,7), 5, 9
0.29430	(1,7)	"
0.30052	(1,6)	"
0.30115	(3,7)	"
0.30238	(3,6)	"
0.31408	(7,8)	"
0.32150	(6,8)	"
0.32169	(1,3)	"
0.33203	(1,2)	"
0.33827	(2,7)	"
0.33986	(2,6)	"
0.35096	(3,8)	"
0.35475	(1,4)	"
0.36228	(2,8)	(1,2,3,8), (4,6,7), 5, 9
0.37808	(4,8)	"
0.40462	(3,4)	"
0.43665	(2,4)	(1,2,3,4,6,7,8), 5, 9
0.53590	(8,9)	"
0.57557	(1,9)	"
0.58109	(4,5)	"
0.66801	(7,9)	"
0.67087	(6,9)	"
0.72464	(3,9)	"
0.73600	(5,7)	"
0.73939	(5,6)	"
0.74151	(2,9)	"
0.74240	(4,9)	(1,2,3,4,6,7,8,9), 5
0.89311	(1,5)	"
0.91444	(5,8)	"
0.94507	(3,5)	"
0.97134	(2,5)	"
1.21389	(5,9)	(1,2,3,4,5,6,7,8)

4.4.1.2 Fault on bus 19 For the sake of brevity in the following example only, a table and drawings describing the coherency indices and the swing curves of the resultant coherent groups are provided. However, pertinent commentaries about the selection of the coherent groups are given to complement the information provided by the table and drawings.

The vector of accelerating powers, $\underline{u}$, used in this example is

$$\underline{u} = [4.5161 \quad 9.0418 \quad 9.4884 \quad 39.657 \quad 34.9544 \quad 16.7381 \quad 18.3963 \quad 9.8501 \quad 11.3686]^T$$

The set of coherent groups selected for a coherency threshold $\varepsilon' = 0.1925$ ($\varepsilon = 0.0873$) are

Group 1: (6,7)
Group 2: (1,2,3,8)
Group 3: 4
Group 4: 5
Group 5: 9
Group 6: 10

Table 4.2 shows that a different set of coherent groups is obtained when the fault is shifted from bus 29 to bus 19. This change in grouping is a direct result of the change in fault location. Since the fault on bus 19 is close to generators 4 and 5, it was expected that these generators would not be coherent. This is in fact what Table 4.2 shows. It is noted that several pairs of generators, e.g. 6 and 7, are coherent for both fault locations and this has also been seen in several other studies not reported here; however, no general conclusions are warranted.

Table 4.2 Three-phase fault on bus 19, New England System
$\varepsilon' = 0.1925 \quad \|r_k\| = 0.641 \quad k=5$

Coherency Indices α_{ij}	Pair (i,j)	Coherent Groups of Generators
0.02250	(6,7)	1, 2, 3, 4, 5, (6,7), 8, 9
0.03916	(2,3)	1, (2,3), 4, 5, (6,7), 8, 9
0.10009	(1,8)	(1,8), (2,3), 4, 5, (6,7), 9
0.12765	(1,2)	"
0.13587	(2,8)	"
0.14257	(1,3)	"
0.14272	(3,8)	(1,2,3,8), 4, 5, (6,7), 9
0.17460	(3,7)	"
0.18315	(3,6)	"
0.20673	(2,7)	"
0.21521	(2,6)	"
0.23827	(7,8)	"
0.24505	(6,8)	"
0.25679	(1,7)	"
0.26360	(1,6)	(1,2,3,6,7,8), 4, 5, 9
0.31547	(8,9)	"
0.33026	(7,9)	"
0.33371	(4,7)	"
0.33412	(6,9)	"
0.33490	(3,9)	"
0.34738	(1,9)	"
0.34924	(2,9)	(1,2,3,6,7,8,9), 4, 5
0.35329	(4,6)	"
0.36299	(3,4)	"
0.37677	(2,4)	"
0.38866	(5,6)	"
0.39119	(5,7)	"
0.41911	(4,8)	"
0.41935	(1,4)	"
0,47365	(4,9)	(1,2,3,4,6,7,8,9), 5
0.48298	(4,5)	"
0.52998	(3,5)	"
0.55503	(2,5)	"
0.57862	(5,8)	"
0.58595	(1,5)	"
0.67382	(5,9)	(1,2,3,4,5,6,7,8,9)

The results reported in Table 4.2 compare favorably with swing curves obtained with the Philadelphia Electric Company stability program as shown in Fig. 4.2 and Fig. 4.3.

4.4.2 The Modified Iowa system

Summary results for the Modified Iowa System (Fig. 3.2) with a fault on bus 435 are presented here. The clearing time and coherency threshold are the same as those used for the New England System. The generator at Davenport (machine 17) was used as reference. The input vector $\underline{u}$ containing the accelerating powers for this example is given by

$$\underline{u} = [1.0651 \quad 11.0014 \quad 1.4166 \quad 0.5448 \quad 12.0431 \quad 18.0754 \quad 5.4625$$
$$15.0718 \quad 4.6826 \quad 17.6229 \quad 20.3229 \quad 22.6140 \quad 14.8857$$
$$-0.5476 \quad 0.6274 \quad 8.0859]^T$$

Any change in fault location will cause the above vector to be modified. Table 4.3 gives only a sufficient number of coherency indices to satisfy the stated coherency threshold.

The coherent groups obtained with a threshold value of $\varepsilon = 0.0873$ (or 5° electrical degrees) are

Group 1: (1,2,12,13)
Group 2: (3,4,15)
Group 3: (5,6)
Group 4: (7,8,9,14)
Group 5: 10
Group 6: 11
Group 7: 16
Group 8: 17

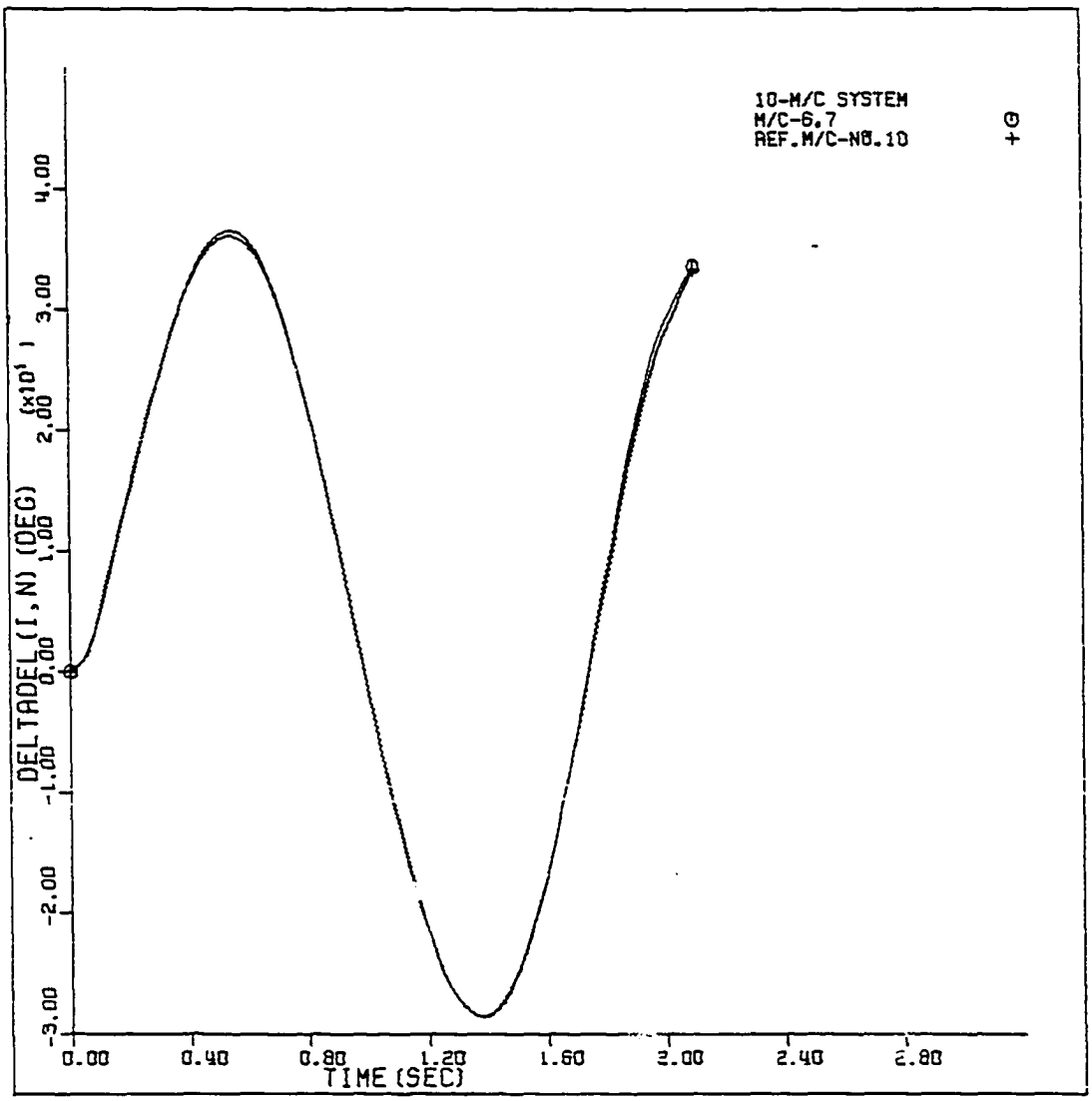

Fig. 4.2 Coherent group 1: machines 6 and 7 when a three-phase fault is placed on bus 19 in the New England system

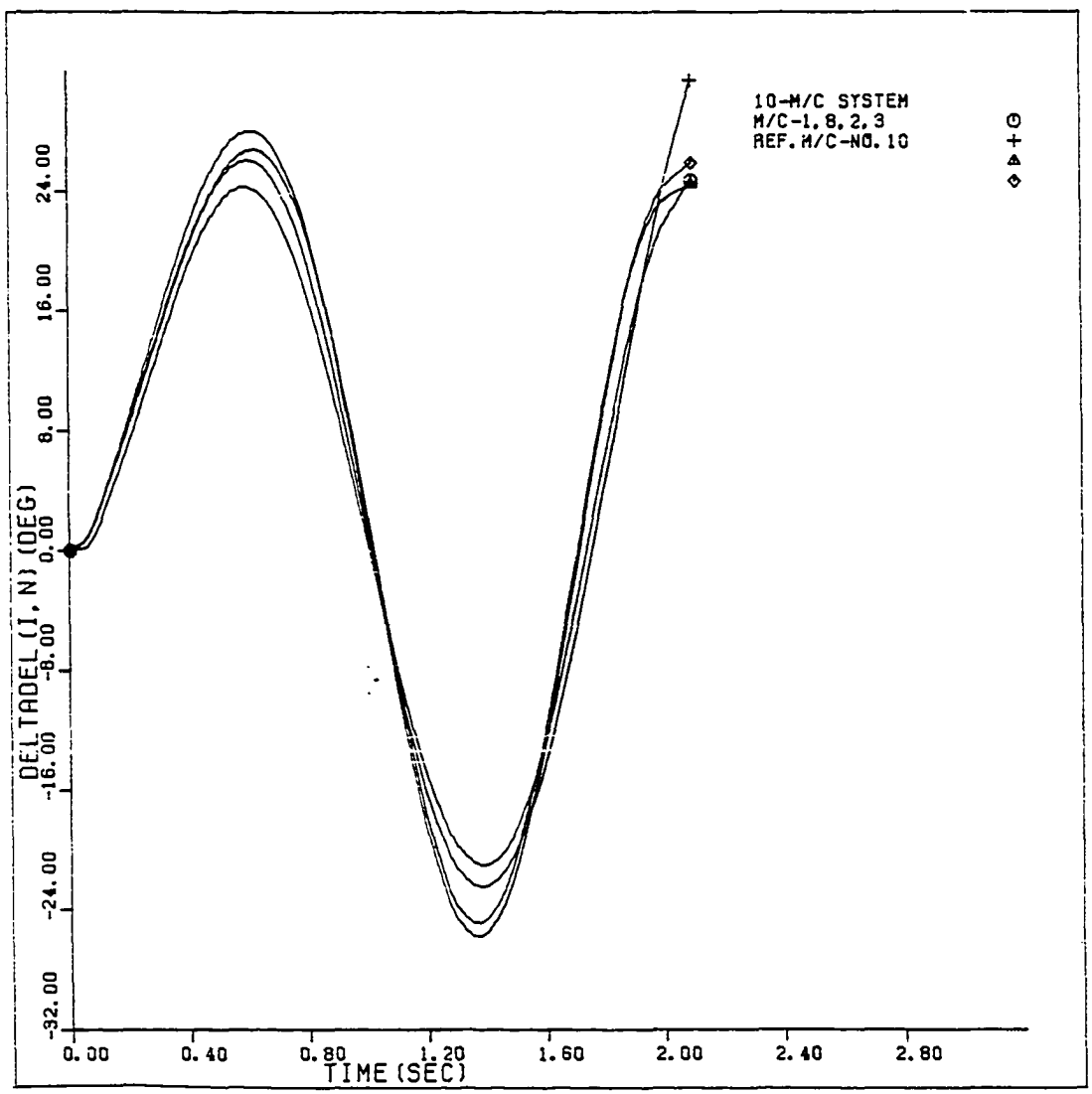

Fig. 4.3 Coherent group 2: machines 1, 8, 2 and 3, when a three-phase fault is placed on bus 19 in the New England system

Table 4.3 Three-phase fault on bus 435 Sycamore
$\varepsilon' = 0.7140 \quad \|r_k\| = 0.17284 \quad k=11$

Coherency Indices α_{ij}	Pair (i,j)	Coherent Groups of Generators
0.14094	(4,15)	1, 2, 3, (4,15), 5, 6, 7, 8, 9, 10, 11, 12, 13, 14, 16
0.23496	(7,9)	1, 2, 3, (4,15), 5, 6, (7,9), 8, 10, 11, 12, 13, 14, 16
0.32307	(7,8)	"
0.36585	(12,13)	1, 2, 3, (4,15), 5, 6, (7,9), 8, 10, 11, (12,13), 14, 16
0.41089	(8,9)	1, 2, 3, (4,15), 5, 6, (7,8,9), 10, 11, (12,13), 14, 16
0.43722	(5,6)	1, 2, 3, (4,15), (5,6), (7,8,9), 10, 11, (12,13), 14, 16
0.45781	(7,14)	"
0.47432	(6,12)	"
0.47619	(8,14)	"
0.49051	(1,12)	"
0.40909	(10,12)	"
0.51649	(8,12)	"
0.52754	(7,15)	"
0.52817	(4,8)	"
0.53059	(1,13)	"
0.53389	(8,15)	(1,12,13), 2, 3, (4,15), (5,6), (7,8,9), 10, 11, 14, 16
0.54163	(6,8)	"
0.54191	(4,7)	"
0.54547	(2,13)	"
0.55349	(9,15)	"
0.55574	(2,12)	"

Table 4.3 (continued)

Coherency Indices α_{ij}	Pair (i,j)	Coherent Groups of Generators
0.56344	(9,14)	(1,12,13), 2, 3, (4,15), (5,6), (7,8,9,14), 10, 11, 16
0.57437	(4,9)	"
0.58628	(6,13)	"
0.58650	(3,4)	"
0.59736	(10,13)	"
0.60157	(3,15)	(1,12,13), 2, (3,4,15), (5,6), (7,8,9,14), 10, 11, 16
0.63479	(8,13)	"
0.63830	(1,14)	"
0.64229	(1,2)	(1,2,12,13), (3,4,15), (5,6), (7,8,9,14), 10, 11, 16
0.64453	(1,8)	"
0.64839	(12,14)	"
0.65249	(6,10)	"
0.65298	(8,10)	"
0.65393	(7,12)	"
0.67561	(3,8)	"
0.68168	(6,7)	"
0.68458	(1,10)	"
0.68461	(2,11)	"
0.68838	(4,6)	"
0.68981	(3,12)	"
0.69426	(1,6)	"
0.71002	(1,7)	"
0.71096	(3,6)	"
0.71266	(12,16)	" threshold

Swing curves were also determined using the Philadelphia Electric Company stability program and are shown in Figures 4.4, 4.5, 4.6 and 4.7 for the four groups of more than one machine. The results predicted by the direct coherency method are substantially in agreement with those given by the swing curves. The small differences existing between these results are due in part to the nonlinear model used in the stability program. These small discrepancies are more apparent after the first swing and thus are of less interest as far as the determination of the transient stability of the system is concerned. It is also interesting to notice that generators 10 and 12, which are both located in Council Bluffs, are in different coherent groups. This decoupling appears to be produced by the large inertia constant ratio ($H_{12} \simeq 4H_{10}$). For those machines which are not coherent with no other machines in the system, i.e., machines 10, 11, 16 and 17, the swing curves given by the Philadelphia Electric Company stability program show that they are indeed not coherent with no other machines.

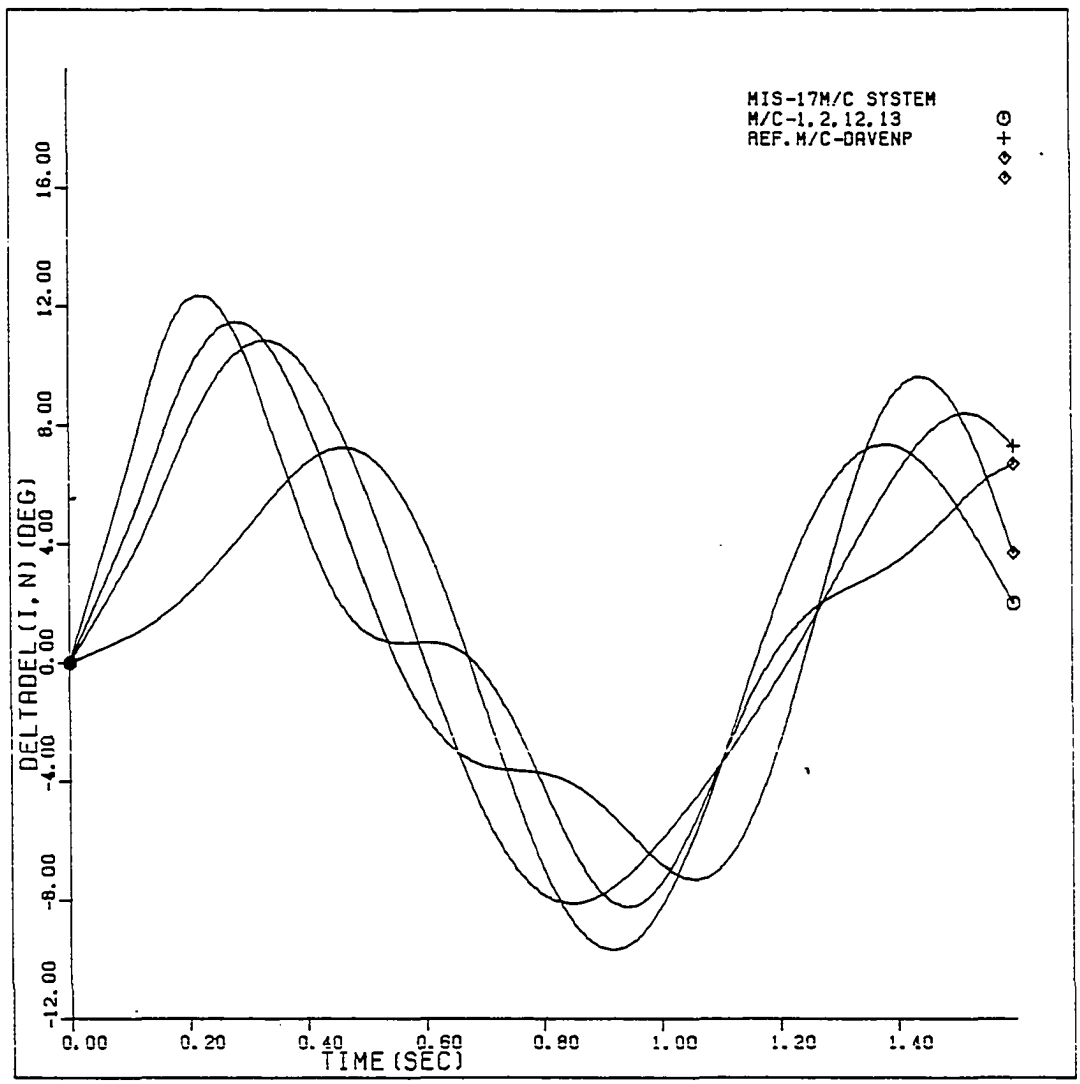

Fig. 4.4 Coherent group 1: machines 1, 2, 12 and 13 when a three-phase fault is placed on bus 435 Sycamore in the Modified Iowa system

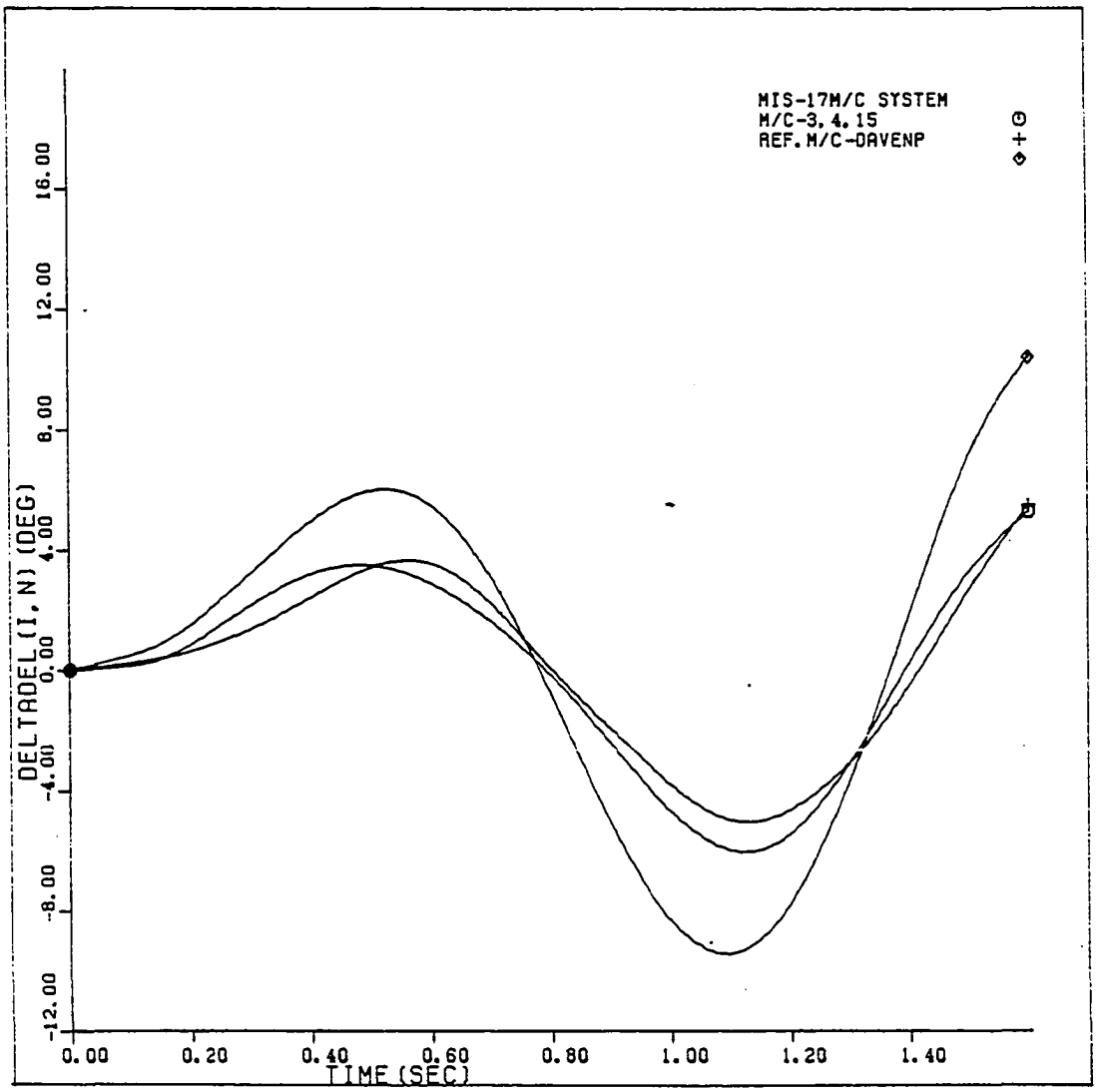

Fig. 4.5 Coherent group 2: machines 3, 4 and 15 when a three-phase fault is placed on bus 435 Sycamore in the Modified Iowa system

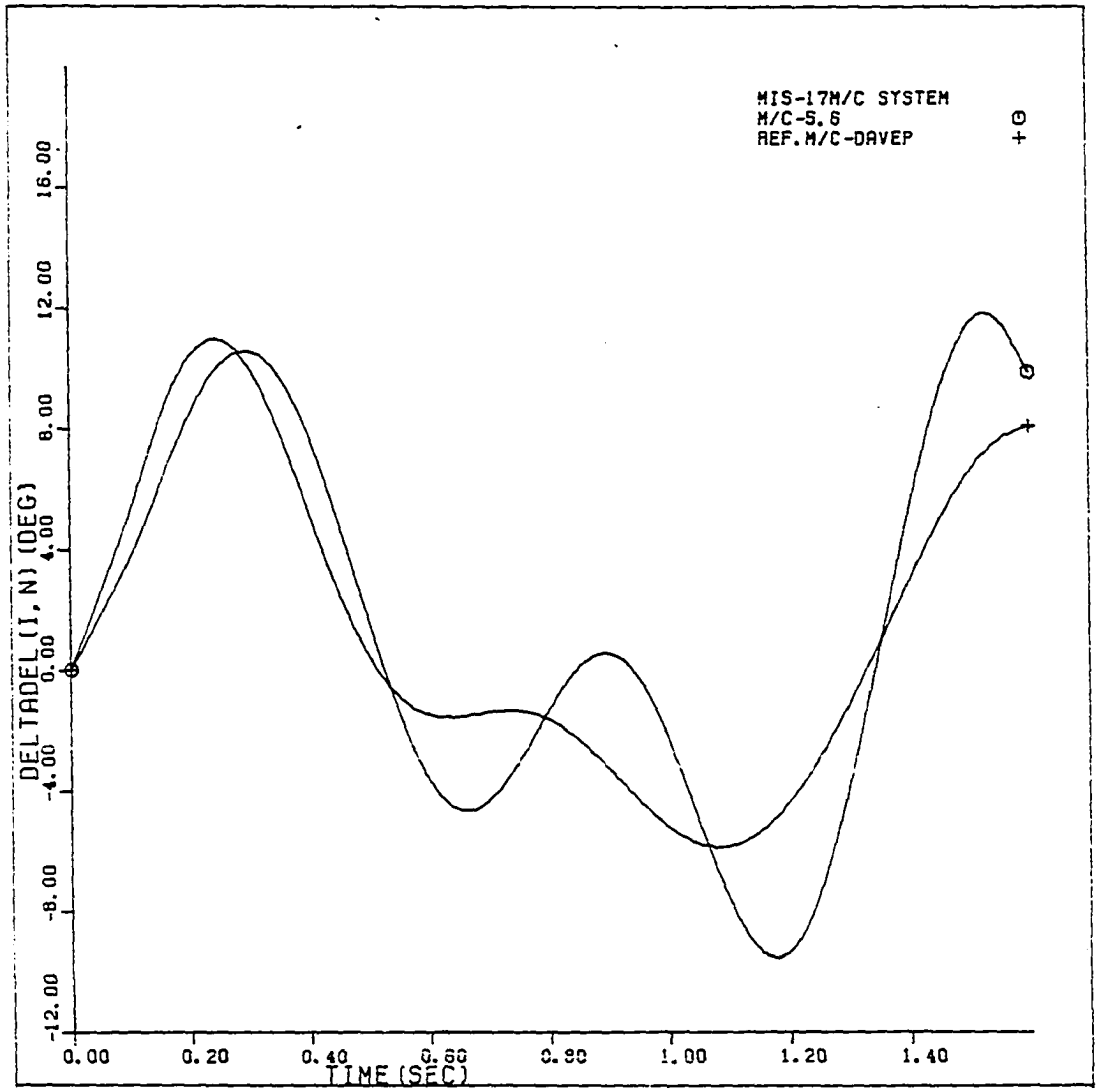

Fig. 4.6 Coherent group 3: machines 5 and 6 when a three-phase fault is placed on bus 435 Sycamore in the Modified Iowa system

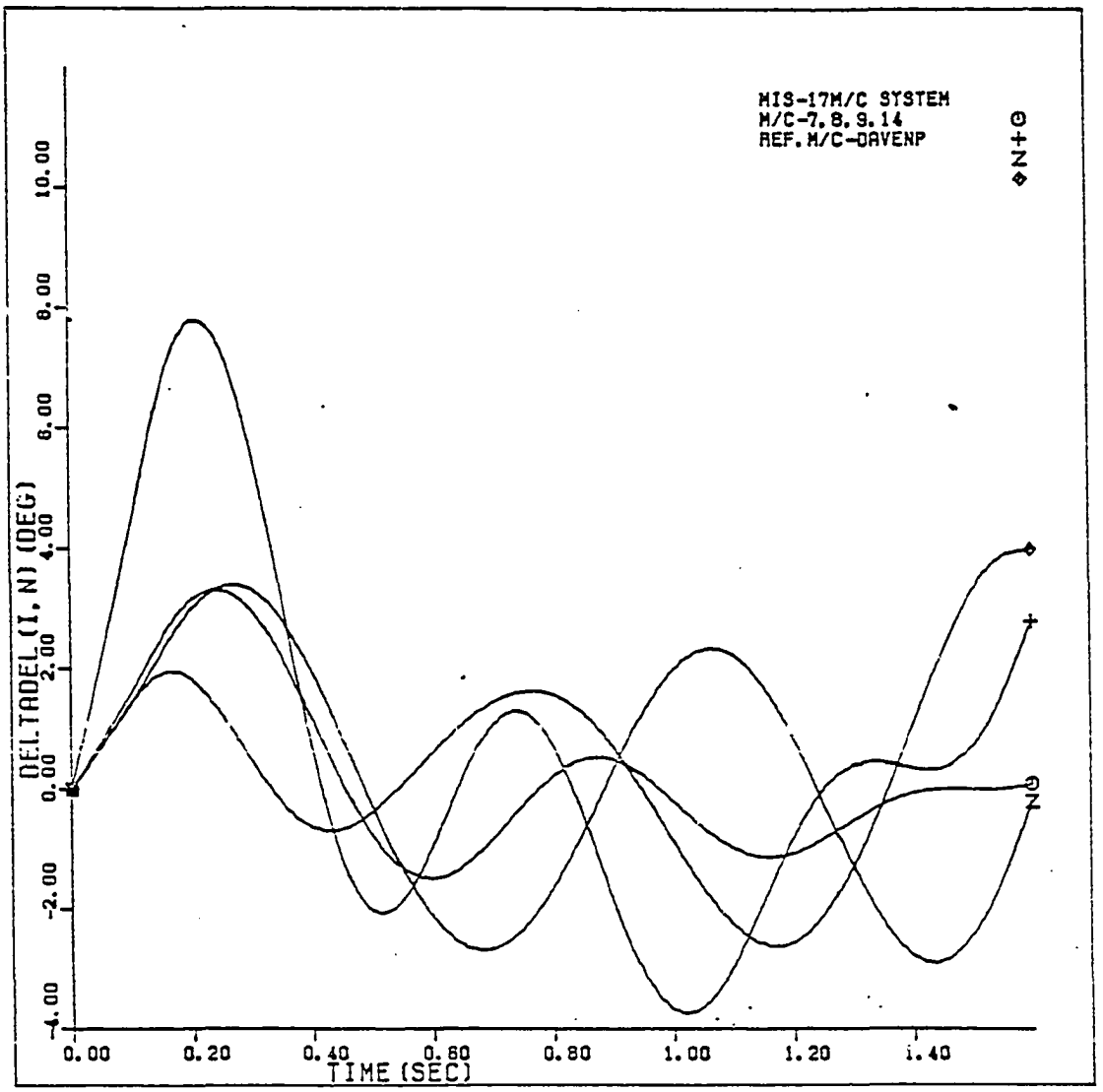

Fig. 4.7 Coherent group 4: machines 7, 8, 9 and 14 when a three-phase fault is placed on bus 435 Sycamore in the Modified Iowa system

5. REDUCED ORDER MODELLING USING SINGULAR PERTURBATION THEORY

5.1 Introduction

As discussed in Chapter 1, a linearized model of the form

$$\dot{\underline{\omega}} = \underline{\underline{A}}\underline{x} + \underline{\underline{B}}\underline{u}; \; \underline{\omega}(0) = \underline{\omega}^{o} \tag{5.1}$$

where $\underline{\omega}$ and $\underline{u}$ are now redefined to be the incremental variables $\Delta\underline{x}$ and $\Delta\underline{u}$, is extensively used in dynamic stability studies as well as in the design of the control units associated with synchronous generators. The recent trend of representing the generating units in great detail has resulted in an increase in the dimension of the model and the numerical stiffness of the system equations.

The problem of dimensionality appears because of the inclusion in the generating unit model of the electrical transients in the machine windings and the characteristics of the voltage regulator-exciter and governor-turbine systems. The numerical stiffness of the system equations results from the presence of small time constants introduced by the machine windings and the voltage regulator-exciter. The neglect of the effects of these time constants in the simplified model resulted in a less accurate representation. There is a need for a technique for simplifying equation (5.1) including the effect of such time constants in order to improve accuracy. Such a technique based on singular perturbation theory is presented in this chapter.

First, an algorithm to formulate the model, equation (5.1), for a multimachine power system using a detailed representation of the

generating units is presented. Then, the model is cast in the singular perturbation form, equation (1.11), by partitioning the system state vector into slow and fast variables. The decomposition is based on a qualitative knowledge of the time rate of change of the different state variables. When this information is not available, physical parameters such as time constants, loop gains and energy storage constants (e.g., masses, inertias, inductances, etc.) are examined to determine which states are slow and which are fast. A solution of the system of the ordinary differential equations in the singular perturbation form using asymptotic expansions is then presented. Since the results obtained from these asymptotic expansions [30] are functions of the number of terms of the expansions, a general procedure is outlined so that any number in terms can be used in the construction of the time solution for the slow and fast system variables. Although a first order approximation ($\underline{x}(t) \sim \underline{X}_o(t) + \varepsilon[\underline{X}_1(t) + \underline{p}_o(\tau)]$) and $\underline{y}(t) \sim \underline{Y}_o(t) + \underline{q}_o(\tau) + \varepsilon[\underline{Y}_1(t) + \underline{q}_1(\tau)]$, where $\underline{x}(t)$ and $\underline{y}(t)$ are the vectors containing the slow and fast variables, respectively) is constructed here, a zero order approximation ($\underline{x}(t) \sim \underline{X}_o(t)$ and $\underline{y}(t) \sim \underline{Y}_o(t) + \underline{q}_o(\tau)$) is used in the dynamic simulation of the numerical example described at the end of this chapter. The accuracy obtainable with the latter is adequate.

5.2 Power System Model

A power system model for dynamic stability studies consists of a linearized set of ordinary differential equations representing the generating unit dynamics and a set of algebraic equations describing the

system network interconnections. The ordinary differential equations are cast in the state space form of equation (5.1) by eliminating the nonstate variables. A generating unit consists of a synchronous generator, a voltage regulator-exciter system and a governor-turbine system. Detailed descriptions of the models for these elements are given in Appendix B.

5.2.1 The generating unit model

Consider a power system having n generating units. The state-space representation of the i^{th} generating unit is obtained by linearization of the system differential equations around the prefault operating point. The synchronous generator of the i^{th} unit is modeled by the hybrid characterization proposed in [32], models for the voltage regulator-exciter and governor-turbine systems have been taken from the IEEE standards used in [4]. The state variables of each of the system units are given with respect to its own d-q axes, with the d-axis leading the q-axis. A pictorial sketch of the system and synchronous generator rotating references is given in Fig. 5.1.

The linearization of the generating unit differential equations is based on the following assumptions.

i) Subtransient saliency can be neglected (i.e., $x''_d = x''_q$).
ii) Stator transient phenomena can be neglected.
iii) Saturation of machine and exciter can be neglected.
iv) Loads can be represented by constant admittances.
v) Armature resistance is negligible.

The hybrid model equations of the i^{th} synchronous generator are

$$\frac{d}{dt} E'_{q_i} = K_1 E'_{q_i} + K_2 E''_{q_i} + K_3 I_{d_i} + \frac{1}{T'_{d_o}} E_{FD_i} \qquad (5.2a)$$

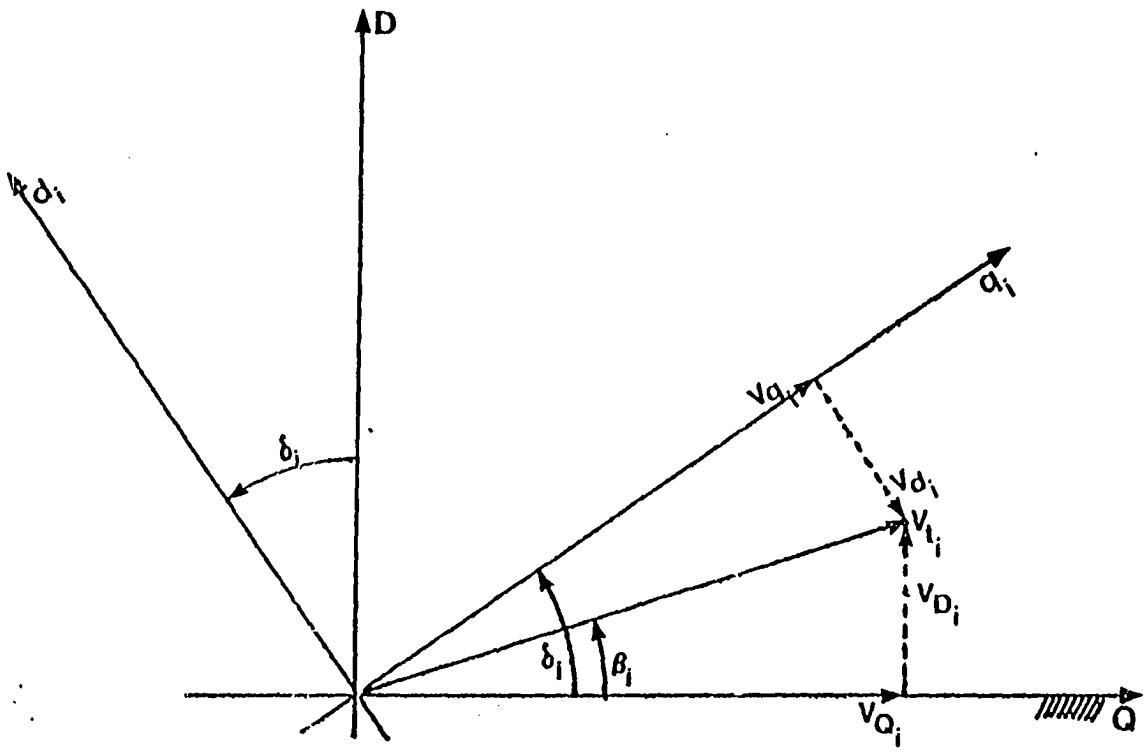

Fig. 5.1 Network and i^{th} machine synchronous rotating references axes

$$\frac{d}{dt} E''_{q_i} = \left(\frac{1}{T_1}\right) E'_{q_i} - \left(\frac{1}{T_2}\right) E''_{q_i} + K_4 I_{d_i} + K_5 E_{FD_i} \tag{5.2b}$$

$$\frac{d}{dt} E''_{d_i} = -\left(\frac{1}{T''_{q_o}}\right) E''_{d_i} + K_6 I_{q_i} \tag{5.2c}$$

$$2H_i \frac{d\omega_i}{dt} = P_{m_i} - P_{e_i} = P_{m_i} - E''_{q_i} I_{q_i} - E''_{d_i} I_{d_i} \tag{5.2d}$$

$$\frac{d}{dt} \delta_i = \omega_R(\omega_i - 1.0) \tag{5.2e}$$

where constants K_1, K_2, K_3, K_4, K_5, K_6, T_1 and T_2 and the time constants T''_{q_o} and T'_{d_o} are defined in Appendix B. Other symbols in the above equations and the following are listed in the list of symbols.

The equations governing the performance of voltage regulator-exciter and governor-turbine systems are given below.

i) For the voltage regulator-exciter system.

$$\frac{d}{dt} V_{1_i} = \left(\frac{K_R}{T_R}\right) V_{t_i} - \left(\frac{1}{T_R}\right) V_{1_i} \tag{5.3a}$$

$$\frac{d}{dt} V_{3_i} = \left(\frac{K_F}{T_F}\right)\left[\left(\frac{1}{T_E}\right) V_{R_i} - \left(\frac{K_E}{T_E}\right) E_{FD_i}\right] \tag{5.3b}$$

$$\frac{d}{dt} V_{R_i} = -\left(\frac{K_A}{T_A}\right)[V_{1_i} + V_{3_i}] - \left(\frac{1}{T_A}\right) V_{R_i} + \left(\frac{K_A}{T_A}\right) V_{REF_i} \tag{5.3c}$$

$$\frac{d}{dt} E_{FD_i} = \left(\frac{1}{T_E}\right) V_{R_i} - \left(\frac{K_E}{T_E}\right) E_{FD_i} \tag{5.3d}$$

ii) For the governor-turbine system.

$$\frac{d}{dt}\theta_{1_i} = \left(\frac{K'}{\tau_1}\right)(\omega_i - 1.0) + \left(\frac{\tau_2 K'}{2H_i\tau_1}\right)[P_{m_i} - E''_{q_i} I_{q_i} - E''_{d_i} I_{d_i}] - \left(\frac{1}{\tau_1}\right)\theta_{1_i} \quad (5.4a)$$

$$\frac{d}{dt}\theta_{2_i} = \left(\frac{1}{\tau_3}\right)\theta_{1_i} - \left(\frac{1}{\tau_3}\right)\theta_{2_i} + \left(\frac{1}{\tau_3}\right)P_{mo_i} \quad (5.4b)$$

$$\frac{d}{dt}P_{m_i} = \left(\frac{F}{\tau_3}\right)\theta_{1_i} + \left[\left(\frac{1}{\tau_5}\right) - \left(\frac{F}{\tau_3}\right)\right]\theta_{2_i} - \left(\frac{1}{\tau_5}\right)P_{m_i} + \left(\frac{F}{\tau_3}\right)P_{mo_i} \quad (5.4c)$$

The gains and time constants used in the above equations are defined in Appendix B.

Linearization of the equations for the i^{th} generating unit give rise to the following matrix representation.

$$\begin{bmatrix} \Delta\dot{\underline{x}}_{m_i} \\ \Delta\dot{\underline{x}}_{e_i} \\ \Delta\dot{\underline{x}}_{t_i} \end{bmatrix} = \begin{bmatrix} \underline{A}_{m_i} & \underline{D}_{me_i} & \underline{D}_{mt_i} \\ \underline{D}_{em_i} & \underline{A}_{e_i} & \underline{0} \\ \underline{D}_{tm_i} & \underline{0} & \underline{A}_{t_i} \end{bmatrix} \begin{bmatrix} \Delta\underline{x}_{m_i} \\ \Delta\underline{x}_{e_i} \\ \Delta\underline{x}_{t_i} \end{bmatrix} + \begin{bmatrix} \underline{D}_{m_i} \\ \underline{D}_{e_i} \\ \underline{D}_{t_i} \end{bmatrix} \Delta\underline{I}_{m_i} + \begin{bmatrix} \underline{b}_{m_i} \\ \underline{b}_{e_i} \\ \underline{b}_{t_i} \end{bmatrix} \Delta\underline{u}_{m_i} \quad (5.5)$$

$$i=1,2,3,..,n$$

where

$$\Delta\underline{x}_{m_i} = [\Delta E_{q_i}\ \Delta E_{q_i}\ \Delta E_{d_i}\ \Delta\omega_i\ \Delta\delta_i]^T \quad (5.6a)$$

$$\Delta\underline{x}_{e_i} = [\Delta V_{1_i}\ \Delta V_{3_i}\ \Delta V_{R_i}\ \Delta E_{FD_i}]^T \quad (5.6b)$$

$$\Delta\underline{x}_{t_i} = [\Delta\theta_{1_i}\ \Delta\theta_{2_i}\ \Delta P_{m_i}]^T \quad (5.6c)$$

$$\Delta\underline{I}_{m_i} = [\Delta I_{q_i}\ \Delta I_{d_i}]^T \quad (5.6d)$$

$$\Delta\underline{u}_{m_i} = [\Delta P_{mo_i}\ \Delta V_{REF_i}]^T \quad (5.6e)$$

The submatrices in equation (5.5) are

$$\underline{A}_{m_i} = \begin{bmatrix} K_1 & K_2 & 0 & 0 & 0 \\ 1/T_1 & -1/T_2 & 0 & 0 & 0 \\ 0 & 0 & -1/T''_{q_o} & 0 & 0 \\ 0 & (1/2H)\bar{i}_q^o & -(1/2H)I_d^o & 0 & 0 \\ 0 & 0 & 0 & R & 0 \end{bmatrix} \tag{5.7a}$$

$$\underline{D}_{m_i} = \begin{bmatrix} 0 & 0 & 0 & 1/T'_{d_o} \\ 0 & 0 & 0 & K_5 \\ 0 & 0 & 0 & 0 \\ 0 & 0 & 0 & 0 \\ 0 & 0 & 0 & 0 \end{bmatrix} \tag{5.7b}$$

$$\underline{D}_{t_i} = \begin{bmatrix} 0 & 0 & 0 \\ 0 & 0 & 0 \\ 0 & 0 & 0 \\ 0 & 0 & (1/2H) \\ 0 & 0 & 0 \end{bmatrix} \tag{5.7c}$$

$$\underline{A}_{e_i} = \begin{bmatrix} -1/T_R & 0 & 0 & 0 \\ 0 & -1/T_F & K_F/T_F T_E & -K_F/T_F T_E \\ -K_A/T_A & -K_A/T_A & -1/T_A & 0 \\ 0 & 0 & 1/T_E & -K_E/T_E \end{bmatrix} \tag{5.8a}$$

$$\underline{D}_{em_i} = \begin{bmatrix} 0 & V_q^o/V_t^o & V_d^o/V_t^o & 0 & 0 \\ 0 & 0 & 0 & 0 & 0 \\ 0 & 0 & 0 & 0 & 0 \\ 0 & 0 & 0 & 0 & 0 \end{bmatrix} \qquad (5.8b)$$

$$\underline{A}_{t_i} = \begin{bmatrix} -1/\tau_1 & 0 & (1/2H)K'\tau_2/\tau_1 \\ 1/\tau_3 & -1/\tau_3 & 0 \\ F/\tau_3 & (1/\tau_5 - F/\tau_3) & -1/\tau_5 \end{bmatrix} \qquad (5.9a)$$

$$\underline{D}_{tm_i} = \begin{bmatrix} 0 & -(1/2H)\tau_2 K' I_q^o/\tau_1 & -(1/2H)\tau_2 K' I_d^o & K'/\tau_1 & 0 \\ 0 & 0 & 0 & 0 & 0 \\ 0 & 0 & 0 & 0 & 0 \end{bmatrix} \qquad (5.9b)$$

$$\underline{D}_{m_i} = \begin{bmatrix} 0 & K_3 \\ 0 & K_4 \\ K_6 & 0 \\ -(1/2H)E_q^{o\prime\prime} I_d^o & (1/2H)E_d^{o\prime\prime} I_q^o \\ 0 & 0 \end{bmatrix} \qquad (5.10a)$$

$$\underline{D}_{e_i} = \begin{bmatrix} -x_q''(V_q^o + V_d^o)/V_t^o & -r(V_q^o + V_d^o)/V_t^o \\ 0 & 0 \\ 0 & 0 \\ 0 & 0 \end{bmatrix} \qquad (5.10b)$$

$$\underline{D}_{t_i} = \begin{bmatrix} -(1/2H)K\ E_q^{o\prime\prime}/\tau_1 & -(1/2H)K'E_d^{o\prime\prime}/\tau_1 \\ 0 & 0 \\ 0 & 0 \end{bmatrix} \qquad (5.10c)$$

$$\underline{b}_{m_i} = \begin{bmatrix} 0 & 0 \\ 0 & 0 \\ 0 & 0 \\ (1/2H) & 0 \\ 0 & 0 \end{bmatrix} \qquad (5.11a)$$

$$\underline{b}_{e_i} = \begin{bmatrix} 0 & 0 \\ 0 & 0 \\ 0 & K_A/T_A \\ 0 & 0 \end{bmatrix} \qquad (5.11b)$$

$$\underline{b}_{t_i} = \begin{bmatrix} 0 & 0 \\ 1/\tau_3 & 0 \\ F/\tau_3 & 0 \end{bmatrix} \qquad (5.11c)$$

The "o" superscript indicates the steady-state equilibrium condition.

5.2.2 Generator-network change of reference frame

The following transformations are used to change from the DQ network reference frame to the dq reference frame and vice versa.

i) The transformation $\underline{T}_{DQ_i}$ maps vectors in the DQ vector space into the dq vector space. Thus, for the i^{th} machine

$$\underline{T}_{DQi} = \begin{bmatrix} \cos\delta_i & \sin\delta_i \\ -\sin\delta_i & \cos\delta_i \end{bmatrix} \qquad i=1,2,3,\ldots,n. \tag{5.12}$$

ii) The inverse transformation, $\underline{T}_{DQ}^{-1} = \underline{T}_{dq}$, maps vectors in the dq vector space into the DQ vector space. Thus, for the i^{th} machine

$$\underline{T}_{dqi} = \begin{bmatrix} \cos\delta_i & -\sin\delta_i \\ \sin\delta_i & \cos\delta_i \end{bmatrix} \qquad i=1,2,3,\ldots,n. \tag{5.13}$$

Note that $\underline{T}_{dq_i}$ and $\underline{T}_{DQ_i}$ are orthogonal transformations.

The linearization of the equations $\underline{I}_{m_i} = \underline{T}_{DQ_i}\underline{I}_{N_i}$ and $\underline{E}'_{m_i} = \underline{T}_{DQ_i}\underline{E}'_{N_i}$ results in

$$\Delta\underline{I}_{m_i} = \underline{T}^{o}_{DQ_i}\Delta\underline{I}_{N_i} + \underline{J}_i\Delta\delta_i \tag{5.14a}$$

$$\Delta\underline{E}_{m_i} = \underline{T}^{o}_{DQ_i}\Delta\underline{E}_{N_i} + \underline{K}^{o}_{i}\Delta\delta_i \qquad i=1,2,3,\ldots,n. \tag{5.14b}$$

where

$$\underline{T}^{o}_{DQ_i} = \begin{bmatrix} \cos\delta^{o}_i & \sin\delta^{o}_i \\ -\sin\delta^{o}_i & \cos\delta^{o}_i \end{bmatrix} \tag{5.15a}$$

$$\Delta\underline{I}_{N_i} = [\Delta I_Q \quad \Delta I_D]^T \tag{5.15b}$$

$$\Delta\underline{E}'_{N_i} = [\Delta E'_Q \quad \Delta E'_D]^T \tag{5.15c}$$

$$\underline{J}^{o}_{i} = [I^{o}_{d} \quad -I^{o}_{q}]^T \tag{5.15d}$$

$$\underline{K}_i^o = [E_d^{o\prime\prime} \quad -E_q^{o\prime\prime}]^T \tag{5.15e}$$

The superscript "o" indicates the steady-state equilibrium condition.

5.2.3 The network equations

Using the internal node representation in the network equations, the load-flow equations describing the interconnections among generators are

$$\begin{bmatrix} \Delta I_{Q1} \\ \Delta I_{D1} \\ \vdots \\ \Delta I_{Qn} \\ \Delta I_{Dn} \end{bmatrix} = \left[\begin{array}{cc|cc|c|cc} G_{11} & -B_{11} & G_{12} & -B_{12} & & G_{1n} & -B_{1n} \\ B_{11} & G_{11} & B_{12} & G_{12} & \cdots & B_{1n} & G_{1n} \\ \hline \vdots & & \vdots & & & \vdots & \\ \hline G_{1n} & -B_{1n} & G_{2n} & -B_{2n} & & G_{nn} & -B_{nn} \\ B_{1n} & G_{1n} & B_{2n} & G_{2n} & \cdots & B_{nn} & G_{nn} \end{array}\right] \begin{bmatrix} \Delta E'_{Q1} \\ \Delta E'_{D1} \\ \vdots \\ \Delta E'_{Qn} \\ \Delta E'_{Dn} \end{bmatrix} \tag{5.16}$$

where

$$\Delta \underline{E}'_{N_i} = \Delta E'_{Q_i} + j\Delta E'_{D_i} \tag{5.17}$$

and

$$Y_{ij} = G_{ij} + jB_{ij} \qquad i=1,2,\ldots,n, \quad j=1,2,\ldots,n \tag{5.18}$$

The linearization of the equations $\underline{E}'_{N_i} = \underline{T}_{dq_i}\underline{E}'_{m_i}$ and $\underline{I}_{N_i} = \underline{T}_{dq_i}\underline{I}_{m_i}$ results in

$$\Delta \underline{E}_{N_i} = \underline{T}^o_{dq_i}\Delta \underline{E}_{m_i} + \underline{D}^o_i \Delta\delta_i \tag{5.19a}$$

$$\Delta \underline{I}_{N_I} = \underline{T}^o_{dq_i}\Delta \underline{I}_{m_i} + \underline{F}^o_i \Delta\delta_i \qquad i=1,2,3,\ldots,n \tag{5.19b}$$

where

$$\underline{T}^{o}_{dq_i} = \begin{bmatrix} \cos\delta^{o}_i & -\sin\delta^{o}_i \\ \sin\delta^{o}_i & \cos\delta^{o}_i \end{bmatrix} \tag{5.20a}$$

$$\Delta\underline{E}_{m_i} = [\Delta E''_q \quad \Delta E''_d]^T \tag{5.20b}$$

$$\underline{D}^{o}_i = [-E^{o}_D{}'' \quad E^{o}_Q{}'']^T \tag{5.20c}$$

$$\underline{F}^{o}_i = [-I^{o}_D \quad I^{o}_Q]^T \tag{5.20d}$$

5.2.4 The system matrix

The system matrix is formed by arranging equation (5.5) for n generating units and eliminating the nonstate variables $\Delta\underline{I}_m$, i.e., $\Delta\underline{I}_m = [\Delta I_{m_1} \quad \Delta I_{m_2} \ldots \Delta I_{m_n}]^T$, as shown in Fig. 5.2. The resulting system of equations is given by equation (5.1), where the state and input vectors are

$$\underline{\omega} = [\Delta\underline{x}^T_{g_1} \quad \Delta\underline{x}^T_{g_2} \ldots \Delta\underline{x}^T_{g_n}]^T$$

$$\Delta\underline{x}_{g_i} = [\Delta\underline{x}^T_{m_i} \quad \Delta\underline{x}^T_{e_i} \quad \Delta\underline{x}^T_{t_i}]^T$$

and

$$\underline{u} = [\Delta\underline{u}^T_{m_1} \quad \Delta\underline{u}^T_{m_2} \ldots \Delta\underline{u}^T_{m_n}]^T$$

The rotor angles in (5.1) can be expressed with respect to the synchronous rotating axis of a reference machine, thereby reducing the order of the system by one in accordance with the procedure given in [49].

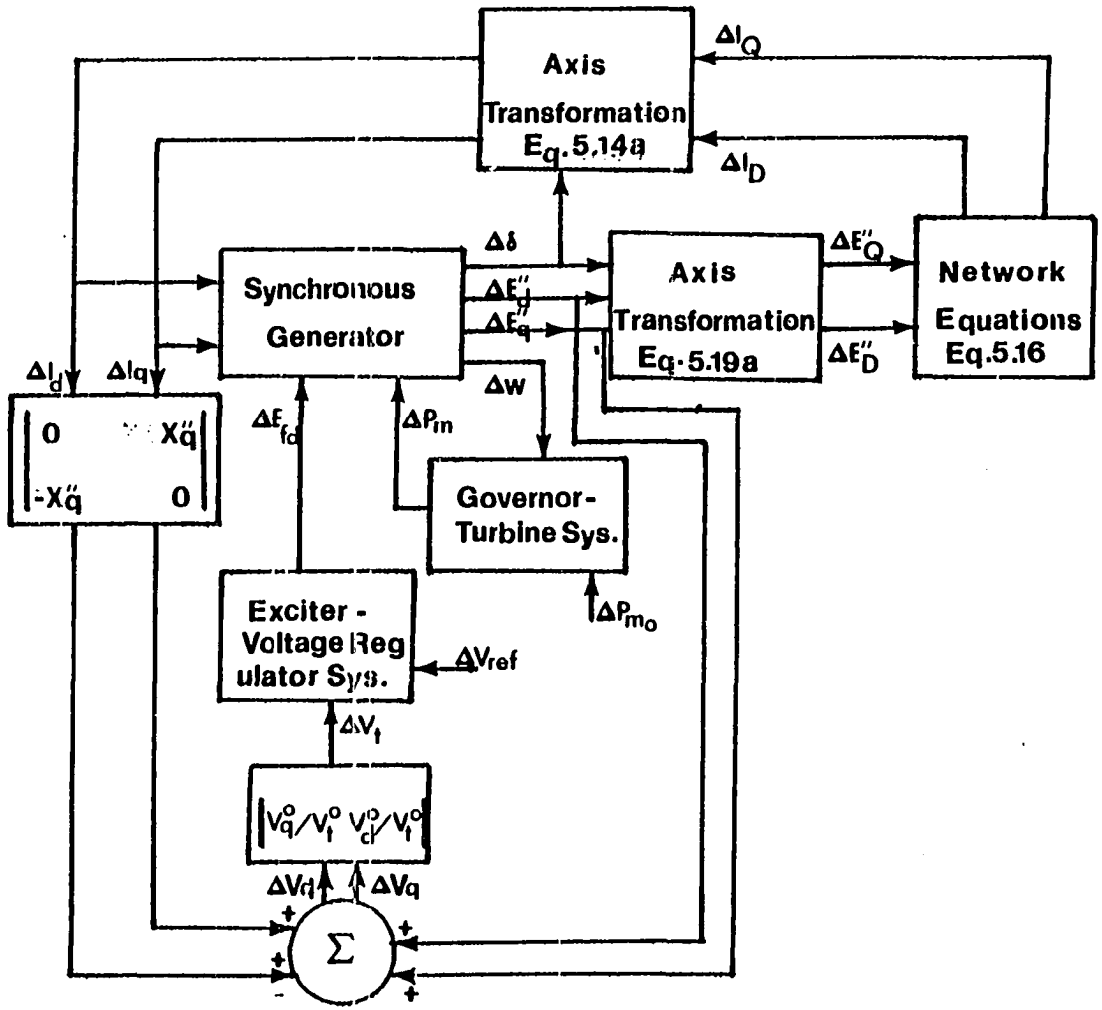

Fig. 5.2 Determination of the generating unit model equations in the state-space form by elminating those nonstate variables

Without loss of generality, let us assume that the dimensions of the vectors $\underline{\omega}$ and $\underline{u}$ are L and M respectively. Given that we are concerned with the simulation and dynamic simplification of equation (5.1), it is necessary to present a brief review of singular perturbation theory as it is applied to the solution of the initial value problem for linear time invariant systems.

5.3 Singular Perturbation Theory

Let us suppose the equation (5.1) is written in the singular perturbation form as

$$\begin{bmatrix} \dot{\underline{x}} \\ \hline \varepsilon\dot{\underline{y}} \end{bmatrix} = \left[\begin{array}{c|c} \underline{A}_{11} & \underline{A}_{12} \\ \hline \underline{A}'_{21} & \underline{A}'_{22} \end{array}\right] \begin{bmatrix} \underline{x} \\ \hline \underline{y} \end{bmatrix} + \begin{bmatrix} \underline{B}_1 \\ \hline \underline{B}'_2 \end{bmatrix} \underline{u} \tag{5.21}$$

where the matrices $\underline{A}'_{21}$, $\underline{A}'_{22}$ and $\underline{B}'_2$ are given by

$$\underline{A}'_{21} = \varepsilon\underline{A}_{21}$$

$$\underline{A}'_{22} = \varepsilon\underline{A}_{22}$$

$$\underline{B}'_2 = \varepsilon\underline{B}_2$$

The initial conditions of equation (5.21) are $\underline{x}(0) = \underline{x}^o$ and $\underline{y}(0) = \underline{y}^o$ respectively, and the dimension of the vectors $\underline{x}$ and $\underline{y}$ are ℓ_1 and ℓ_2 such that $\ell_1 + \ell_2 = L$. Moreover, assume that

i) The perturbation parameter ε is small and greater than zero.

ii) The matrix $\underline{A}_{22}$ is nonsingular, stable and not numerically stiff.

It should be mentioned that in physical systems the use of the perturbation parameter ε is symbolic and represents the presence of fast and slow subsystems described by $\underline{y}(t)$ and $\underline{x}(t)$ respectively. Hence, the presence of ε amounts to the verification of the presence of these two subsystems in equation (5.1) and the partitioning of the vector $\underline{\omega}$ as shown in (5.21).

The asymptotic solution of (5.21) is an additive function of the time variable t and the stretched variable $\tau = t/\varepsilon$. The solution sought is of the form [30]

$$\underline{x}(t,\varepsilon) = \underline{X}(t,\varepsilon) + \varepsilon\underline{p}(\tau,\varepsilon) \tag{5.22a}$$

$$\underline{y}(t,\varepsilon) = \underline{Y}(t,\varepsilon) + \underline{q}(\tau,\varepsilon) \tag{5.22b}$$

where $(\underline{X},\underline{Y})$ is the outer solution (i.e., the solution away from t=0) and $(\varepsilon\underline{p},\underline{q})$ is the so-called boundary layer correction (i.e., the solution that is significant near t=0). The vectors $\underline{X}$, $\underline{Y}$, $\underline{p}$ and $\underline{q}$ all have asymptotic expansions as $\varepsilon \to 0$.

$$\underline{X}(t,\varepsilon) \sim \sum_{j=0}^{\infty} \underline{X}_j(t)\varepsilon^j \tag{5.23a}$$

$$\underline{Y}(t,\varepsilon) \sim \sum_{j=0}^{\infty} \underline{Y}_j(t)\varepsilon^j \tag{5.23b}$$

$$p(\tau,\varepsilon) \sim \sum_{j=0}^{\infty} \underline{p}_j(\tau)\varepsilon^j \tag{5.23c}$$

$$q(\tau,\varepsilon) \sim \sum_{j=0}^{\infty} \underline{q}_j(\tau)\varepsilon^j \tag{5.23d}$$

To obtain the zero and first order approximations, the complete expansion (5.22) and the outer solution are used in the following manner. For any time t, the solution of $(\underline{x},\underline{y})$ would be given by the complete expansion, equation (5.22), such that it must satisfy equation (5.21). Thus,

$$\frac{d}{dt}(\underline{x}) = \frac{d}{dt}(\underline{X}) + \varepsilon \frac{d}{d\tau}(\underline{p}) \frac{d\tau}{dt} \tag{5.24a}$$

$$\frac{d}{dt}(\underline{y}) = \frac{d}{dt}(\underline{Y}) + \frac{d}{d\tau}(\underline{q}) \frac{d\tau}{dt} \tag{5.24b}$$

since $\tau = t/\varepsilon$, $\frac{d\tau}{dt} = \frac{1}{\varepsilon}$ and the above set of equations become

$$\dot{\underline{x}} = \frac{d}{dt}(\underline{X}) + \frac{d}{d\tau}(\underline{p}) \tag{5.25a}$$

$$\varepsilon\dot{\underline{y}} = \varepsilon \frac{d}{dt}(\underline{Y}) + \frac{d}{d\tau}(\underline{q}) \tag{5.25b}$$

After substituting equations (5.22) and (5.25) into equation (5.21) we get

$$\frac{d}{dt}(\underline{X}) + \frac{d}{d\tau}(\underline{p}) = \underline{A}_{11}(\underline{X}+\varepsilon\underline{p}) + \underline{A}_{21}(\underline{Y}+\underline{q}) + \underline{B}_1\underline{u} \tag{5.26a}$$

$$\varepsilon \frac{d}{dt}(\underline{Y}) + \frac{d}{d\tau}(\underline{q}) = \underline{A}'_{21}(\underline{X}+\varepsilon\underline{p}) + \underline{A}'_{22}(\underline{Y}+\underline{q}) + \underline{B}'_2\underline{u} \tag{5.26b}$$

with initial conditions

$$\underline{x}(0) = \underline{X}(0) + \varepsilon\underline{p}(0) \tag{5.26c}$$

$$\underline{y}(0) = \underline{Y}(0) + \underline{q}(0) \tag{5.26d}$$

If the vectors $\underline{X}$, $\underline{Y}$, $\underline{p}$ and $\underline{q}$ in equations (5.26a) and (5.25b) are replaced by their asymptotic expansions and if we equate the coefficients of ε^0 and ε, the following results are obtained.

$$\frac{d}{dt}(\underline{X}_0) + \frac{d}{d\tau}(\underline{p}_0) = \underline{A}_{11}\underline{X}_0(t) + \underline{A}_{12}\underline{Y}_0(t) + \underline{A}_{12}\underline{q}_0(\tau) + \underline{B}_1\underline{u} \tag{5.27a}$$

$$\frac{d}{d\tau}(\underline{q}_0) = \underline{A}'_{21}\underline{X}_0(t) + \underline{A}'_{22}\underline{Y}_0(t) + \underline{A}'_{22}\underline{q}_0(\tau) + \underline{B}'_2\underline{u} \tag{5.27b}$$

and

$$\frac{d}{dt}(\underline{X}_1) + \frac{d}{d\tau}(\underline{p}_1) = \underline{A}_{11}\underline{X}_1(t) + \underline{A}_{12}\underline{Y}_1(t) + \underline{A}_{11}\underline{p}_0(\tau) + A_{12}\underline{q}_1(\tau) \tag{5.28a}$$

$$\frac{d}{dt}(\underline{Y}_0) + \frac{d}{d\tau}(\underline{q}_1) = \underline{A}'_{21}\underline{X}_1(t) + \underline{A}'_{22}\underline{Y}_1(t) + \underline{A}'_{21}\underline{p}_0(\tau) + A'_{22}\underline{q}_1(\tau) \tag{5.28b}$$

Now, since $\tau \to \infty$ as $\varepsilon \to 0$, the solution $(\underline{x},\underline{y})$ will converge to the outer solution $(\underline{X},\underline{Y})$ because the boundary layer correction $(\underline{p},\underline{q})$ converges to zero as $\varepsilon \to 0$. Thus, the outer solution $(\underline{X},\underline{Y})$ must satisfy equation (5.21) for those values of t where the boundary layer correction $(\varepsilon\underline{p},\underline{q})$ vanishes. Hence, equation (5.21) becomes

$$\frac{d}{dt}(\underline{X}) = \underline{A}_{11}\underline{X} + \underline{A}_{21}\underline{Y} + \underline{B}_1\underline{u} \tag{5.29a}$$

$$\varepsilon\frac{d}{dt}(\underline{Y}) = \underline{A}'_{21}\underline{X} + \underline{A}'_{22}\underline{Y} + \underline{B}'_2\underline{u} \tag{5.29b}$$

After substituting equations (5.23) into equations (5.29a) and (5.29b) and equating the coefficients of ε^0 and ε, we obtain

$$\frac{d}{dt}(\underline{X}_0) = \underline{A}_{11}\underline{X}_0(t) + \underline{A}_{12}\underline{Y}_0(t) + \underline{B}_1\underline{u} \tag{5.30a}$$

$$\underline{0} = \underline{A}_{21}'\underline{X}_0(t) + \underline{A}_{22}'\underline{Y}_0(t) + \underline{B}_2'\underline{u} \tag{5.30b}$$

and

$$\frac{d}{dt}(\underline{X}_1) = \underline{A}_{11}\underline{X}_1(t) + A_{12}\underline{Y}_1(t) \tag{5.31a}$$

$$\frac{d}{dt}(\underline{Y}_0) = \underline{A}_{21}'\underline{X}_1(t) + \underline{A}_{22}'\underline{Y}_1(t) \tag{5.31b}$$

By using the results given by equations (5.27), (5.28), (5.30) and (5.31), we are able to construct the following differential equations which will yield the vectors $\underline{p}_0(\tau)$, $\underline{q}_0(\tau)$, $\underline{p}_1(\tau)$ and $\underline{q}_1(\tau)$ present in the zero order approximation of $(\underline{x},\underline{y})$.

$$\frac{d}{d\tau}(\underline{p}_0) = \underline{A}_{12}\underline{q}_0(\tau) \tag{5.32a}$$

$$\frac{d}{d\tau}(\underline{q}_0) = \underline{A}_{22}'\underline{q}_0(\tau) \tag{5.32b}$$

$$\frac{d}{d\tau}(\underline{p}_1) = \underline{A}_{11}\underline{p}_0(\tau) + \underline{A}_{12}\underline{q}_1(\tau) \tag{5.32c}$$

$$\frac{d}{d\tau}(\underline{q}_1) = \underline{A}_{21}'\underline{p}_0(\tau) + \underline{A}_{22}'\underline{q}_1(\tau) \tag{5.32d}$$

Remaining is the computation of the boundary conditions for the equations (5.30a), (5.31a), (5.31b) and (5.32). This is accomplished by substituting equations (5.23) into equations (5.26) and equating the coefficients of ε^0 and ε with the result that

$$\underline{X}_0(0) = \underline{x}(0) = \underline{x}^0 \tag{5.33a}$$

$$\underline{X}_1(0) + \underline{p}_0(0) = \underline{0} \tag{5.33b}$$

and

$$\underline{p}_0(\infty) = \underline{0} \quad \text{as} \quad \varepsilon \to 0 \tag{5.33c}$$

$$\underline{Y}_0(0) + \underline{q}_0(0) = \underline{y}(0) = \underline{y}^o \tag{5.33d}$$

$$\underline{Y}_1(0) + \underline{q}_1(0) = \underline{0} \tag{5.33e}$$

Having obtained all the differential equations and their initial conditions necessary to construct the zero and first order approximations, a procedure leading to such results is now outlined.

i) The zero order approximation.

$$\underline{x}(t,\varepsilon) = \underline{X}_0(t) + \underline{0}(\varepsilon) \tag{5.34a}$$

$$\underline{y}(t,\varepsilon) = \underline{Y}_0(t) + \underline{q}_0(\tau) + \underline{0}(\varepsilon) \tag{5.34b}$$

where $\underline{X}_0$, $\underline{Y}_0$ and $\underline{q}_0$ are computed from

$$\frac{d}{dt}(\underline{X}_0) = [\underline{A}_{11} - \underline{A}_{12}\underline{A}_{22}^{-1}\underline{A}_{21}]\underline{X}_0(t) + (\underline{B}_1 - \underline{A}_{12}\underline{A}_{22}^{-1}\underline{B}_2)\underline{u}]$$

$$\underline{X}_0(0) = \underline{x}^o \tag{5.35a}$$

$$\underline{Y}_0(t) = -\underline{A}_{22}^{-1}\underline{A}_{21}\underline{X}_0(t) - \underline{A}_{22}^{-1}\underline{B}_2\underline{u} \tag{5.35b}$$

$$\frac{d}{d\tau}(\underline{q}_0) = \underline{A}_{22}\underline{q}_0(\tau); \quad \underline{q}_0(0) = \underline{y}^o - \underline{Y}_0(0) \tag{5.35c}$$

ii) The first order approximation.

$$\underline{x}(t,\varepsilon) = \underline{X}_0(t) + \varepsilon[\underline{p}_0(\tau) + \underline{X}_1(t)] + \underline{0}(\varepsilon^2) \tag{5.36a}$$

$$\underline{y}(t,\varepsilon) = \underline{Y}_0(t) + \underline{q}_0(\tau) + \varepsilon[\underline{q}_1(t) + \underline{Y}_1(t)] + \underline{0}(\varepsilon^2) \tag{5.36b}$$

where $\underline{X}_1$, $\underline{p}_0$, $\underline{q}_1$ and $\underline{Y}_1$ are computed from

$$\frac{d}{d\tau}(\underline{p}_0) = \underline{A}_{12}\underline{q}_0(\tau);\ \underline{p}_0(\infty) = 0 \tag{5.37a}$$

$$\frac{d}{dt}(\underline{X}_1) = [\underline{A}_{11} - \underline{A}_{12}\underline{A}_{22}^{-1}\underline{A}_{21}]\underline{X}_1(t) + \underline{A}_{12}\underline{A}_{22}^{-1}[\frac{d}{dt}\underline{Y}_0];$$

$$\underline{X}_1(0) = -\underline{p}_0(0) \tag{5.37b}$$

where

$$\frac{d}{dt}(\underline{Y}_0) = \underline{A}_{21}\underline{X}_0(t) + \underline{A}_{22}\underline{Y}_0(t) + \underline{B}_2\underline{u}$$

$$\underline{Y}_1(t) = -\underline{A}_{22}^{-1}\underline{A}_{21}\underline{X}_1(t) + \underline{A}_{22}^{-1}[\frac{d}{dt}\underline{Y}_0] \tag{5.37c}$$

$$\frac{d}{d\tau}(\underline{q}_1) = \underline{A}_{21}\underline{p}_0(\tau) + \underline{A}_{22}\underline{q}_1(\tau);\ \underline{q}_1(0) = -\underline{Y}_1(0) \tag{5.37d}$$

5.4 Numerical Example

An example of the dynamical simplification of the full scale system equations based on the singular perturbation theory is presented here. A single generator-infinite bus system represented by a set of linearized ordinary differential equations is used. The equations describe the dynamics of the synchronous generator and its control units, the voltage regulator-exciter and governor-turbine systems. Details of the models describing the above subsystems are provided in Appendix B.

Also, selected graphs of some of the most important state variables arrived at by using a conventional method of integration as well as the proposed method based on singular perturbation are shown.

The line diagram of the system is shown in Fig. 5.3. The system data are listed below.

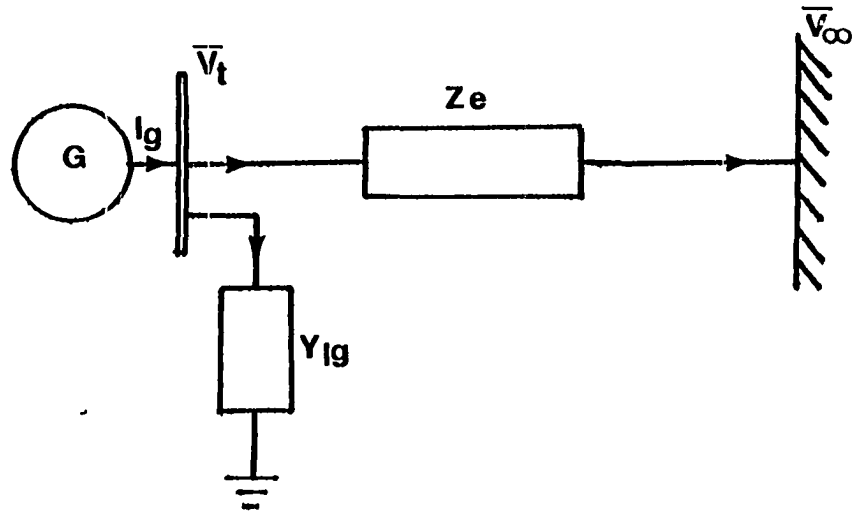

Fig. 5.3 The synchronous machine - infinite bus system

i) The synchronous machine.

rated MVA = 160; rated voltage = 15 KV; Y connected;
excitation voltage = 375V; power factor = 0.85;
H = 2.37 seconds; r_a = 0.001096 p.u., x_q'' = 0.185 p.u.;
x_d'' = 0.185 p.u.; x_q' = 0.380 p.u.; x_d' = 0.245 p.u.;
x_q = 1.64 p.u.; x_d = 1.70 p.u.; T_{do}' = 5.9 seconds;
T_d'' = 0.023 seconds; T_{qo}' = T_{qo}'' = 0.075 seconds; T_{do}'' = 0.03046 seconds.

ii) The voltage regulator-exciter system (IEEE Type I).

K_A = 25 p.u.; K_E = -0.044 p.u.; K_F = 0.0805 p.u.;
K_R = 1.0 p.u.; T_A = 0.2 seconds; T_E = 0.5 seconds;
T_F = 0.35 seconds; T_R = 0.06 seconds; $V_{R_{MAX}}$ = 1.0 p.u.;
$V_{R_{MIN}}$ = -1.0 p.u.; S_E = 0.0 (i.e., saturation is neglected).

iii) The governor-turbine system.

τ_1 = 30.0 seconds; τ_2 = 3.5 seconds; τ_3 = 0.52 seconds;
τ_4 = 0.0 seconds; τ_5 = 0.415 seconds; F = -2.0 p.u.;
P_{max} = 250 MW; K' = 0.333; R = 0.05; f_0 = 60 Hz.

iv) The transmission line.

R_e = 0.02 p.u.; X_e = 0.4 p.u.

v) The local load.

$1/R_0$ = 0.01 p.u.; $1/X_{c_o}$ = 0.01 p.u.

vi) The injected power at the machine terminal bus.

P + jQ = 1.28 + j0.87 p.u.

vii) The voltage at the infinite bus.

$\bar{V}_\infty$ = 0.828 + j0.0 p.u.

The initial conditions obtained from the above operating conditions are as follows.

i) The synchronous machine.

I_q^o = 0.385 p.u.; I_Q^o = 1.174 p.u.

I_d^o = -1.12 p.u.; I_D^o = -0.0802 p.u.

$E_q^{o''} = 0.982$ p.ul; $E_q^{o'} = 1.05$ p.u.

$E_d^{o''} = -0.56$ p.u.; $\delta^o = 66.995$ electrical degrees

$V_q^o = 0.7764$ p.u.; $V_Q^o = 0.4661$ p.u.

$V_d^o = -0.636$ p.u.; $V_D^o = 0.8889$ p.u.

$\omega_R = 1.0$ p.u.

ii) The voltage regulator-exciter system.

$V_1^o = 1.0037$ p.u.; $V_3^o = 0.0$ p.u.; $V_R^o = -0.1173$ p.u.;

$E_{FD}^o = 2.666$ p.u.; $V_{REF}^o = 0.999$ p.u.

iii) The governor-turbine system.

$\theta_1^o = 0.0$ p.u.; $\theta_2^o = 0.0$ p.u.; $P_m^o = 1.0$ p.u.

Since the analysis performed here is for dynamic stability, the initial conditions for the incremental state variables are all equal to zero.

Using the above operating point conditions, system gains and time constants, the following linearized differential equations are obtained.

$$\Delta\dot{E}_q' = -2.76\Delta E_q' + 2.43217\Delta E_q'' + 0.00603\Delta E_d'' - 0.11582\Delta\delta + 0.1689\Delta E_{FD}$$

$$\Delta\dot{E}_q'' = 31.95\Delta E_q' - 35.95\Delta E_q'' + 0.1332\Delta E_d'' - 2.5581\Delta\delta + 0.0624\Delta E_{FD}$$

$$\Delta\dot{E}_d'' = -1.286\Delta E_q'' - 46.3379\Delta E_d'' - 11.5624\Delta\delta$$

$$\Delta\dot{\omega} = -0.296\Delta E_q'' - 0.1101\Delta E_d'' - 0.2739\Delta\delta + 0.211\Delta P_m$$

$$\Delta\dot{\delta} = 377.0\Delta\omega$$

$$\Delta\dot{V}_1 = 8.9817\Delta E_q'' - 7.105\Delta E_d'' - 1.8633\Delta\delta - 16.667\Delta V_1$$

$$\Delta\dot{V}_3 = -2.8571\Delta V_3 + 0.4857\Delta V_R + 0.0214\Delta E_{FD}$$

$$\Delta\dot{V}_R = -125.0\Delta V_1 - 125.0\Delta V_3 - 5.0\Delta V_R + 125.0\Delta V_{REF}$$

$$\Delta\dot{E}_{F_D} = 2.0\Delta V_R + 0.088\Delta E_{FD}$$

$$\Delta\dot{\theta}_1 = -0.0116\Delta E''_q - 0.043\Delta E''_d + 0.0111\Delta\omega - 0.0107\Delta\delta - 0.0333\Delta\theta_1 + 0.0082\Delta P_m$$

$$\Delta\dot{\theta}_2 = 1.9231\Delta\theta_1 - 1.9231\Delta\theta_2 + 1.9231\Delta P_{m_o}$$

$$\Delta\dot{P}_m = -3.8462\Delta\theta_1 + 6.2558\Delta\theta_2 - 2.4096\Delta P_m + 3.8462\Delta P_{m_o}$$

After casting the above equations into a matrix form, the following system matrix $\underline{A}$ results as shown on the following page.

The eigenvalues of matrix $\underline{A}$ are listed below.

$\lambda_1 = -46.10883$ $\lambda_7 = -2.06301$

$\lambda_2 = -37.4932$ $\lambda_8 = -0.37273 + j9.31282$

$\lambda_3 = -16.54938$ $\lambda_9 = -0.37273 - j9.31282$

$\lambda_4 = -3.85673 + j7.52069$ $\lambda_{10} = -0.17363 + j0.928$

$\lambda_5 = -3.85673 - j7.52069$ $\lambda_{11} = -0.17363 - j0.928$

$\lambda_6 = -2.27338$ $\lambda_{12} = -0.02494$

It is evident that the time constants associated with these eigenvalues vary over a wide range (i.e., the system of equations is numerically stiff) and that the time domain responses for the various state variables

$$A = \begin{array}{c} \\ 1 \\ 2 \\ 3 \\ 4 \\ 5 \\ 6 \\ 7 \\ 8 \\ 9 \\ 10 \\ 11 \\ 12 \end{array} \begin{array}{c} \begin{array}{cccccccccccc} 1 & 2 & 3 & 4 & 5 & 6 & 7 & 8 & 9 & 10 & 11 & 12 \end{array} \\ \begin{bmatrix} -2.76 & 2.43217 & 0.00603 & 0.0 & -0.11582 & 0.0 & 0.0 & 0.0 & 0.1689 & 0.0 & 0.0 & 0.0 \\ 31.95 & -35.4199 & 0.1332 & 0.0 & -2.55813 & 0.0 & 0.0 & 0.0 & 0.0624 & 0.0 & 0.0 & 0.0 \\ 0.0 & -1.28603 & -46.33794 & 0.0 & -11.5624 & 0.0 & 0.0 & 0.0 & 0.0 & 0.0 & 0.0 & 0.0 \\ 0.0 & -0.2960 & -0.1101 & 0.0 & -0.2739 & 0.0 & 0.0 & 0.0 & 0.0 & 0.0 & 0.0 & 0.211 \\ 0.0 & 0.0 & 0.0 & 377.0 & 0.0 & 0.0 & 0.0 & 0.0 & 0.0 & 0.0 & 0.0 & 0.0 \\ 0.0 & 8.9817 & -7.105 & 0.0 & -1.8633 & -16.6667 & 0.0 & 0.0 & 0.0 & 0.0 & 0.0 & 0.0 \\ 0.0 & 0.0 & 0.0 & 0.0 & 0.0 & 0.0 & -2.8571 & 0.4857 & 0.0214 & 0.0 & 0.0 & 0.0 \\ 0.0 & 0.0 & 0.0 & 0.0 & 0.0 & -125.0 & -125.0 & -5.0 & 0.0 & 0.0 & 0.0 & 0.0 \\ 0.0 & 0.0 & 0.0 & 0.0 & 0.0 & 0.0 & 0.0 & 2.0 & 0.088 & 0.0 & 0.0 & 0.0 \\ 0.0 & -0.0116 & -0.043 & 0.0111 & -0.0107 & 0.0 & 0.0 & 0.0 & 0.0 & -0.0333 & 0.0 & 0.0082 \\ 0.0 & 0.0 & 0.0 & 0.0 & 0.0 & 0.0 & 0.0 & 0.0 & 0.0 & 1.9231 & -1.9231 & 0.0 \\ 0.0 & 0.0 & 0.0 & 0.0 & 0.0 & 0.0 & 0.0 & 0.0 & 0.0 & -3.8462 & 6.2558 & -2.4096 \end{bmatrix} \end{array}$$

may be of short or long duration depending on which time constants are more significant in each response.

The separation of state variables into slow and fast subsets is largely a matter of insight and experience aided by knowledge of the time constants and gains in the system equations as well as the location of the perturbation in the power system. The perturbation used in the present example is a 10% step change in the input controlling the machine terminal voltage $\bar{V}_t$, i.e., ΔV_{REF}, keeping the other input, ΔP_{m_o}, unchanged. It is thus expected that those variables describing the voltage regulator dynamics will be excited with more intensity than those located in other parts of the model. Based on the foregoing, the outputs of the voltage regulator and stabilizer, ΔV_R and ΔV_3 respectively, were chosen as fast variables. Other potential sets of fast variables, particularly those with very small time constants (e.g., $\Delta E''_q$ and $\Delta E''_d$), were tested with negative results.

The choice of the size of the perturbation parameter, ε, is made by comparing the relative magnitudes of the real parts of the eigenvalues of $\underline{A}$. Experience and insight are again helpful. It was found that $\varepsilon = 0.1$ was an excellent choice for this example. The selection of this value makes the fast time scale 10 times greater than the scale used for the slow variables.

With the above partitioning of state variables, the fast and slow vectors are then

$$\underline{y} = [\Delta V_3 \quad \Delta V_R]^T$$

and

$$\underline{x} = [\Delta E_q' \quad \Delta E_q'' \quad \Delta E_d'' \quad \Delta\omega \quad \Delta\delta \quad \Delta V_1 \quad \Delta E_{F_D} \quad \Delta\theta_1 \quad \Delta\theta_2 \quad \Delta P_m]^T$$

with the matrices $\underline{A}_{11}$, $\underline{A}_{12}$, $\underline{A}_{21}'$ and $\underline{A}_{22}'$ given on the following page. The vectors associated with the step forcing functions ΔP_{m_o} and ΔV_{REF} are partitioned as follows:

$$\underline{B}_1 = \underline{0} \quad \text{(10-dimensional vector)}$$

$$B_2' = [0.0 \quad 12.5]^T$$

Using the above results, the following sets of differential equations giving the reduced order system $(\underline{X}_0, \underline{Y}_0)$, equations (5.30), and the boundary layer correction $q_0(\tau)$, equation (5.32b), are assembled.

i) $\dot{\underline{X}}_0 = [\underline{A}_{11} - \underline{A}_{12}\underline{A}_{22}'^{-1}\underline{A}_{21}']\underline{X}_0(t) + [\underline{B}_{11} - \underline{A}_{12}\underline{A}_{22}'^{-1}\underline{B}_2']\underline{u}(t); \quad \underline{X}(0) = \underline{0}$

$$\dot{X}_{10} = -2.76X_{10} + 2.43217X_{20} + 0.0063X_{30} - 0.11582X_{50} + 0.1689X_{70}$$

$$\dot{X}_{20} = 31.95X_{10} - 35.4199X_{20} + 0.1332X_{30} - 2.55813X_{50} + 0.0624X_{70}$$

$$\dot{X}_{30} = -1.28603X_{20} - 46.3379X_{30} - 11.5624X_{50}$$

$$\dot{X}_{40} = -0.296X_{20} - 0.1101X_{30} - 0.2739X_{50} + 0.211X_{100}$$

$$\dot{X}_{50} = 377.0X_{40}$$

$$\dot{X}_{60} = 8.9817X_{20} - 7.105X_{30} - 1.8633X_{50} - 16.6667X_{60}$$

$$\dot{X}_{70} = -9.5239X_{60} + 0.01666X_{70} + 9.5239\Delta V_{REF}$$

$$\dot{X}_{80} = -0.0116X_{20} - 0.043X_{40} + 0.0111X_{40} - 0.0107X_{50} - 0.0333X_{80} + 0.0082X_{100}$$

$$\underline{A}_{11} = \begin{array}{c} \begin{array}{cccccccccc} 1 & 2 & 3 & 4 & 5 & 6 & 9 & 10 & 11 & 12 \end{array} \\ \left[\begin{array}{cccccccccc} -2.76 & 2.43217 & 0.00603 & 0.0 & -0.11582 & 0.0 & 0.1689 & 0.0 & 0.0 & 0.0 \\ 31.95 & -35.4199 & 0.1332 & 0.0 & -2.55813 & 0.0 & 0.0624 & 0.0 & 0.0 & 0.0 \\ 0.0 & -1.28603 & -46.3379 & 0.0 & -11.5624 & 0.0 & 0.0 & 0.0 & 0.0 & 0.0 \\ 0.0 & -0.2960 & -0.1101 & 0.0 & -0.2739 & 0.0 & 0.0 & 0.0 & 0.0 & 0.211 \\ 0.0 & 0.0 & 0.0 & 377.0 & 0.0 & 0.0 & 0.0 & 0.0 & 0.0 & 0.0 \\ 0.0 & 8.9817 & -7.105 & 0.0 & -1.8633 & -16.6667 & 0.0 & 0.0 & 0.0 & 0.0 \\ 0.0 & 0.0 & 0.0 & 0.0 & 0.0 & 0.0 & 0.088 & 0.0 & 0.0 & 0.0 \\ 0.0 & -0.0116 & -0.043 & 0.0 & -0.0107 & 0.0 & 0.0 & -0.0333 & 0.0 & 0.0082 \\ 0.0 & 0.0 & 0.0 & 0.0 & 0.0 & 0.0 & 0.0 & 1.4231 & -1.9231 & 0.0 \\ 0.0 & 0.0 & 0.0 & 0.0 & 0.0 & 0.0 & 0.0 & -3.8462 & 6.2558 & -2.4096 \end{array}\right] \end{array}$$

$$\underline{A}'_{22} = \begin{array}{c} \begin{array}{cc} 7 & 8 \end{array} \\ \left[\begin{array}{cc} -0.2857 & 0.04857 \\ -12.5 & -0.5 \end{array}\right] \end{array}$$

$$\underline{A}'_{21} = \begin{array}{c} \\ 7 \\ 8 \end{array} \left[\begin{array}{cccccccccc} 0.0 & 0.0 & 0.0 & 0.0 & 0.0 & 0.0 & 0.00214 & 0.0 & 0.0 & 0.0 \\ 0.0 & 0.0 & 0.0 & 0.0 & 0.0 & -12.5 & 0.0 & 0.0 & 0.0 & 0.0 \end{array}\right]$$

$$A_{12}^{T} = \begin{array}{c} \\ 7 \\ 8 \end{array} \left[\begin{array}{cccccccccc} 0.0 & 0.0 & 0.0 & 0.0 & 0.0 & 0.0 & 0.0 & 0.0 & 0.0 & 0.0 \\ 0.0 & 0.0 & 0.0 & 0.0 & 0.0 & 0.0 & 2.0 & 0.0 & 0.0 & 0.0 \end{array}\right]$$

$$\dot{X}_{90} = 1.9231X_{80} - 1.9231X_{90}$$

$$\dot{X}_{100} = -3.8462X_{80} + 6.2558X_{90} - 2.4096X_{100}$$

ii) $\underline{Y}_0(t) = -\underline{A}_{22}^{-1}\underline{A}_{21}\underline{X}_0(t) - \underline{A}_{21}^{-1}\underline{B}_2\underline{u}$

$$Y_{10} = -0.8095X_{60} + 0.0014X_{70} + 0.8095\Delta V_{REF}$$

$$Y_{20} = -4.76196X_{60} - 0.0357X_{70} + 4.76196\Delta V_{REF}$$

iii) $\frac{d}{d\tau}(\underline{q}_0) = \underline{A}_{22}\underline{q}_0(\tau);\ \underline{q}_0(0) = \underline{y}(0) - \underline{Y}_0(0)$

$$\frac{d}{d\tau} q_{10} = -0.2857q_{10} + 0.0486q_{20};\ q_{10}(0) = -Y_{10}(0)$$

$$\frac{d}{d\tau} q_{20} = -12.5q_{10} - 0.5q_{20};\ q_{20}(0) = -Y_{20}(0)$$

The eigenvalues of the matrices $\underline{A}_{EQ} = [\underline{A}_{11} - \underline{A}_{12}\underline{A}_{22}^{-1}\underline{A}_{21}]$ and $\underline{A}_{22}$ used in the zero order approximation are listed below.

$\lambda_1 = -46.1092$ $\qquad$ $\lambda_6 = -0.0624 + j0.9141$

$\lambda_2 = -37.4759$ $\qquad$ $\lambda_7 = -0.0624 - j0.9141$

$\lambda_3 = -16.7372$ $\qquad$ $\lambda_8 = -2.2709$

$\lambda_4 = -0.3624 + j9.3140$ $\qquad$ $\lambda_9 = -2.0660$

$\lambda_5 = -0.3624 - j9.3140$ $\qquad$ $\lambda_{10} = -0.0249$

and

$$\lambda_1 = -3.9286 + j7.7178$$

$$\lambda_2 = -3.9286 - j7.7178$$

A set of graphs showing the fast variables ΔV_3 and ΔV_R and two slow variables, $\Delta\omega$ and $\Delta E'_q$, is provided. Figures 5.4 and 5.5 show the full scale model solution, the reduced order solution and zero order approximation of the variables ΔV_3 and ΔV_R, respectively. Figures 5.6 and 5.7 show the full scale model and zero order approximation responses of the variables $\Delta\omega$ and $\Delta E'_q$. In this case, these being the slow variables, the zero order approximation and the reduced order solution are numerically identical.

It is noted that the graphs showing the reduced order solution for the fast variables ΔV_3 and ΔV_R do not start at the origin while the full scale and zero order approximation solutions do. This sudden jump present in the reduced order solution is due to the absence of the term $\underline{q}_0(\tau)$ which accounts for the fast phenomena, significant near t=0. Such difference in magnitude at t=0 is called boundary layer jump. Now, with regard to the graphs describing the slow variables $\Delta\omega$ and $\Delta E'_q$ it can be seen that the zero order approximation follows the response given by the full scale model very closely. The slight differences in magnitude between responses stem from the fact that the magnitudes of the real parts of the eigenvalues of the equivalent system (slow and fast subsystems) are slightly smaller than those in the original system model.

As one may conclude from this numerical example, this technique is promising for the solution of the problem of dynamic stability in multimachine power systems where generating units are described by complex models. The extension to the multimachine problem is implicit in the procedure described in Section 5.2. In summary, the singular perturbation technique method is simpler and faster than conventional numerical algorithms. This is due to the two time scale decomposition and the use of the asymptotic approximation used for the computation of the time response of the state variables of the system.

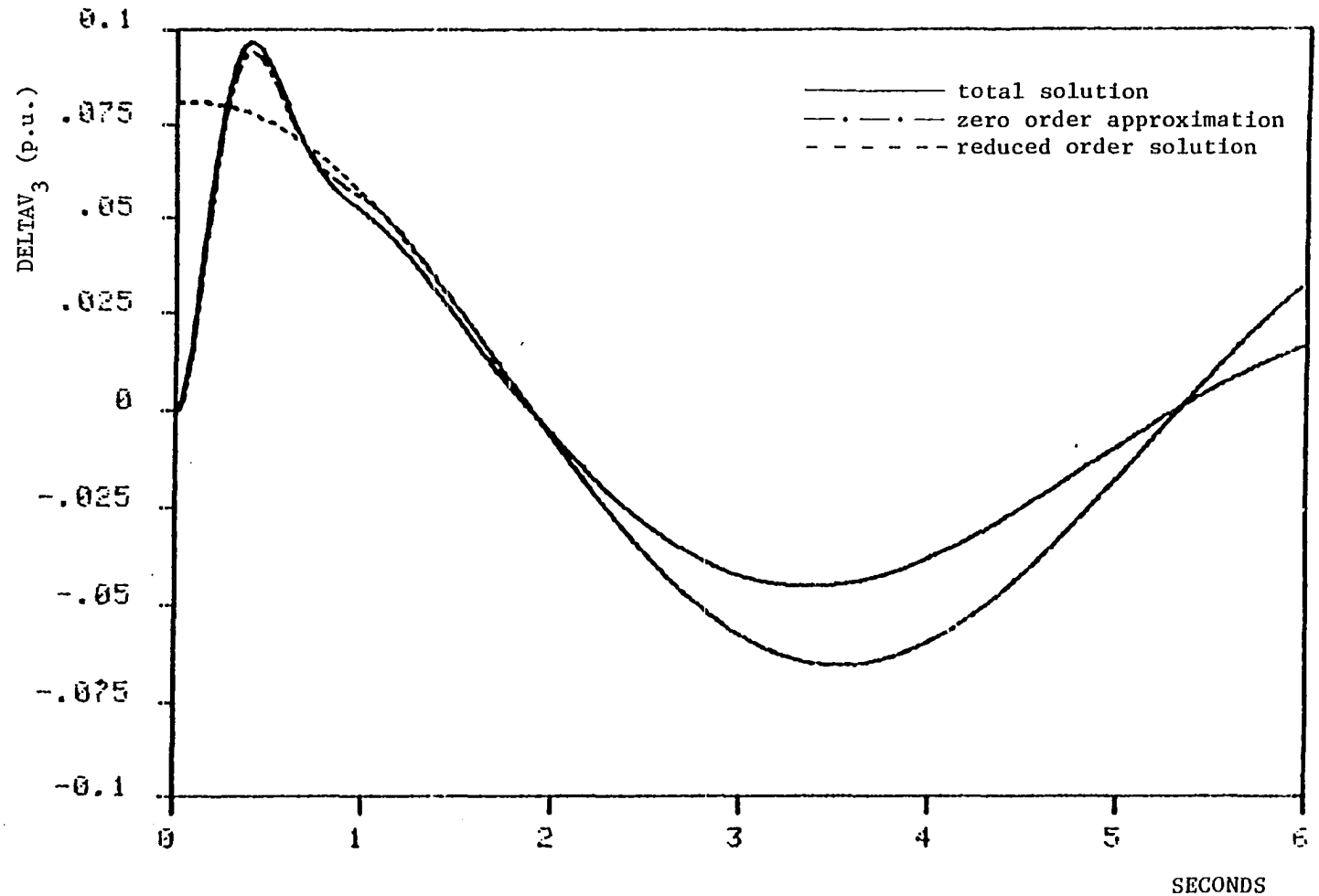

Fig. 5.4 Total, zero approximation and reduced order solutions for the state variable ΔV_3

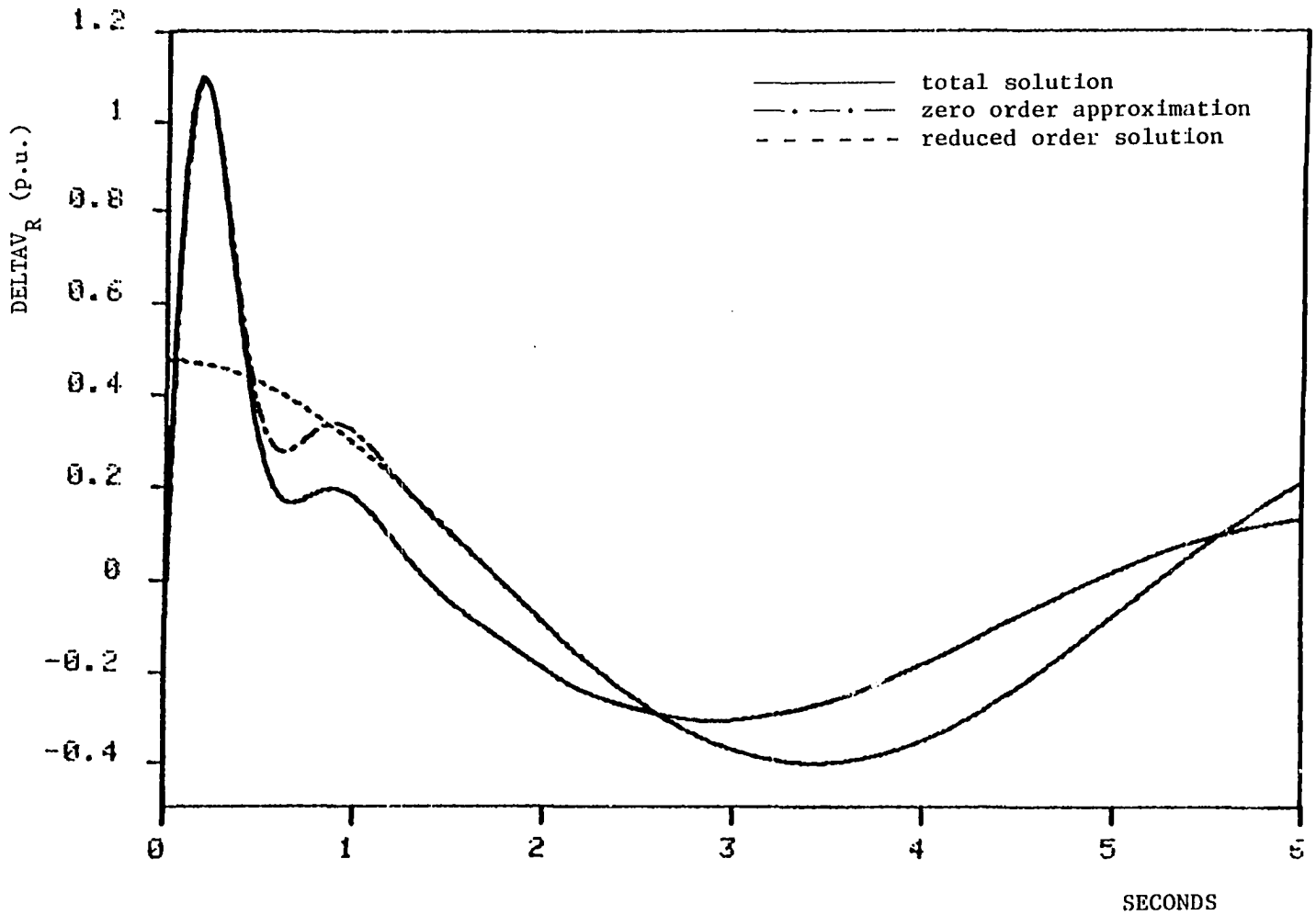

Fig. 5.5 Total, zero order approximation and reduced order solutions for the state variable ΔV_R

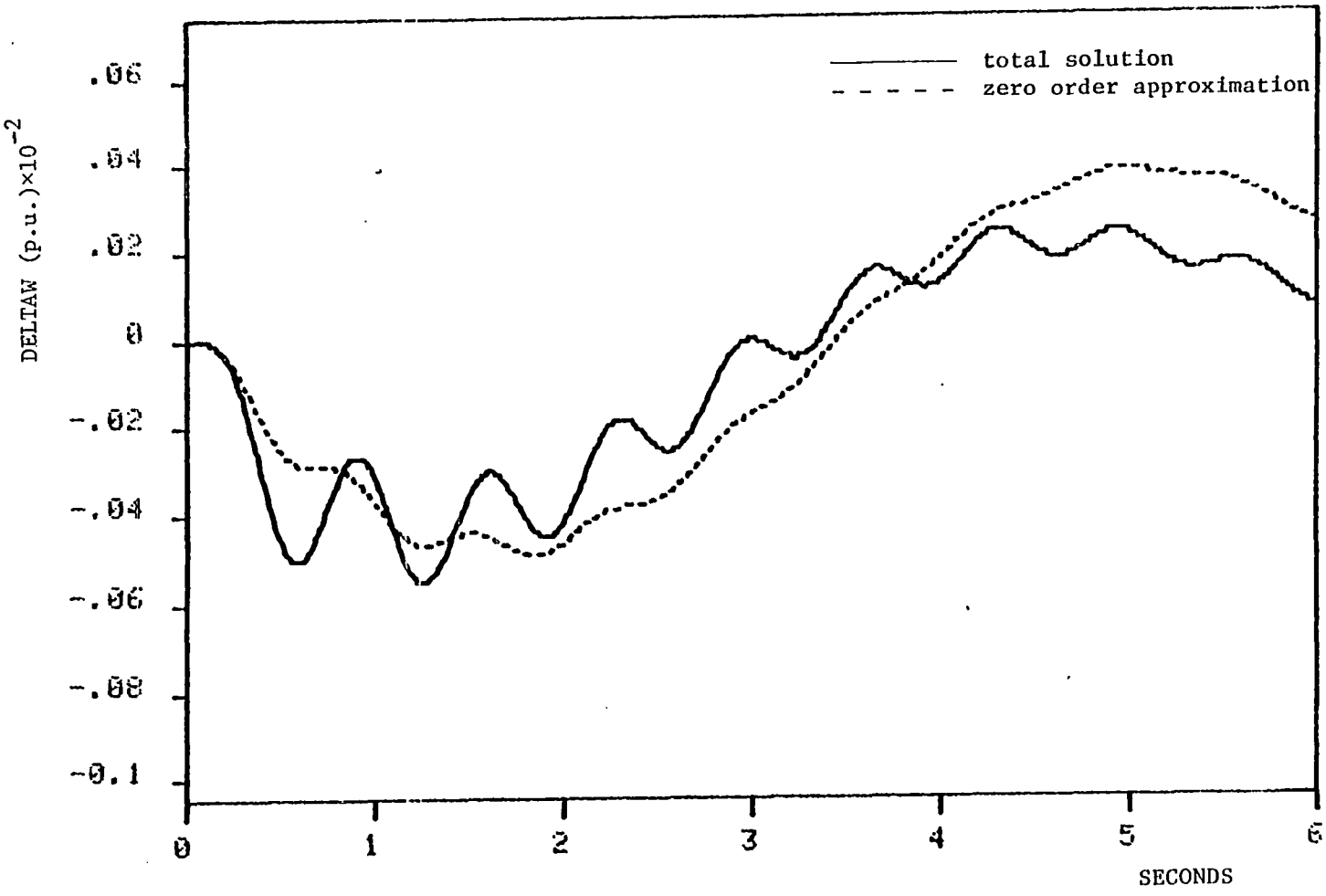

Fig. 5.6 Total and zero order approximation solutions for the state variable $\Delta\omega$

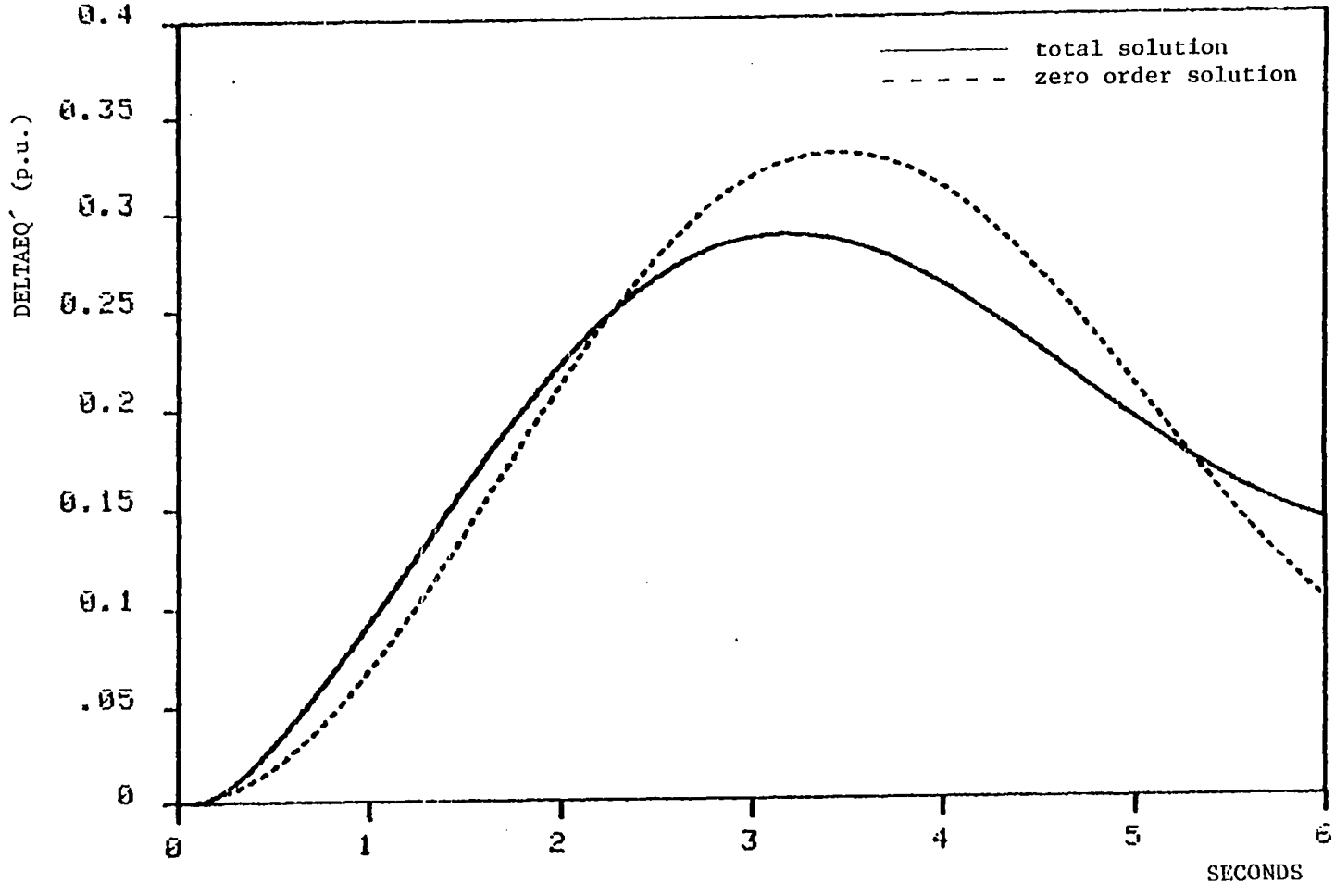

Fig. 5.7 Total and zero order approximation solutions for the state variable $\Delta E'_q$

6. CONCLUSIONS

6.1 Summary and Conclusions

Among existing coherency identification methods, those which use an index or coherency measure [1,5,45] seem to have more acceptance than those which resort to the storage and comparison of swing curve data to determine the sets of coherent generators [35]. It is along these lines that two methods using different coherency criteria are developed.

The first method is based on the slow coherency method described in [5] by a sensitivity based approach. This sensitivity based approach yields the group-reference generators by use of a sensitivity matrix obtained from the sensitivities of the r slow eigenvalues of the system matrix $\underline{\bar{A}}$ with respect to the generator inertia constants. This choice of system parameters, i.e., the inertia constants, was based on the obvious influence of those parameters on the system slow responses. The coherency measure used in this approach is the minimum norm of a matrix $\underline{L}d$ which leads to the determination of a grouping matrix $\underline{L}_g$. To validate this approach, two numerical examples provide results equivalent to those obtained by the method proposed in [5]. The method provides a physical significance to the process of choosing group reference generators, something the method in [5] lacks. This is due to the fact that the Gaussian elimination procedure is based on an abstract mathematical concept with no physical association with the dynamics of the system generators. It was also found, with the help of

numerous cases, that the slow coherency method is largely independent of the fault location as long as the perturbation applied to the system is only a small percentage of the total system generation. Otherwise, the coherent groups may change for large faults at different locations. This seems to contradict the statement made in [5] that the method is independent of fault size and location.

The second method is based on work done in references [15] and [1] and uses a set of coherency indices computed from the root-mean-square value of the rotor angular excursions between pairs of machines during the post-fault period, which are then compared to a prespecified coherency threshold. With the help of a commutative recognition rule and a ranking table [45], the sets of coherent generators are selected according to the coherency threshold. Two numerical examples are used to validate the method by comparison of results with detailed swing curves. These examples demonstrate that the method yields good results.

A third method for order reduction of multimachine power systems based on singular perturbation theory is also described. It consists of a specification of a linearized model for a multimachine power system including the control units of the synchronous generators, a manipulation of the system of equations into a singular perturbed form, and a solution of these equations based on the asymptotic expansion of the system state variables.

A numerical example consisting of a synchronous generating unit tied to an infinite bus is used to validate the method. It was observed in this numerical example that the partitioning of the state

vector, $\underline{\omega}$, into slow and fast subsets is dependent on the location of the system perturbation inputs and involves insight and experience. There are two inputs in this model, ΔV_{REF} and ΔP_{m_o}, leading to two different sets of slow and fast variables as they are separately excited. For instance, the variation in angular velocity, $\Delta\omega$, belongs to the slow subset of slow variables for the input ΔV_{REF} but belongs to the fast set of variables when the input is ΔP_{m_o}. These results also demonstrate that a close approximation to the full order model response is obtained by considering only the zero order approximation of the singular perturbed system. The first order approximation requires the solution of final value differential equations, equations (5.37a), and a set of initial value differential equations, equations (5.37b), (5.37c) and (5.37d), requiring considerable computation but with only a small gain in accuracy. Furthermore, the savings in computer time for the zero order approximation are substantial when compared with the time required in the numerical solution of the full scale model equations using conventional numerical techniques. It is emphasized that these observations are based on the results for the simple example used here and should not be interpreted as applying in toto to more general systems.

The singular perturbation technique is versatile in that it accommodates many possible variations in the modelling of the generating units. In addition, it has the feature of preserving the physical identities of the original state variables as they are expressed in the new singular perturbed model. As a consequence, the method is attractive for interaction with conventional dynamic stability algorithms.

6.2 Scope for Further Research

The singular perturbation method offers the best opportunities for further research. Some suggestions are

i) Simulation of power systems for transient stability studies. No successful attempt has been made up to the present time to solve this problem which requires the solution of the nonlinear differential equations describing the generating units and power equations for the network. There is thus much room for research in transient stability studies.

ii) There is a need for a better understanding of what is an optimal separation of variables into fast and slow subsets and for procedures and criteria to accomplish such a separation. Such research might lead to an explicit algorithm but is more likely to result in more intuitive insights resulting from experience.

iii) While the general development in Section 5.2 can be extended to systems larger than the example used, experience in accomplishing the details is needed.

iv) The observations made in ii) also apply to the selection of the perturbation parameter ε.

7. BIBLIOGRAPHY

1. Adgoankar, R. P., "Dynamic Equivalents for Power System Studies." Ph.D. Thesis, Indian Institute of Technology, Kanpur, India, 1979.

2. Altabib, H. V. and Krause, P. C., "Dynamic Equivalents of Reduced Order Models of Systems Components." IEEE Transactions on Power Apparatus and Systems, PAS 95, No. 5 (Sept./Oct. 1976):1535-1544.

3. Anderson, P. M., Faulted Power Systems, Ames, Iowa: The Iowa State University Press, 1976.

4. Anderson, P. M. and Fouad, A., Power System Control and Stability, Ames, Iowa: The Iowa State University Press, 1977.

5. Avramovic, B., "Time Scales, Coherency, and Weakening Coupling," Final Report R-895. University of Illinois-Urbana, Illinois, Oct. 1980.

6. Brown, H. E., Shippley, R. B., Coleman, D. and Nied, R. E., "Study of Stability Equivalents." IEEE Transactions on Power Apparatus and Systems, PAS 88, No. 3 (March 1969):200-206.

7. Chang, E. and Adibi, M. M., "Power System Dynamic Equivalents." IEEE Transactions on Power Apparatus and Systems, PAS 89, No. 8 (Nov./Dec. 1970):1737-1743.

8. Chen, C. T., Introduction to Linear System Theory. New York: Holt, Rinehart and Winston, Inc., 1970.

9. Chow, J. H., Allemong, J. J. and Kokotovic, P. V., "Singular Perturbation Analysis with Sustained High Frequency Oscillations." Automatica, 14, No. 3 (May/June 1978):271-279.

10. Conte, S. D. and deBoor, C., Elementary Numerical Analysis. Tokyo, Japan: McGraw-Hill Kogakusha, Ltd., 1972.

11. Cruz, J. B., editor, System Sensitivity Analysis: Benchmark Papers in Electrical Engineering and Computer Science. Stroudsburg, Pennsylvania: Dowden, Hutchingson and Ross, Inc., 1973.

12. Davison, E. J., "A Method for Simplifying Linear Dynamic Systems." IEEE Transactions on Automatic Control, AC 11, No. 1 (Jan. 1966): 93-101.

13. Davison, E. J., "A New Method for Simplifying Large Linear Dynamic Systems," IEEE Transactions on Automatic Control, AC 13, No. 2 (Apr. 1968):214-215.

14. Davison, E. J. and Chidambara, M. R., "Further Remarks on Simplifying Linear Dynamic Systems." IEEE Transactions on Automatic Control, AC 12, No. 2 (Apr. 1967):119-120.

15. Desoer, C. A., "Modes in Linear Circuits." IRE Transactions on Circuit Theory, 7, No. 3 (March 1960):211-213.

16. Dharmarao, N. and Sarkar, A. D., "Dynamic System Simplification and an Application to Power System Solutions." IEE Proceedings, 119, (1972):904-910.

17. Efimov, N. V., and Rozendorn, E. R., Linear Algebra and Multidimensional Geometry. Moscow, USSR: MIR Publishers, 1975.

18. Elangovan, S. and Kuppurajulu, A., "System Analysis by Simplified Models." IEEE Transactions on Automatic Control, AC 15, No. 2 (Apr. 1970):234-237.

19. Fadeev, D. K. and Faddeeva, V. N., Computational Methods of Linear Algebra. San Francisco, California: W. H. Freeman and Co., 1963.

20. Hammond, T. J. and Winning, D. J., "Comparisons of Synchronous Machine Models in the Study of the Transient Behavior of Electrical Power Systems." IEE Proceedings, 118, No. 10 (Oct. 1971):1442-1458.

21. Henrici, P., Discrete Variable Methods in Ordinary Differential Equations. New York: John Wiley and Sons, Inc., 1972.

22. Jordan, D. N. and Smith, P., Nonlinear Ordinary Differential Equations. Oxford: Oxford University Press, 1977.

23. Kuppurajulu, A. and Elangovan, S., "Simplified Power System Models for Dynamic Stability Studies." IEEE Transactions on Power Apparatus and Systems, PAS 90, No. 1 (Jan./Feb. 1971):11-12.

24. Lee, S.T.Y. and Schweppe, C., "Distance Measures and Coherency Recognition for Transient Stability Studies." IEEE Transactions on Power Apparatus and Systems, PAS 93, No. 5 (Sept./Oct. 1973): 1550-1557.

25. Lawler, J. S. and Schleuter, R. A., "Computational Algorithms for Constructing Modal-Coherent Dynamic Equivalents." IEEE Power Summer Meeting, Paper No. 81, SM 427-4, Portland, Oregon, July 26-31, 1981.

26. Miranker, W. L., Numerical Methods for Stiff Equations and Singular Perturbation Problems. Boston, Massachusetts: D. Reidel Publishing Company, 1981.

27. Nayfeh, A. M., Introduction to Perturbation Techniques. New York: John Wiley and Sons, Inc., 1981.

28. Nayfeh, A. M., Perturbation Methods. New York: John Wiley and Sons, Inc., 1973.

29. Okobo, S. Suzuki, H. and Vemura, K., "Modal Analysis for Power Dynamic Stability." IEEE Transactions on Power Apparatus and Systems, PAS 97, No. 4 (July/Aug. 1978):1313-1318.

30. O'Malley, R. E., Jr., Introduction to Singular Perturbation Techniques. New York: Academic Press, 1974.

31. Pai, M. A., Computer Techniques in Power Systems Analysis. New Delhi: Tata McGraw-Hill Publishing Company Limited, 1979.

32. Pai, M. A. and Shetty, P. S., "System Matrix Formulation without Matrix Inversion for Multimachine Power Systems," Journal of the Institution of Engineers (India), 59, No. 10 (Oct. 1978): 109-114.

33. Pai, M. A. and Adgoankar, R. P., "Dynamic Equivalents of Power Systems Using Singular Perturbation Techniques." IFAC Symposium on Computer Applications in Large Scale Power Systems. New Delhi, India, (Aug. 16-18; 1978):33-40.

34. Peréz-Arriaga, I. J., Schweppe, F. C. and Verghese, G. C., "Selective Modal Analysis: Basic Results." IEEE PES Winter Meeting, New York (1980):649-656.

35. Pai, M. A. and Adgoankar, R. P., "Identification of Coherent Generators Using Weighted Eigenvectors." IEEE PES Winter Power Meeting, Paper AZ9-022-5, New York, 1929.

36. Pai, M. A., Power System Stability Analysis by Direct Method of Lyapunov. New York: North-Holland Publishing Co., 1982.

37. Podmore, R., "Identification of Coherent Generators for Dynamic Equivalents." IEEE Transactions on Power Apparatus and Systems, PAS 97, No. 4 (July/Aug. 1978):1344-1354.

38. Podmore, R. and Germond, A. J., "Development of Dynamic Equivalents for Transient Stability Studies." Final Report on EPRI Project RP763, May 1977.

39. Podmore, R. Athay, T., Germond, A. J. and Virmani, S., "New Techniques for Analysis of Power Systems Transient Stability." Sixth PSCC, Darmdtadst, Germany, Aug. 21-25, 1978, p. 819-822.

40. Quazza, G., "Large Scale Control Problems in Electric Power Systems," Automatica, 13, No. 6 (Nov./Dec. 1977):579-593.

41. Sacommano, F., Marconato, F. and Mariani, E., "Application of Simplified Dynamic Models to the Italian Power Systems." IEEE PICA Conference (1973), (1973):118-126.

42. Sacommano, F., "Development and Evaluation of Simplified Dynamic Models for Multimachine Electric Power Systems." Fourth PSCC, Grenoble, France, Sept. 11-16, 1972, pp. 11-16.

43. Santi, P., O'Malley, R. E. and Kokotovic, P. V., "Singular Perturbations and Order Reduction in Control Theory - An Overview." Automatica, 12, No. 2 (March/Apr. 1976):123-132.

44. Satsangi, P. S., Paliwal, L. N., Rao, D. and Nanda, J., "Graph Theory in Dynamic Equivalencing for Large Scale Power System Studies." Paper presented at the IFAC Symposium, New Delhi, 1979.

45. Schlueter, R. A., Akthar, H. and Modir, H., "An RMS Coherency Measure: A Basic for Unification of Coherence and Modal Analysis Model Aggregation Techniques." IEEE PES Summer Power Meeting, Paper A78 533-2, 1978.

46. Spalding, B. D., Yee, H. and Goudie, D. B., "Coherency Recognition for Transient Stability Studies Using Singular Points." IEEE Transactions on Power Apparatus and Systems, PAS 96, No. 4

47. Stanton, K. N., "Dynamic Energy Balance Studies for Simulation of Power Frequency Transients." IEEE Transactions on Power Apparatus and Systems, PAS 91, No. 1 (Jan./Feb. 1972):110-117.

47b. Stanton, K., Kruempel, K., Vittal, V. and Fouad, A., "Transient Stability Margin as a Tool for Dynamic Security Assessment." Electric Power Research Institute Report (Iowa State University, EL-1755, March 1981).

48. Undrill, J. M., "Dynamic Stability Calculations for an Arbitrary Number of Interconnected Synchronous Machines." IEEE Transactions on Power Apparatus and Systems, PAS 87, No. 3 (Mar. 1968):835-844.

49. Undrill, J. M. and Turner, A. E., "Construction of Power System Electromechanical Equivalents by Modal Analysis." IEEE Transactions on Power Apparatus and Systems, PAS 90, No. 5 (Sept./Oct. 1971):2049-2059.

50. Uyemura, K. and Matzuki, J., "A Computational Algorithm for Evaluating Unstable Equilibrium Points in Power Systems." Elect. Eng. in Japan, No. 4 (July/Aug. 1972):41-47.

51. Van Ness, J. E., "Improving Reduced Dynamic Models of Power Systems." IEEE PICA Conference (1975):155-157.

52. Van Ness, J. E., Boyle, J. M. and Imad, F. P., "Sensitivities of Large Multiple Loop Control Systems." IEEE Transactions on Automatic Control, AC 10, No. 3 (July 1965):308-315.

53. Van Ness, J. E., Zimmer, H. and Cultu, M., "Reduction of Dynamic Models of Power Systems." IEEE PICA Conference (1973):15-112.

54. Willems, J. C., "Lyapunov Functions for Diagonally Dominant Systems." Automatica, 12, (Dec. 1976):519-523.

55. Winkelman, J. R., Allemong, J. J. and Kokotovic, P. V., "Singular Perturbation Methods in Multiple Time Scale Power System Simulation." IEEE Proceedings (1979):375-384.

56. Winkelman, J. R., Avramovic, B., Chow, J. H. and Kokotovic, P. V., "Area Decomposition for Electromechanical Models of Power Systems." IFAC Symposium on Large Scale System Theory and Application, Toulousse, France, 1980.

57. Wu, F. F. and Narasimhamusthi, N., "Coherence Identification for Power Systems Dynamic Equivalents." Memo No. UCB/ERL M77/75. University of California, Berkeley, Aug. 26, 1977.

58. Zein El-Sin, H. M. and Elden, R.T.H., "A Computer Based Eigenvalue Approach for Power System Dynamic Stability Evaluation." IEEE PICA Conference (1977):186-192.

8. ACKNOWLEDGEMENTS

The author wishes to express his appreciation to all members of his committee, Dr. H. W. Hale, Dr. K. C. Kruempel, Dr. R. J. Lambert, Dr. A. A. Fouad and Dr. R. G. Brown. Special thanks are given to Dr. M. A. Pai for suggesting the topic of this dissertation and his continuous encouragement throughout the development of this work, to his major professor, Dr. H. W. Hale, for his constructive criticism and discussion and to Dr. K. C. Kruempel for his invaluable assistance in the stability runs of the different numerical examples presented in this dissertation.

Also, the author expresses his deepest gratitude to the Electrical Engineering Department of Iowa State University for its financial support.

Last but not least, the author wishes to thank his parents and sisters for their encouragement and love.

9. APPENDIX A: THE NEW ENGLAND, THE MODIFIED IOWA (MIS) AND WSCC POWER SYSTEM DATA

9.1 The New England System [35]

Number of buses: 39 (See Fig. 3.1)

Number of Lines: 47

Number of Shunt Loads: 19

Number of Machines: 10

MVA Base: 100

i) Line Data.

All of the quantities shown in Table 9.1 are in p.u.

Table 9.1 Line data of the New England System

From Bus No.	To Bus No.	Resistance	Reactance	Susceptance	Transformer Tap
1	2	0.0035	0.0411	0.6987	0.0000
1	39	0.0010	0.0250	0.7500	0.0000
2	3	0.0013	0.0151	0.2572	0.0000
2	25	0.0070	0.0086	0.1460	0.0000
3	4	0.0013	0.0213	0.2214	0.0000
3	18	0.0011	0.0133	0.2138	0.0000
4	5	0.0008	0.0128	0.1342	0.0000
4	14	0.0008	0.0129	0.1382	0.0000
5	6	0.0002	0.0026	0.0434	0.0000
5	8	0.0008	0.0112	0.1476	0.0000
6	7	0.0006	0.0092	0.1130	0.0000
6	11	0.0007	0.0082	0.1389	0.0000
7	8	0.0004	0.0046	0.0780	0.0000
8	9	0.0023	0.0363	0.3804	0.0000
9	39	0.0010	0.0250	1.2000	0.0000
10	11	0.0004	0.0043	0.0729	0.0000
10	13	0.0004	0.0043	0.0729	0.0000
13	14	0.0009	0.0101	0.1723	0.0000
14	15	0.0018	0.0217	0.3660	0.0000
15	16	0.0009	0.0094	0.1710	0.0000
16	17	0.0007	0.0089	0.1342	0.0000
16	19	0.0016	0.0195	0.3040	0.0000
16	21	0.0008	0.0135	0.2548	0.0000
16	24	0.0003	0.0059	0.0680	0.0000
17	18	0.0007	0.0082	0.1319	0.0000
17	27	0.0013	0.0173	0.3216	0.0000
21	22	0.0008	0.0135	0.2548	0.0000
22	23	0.0006	0.0096	0.1846	0.0000
23	24	0.0022	0.0350	0.3610	0.0000
25	26	0.0032	0.0323	0.5130	0.0000
26	27	0.0014	0.0147	0.2396	0.0000
26	28	0.0043	0.0474	0.7802	0.0000
26	29	0.0057	0.0625	1.0290	0.0000
28	29	0.0014	0.0151	0.2490	0.0000
12	11	0.0016	0.0435	0.0000	1.0060
12	13	0.0016	0.0435	0.0000	1.0060
6	31	0.0000	0.0250	0.0000	1.0700
10	32	0.0000	0.0200	0.0000	1.0700
19	33	0.0007	0.0142	0.0000	1.0700
20	34	0.0009	0.0180	0.0000	1.0090
22	35	0.0000	0.0143	0.0000	1.0250
23	36	0.0005	0.0272	0.0000	1.0000
25	37	0.0006	0.0232	0.0000	1.0250
2	30	0.0000	0.0181	0.0000	1.0250
29	38	0.0008	0.0156	0.0000	1.0250
19	20	0.0007	0.0138	0.0000	1.0600

ii) Shunt load data.

The shunt loads at any other system bus not present in the Table below are assumed to be zero MW and zero MVAR.

Table 9.2 Shunt load data of the New England system

Bus No.	MW	MVAR
3	322.0	2.4
4	500.0	184.0
7	233.8	84.0
8	522.0	176.6
12	7.5	88.0
15	320.0	153.0
16	329.4	32.3
18	158.0	30.0
20	628.0	103.0
21	274.0	115.0
23	274.5	84.6
24	308.6	-92.2
25	224.0	47.2
26	139.0	17.0
27	281.0	75.5
28	206.0	27.6
29	283.5	26.9
31	9.2	4.6
39	1104.0	250.0

iii) Generator data.

In Table 9.3, inertia constants are given in seconds, reactances in p.u. and time constants in seconds.

Table 9.3 Generator data of the New England system

Unit No.	Load Flow Bus No.	H	X'_d	X'_q	X_d	X_q	T'_{do}	τ_{qo}	X_ℓ
1	30	42.0	0.031	0.031	0.100	0.069	10.2	0.0	0.0125
2	31	30.3	0.0647	0.0697	0.295	0.282	6.56	1.5	0.0350
3	32	35.8	0.0531	0.0531	0.2495	0.237	5.7	1.5	0.0304
4	33	28.6	0.0436	0.0436	0.262	0.258	5.69	1.5	0.0295
5	34	26.0	0.1320	0.0132	0.670	0.620	5.40	0.44	0.0540
6	35	34.8	0.0500	0.0500	0.254	0.241	7.3	0.40	0.0224
7	36	26.4	0.0490	0.0490	0.295	0.292	5.66	1.50	0.0322
8	37	24.3	0.0570	0.0570	0.290	0.280	6.70	0.41	0.0280
9	38	34.5	0.0570	0.0570	0.2106	0.205	4.79	1.96	0.0298
10	39	500.0	0.0310	0.0310	0.100	0.069	10.20	0.0	0.0125

iv) Initial Conditions.

All quantities shown in Table 9.4 are in p.u. The voltages here specified are the voltages behind transient reactance used in the classical representation of synchronous machines.

Table 9.4 Initial conditions used in the computation of the system matrix $\underline{A}$

Bus No.	Voltage	
	Magnitude	Angle (electrical degrees)
30	1.0929	-0.4985°
31	1.1915	19.2738°
32	1.1491	19.5800°
33	1.0808	17.1030°
34	1.1061	12.2590°
35	1.1910	19.3400°
36	1.1394	20.0480°
37	1.0709	17.5890°
38	1.1368	30.5680°
39	1.0206	-11.2609°

9.2 The Modified Iowa System (MIS) [47b]

Number of Buses: 163 (See Fig. 3.2)

Number of Lines: 304

Number of Machines: 17

MVA Base: 100

i) Line data.

Refer to [47b] for specific line data.

ii) Generator data.

The units for machine inertia constants are given in seconds and the reactances in p.u.

Table 9.5 Generator data of the Modified Iowa system

Unit No.	Load Flow Bus No.	H	X_d'
1	393	100.00	0.0040
2	998	34.56	0.0437
3	268	80.00	0.0100
4	635	80.00	0.0050
5	1246	16.79	0.0507
6	1247	32.49	0.0206
7	1252	6.65	0.1131
8	1254	2.66	0.3115
9	1265	29.60	0.0535
10	1267	5.00	0.1770
11	1270	11.31	0.1049
12	1271	19.79	0.0297
13	339	20.66	0.0544
14	1201	200.00	0.0020
15	539	100.00	0.0040
16	733	28.60	0.0559
17	480	200.00	0.0020

iii) Initial conditions.

The voltage here specified in p.u. are the voltages behind transient reactance used in the classical representation of synchronous machines.

Table 9.6 Initial conditions used in the computation of the system matrix $\underline{\bar{A}}$

Bus No.	Voltage Magnitude	Angle (electrical radians)
393	1.0032	-0.4874
998	1.1333	-0.0240
268	1.0302	-0.2842
635	1.0008	-0.4554
1246	1.0678	-0.1090
1247	1.0505	-0.0790
1252	1.0163	-0.4018
1254	1.1235	-0.4705
1265	1.1195	-0.2166
1267	1.0652	-0.1942
1270	1.0777	-0.4242
1271	1.0609	-0.1764
339	1.0103	-0.4906
1201	1.0206	-0.4672
539	1.0182	-0.3682
733	1.1243	-0.1171
480	1.1116	-0.0760

9.3 The WSCC System [4]

Number of Buses: 9 (See Fig. 2.1)

Number of Lines: 9

Number of Shunt Loads: 3

Number of Generators: 3

MVA Base: 100

i) Line data.

All resistances and reactances shown in Table 9.7 are in p.u.

Table 9.7 Line data of the WSCC system

From Bus No.	To Bus No.	Resistance	Reactance	Susceptance
1	9	0.0000	0.0586	0.0000
2	7	0.0000	0.0625	0.0000
3	4	0.0000	0.0576	0.0000
4	5	0.0100	0.0850	0.1660
4	6	0.0170	0.0920	0.1580
5	7	0.0320	0.1610	0.3060
6	9	0.0390	0.1700	0.3580
7	8	0.0085	0.0720	0.1490
8	9	0.0119	0.1008	0.2090

ii) Shunt load data.

Data given in Table 9.8 are in WN and MVAR.

Table 9.8 Shunt load data of the WSCC system

Bus No.	MW	MVAR
5	125.0	50.0
6	90.0	30.0
8	100.0	35.0

iii) Generator data.

In Table 9.9, inertia constants are given in seconds, reactances in p.u. and time constants in seconds.

Table 9.9 Generator data of the WSCC system

Unit No.	Load Flow Bus No.	H	X_d'	X_q'	X_d	X_q	T_{do}'	T_{qo}'	X_ℓ
1	1	3.01	0.1813	0.25	1.3125	1.2578	5.89	0.600	0.0742
2	2	6.50	0.1198	0.1969	0.8958	0.8645	6.00	0.535	0.0521
3	3	23.64	0.0608	0.0969	0.1460	0.0969	8.96	0.000	0.0336

10. APPENDIX B: GENERATOR UNIT MODEL

10.1 The Synchronous Machine

Consider a five winding model of a synchronous generator as shown in Fig. 10.1. The flux linkage-current relationships in the hybrid characterization with the assumption of a common flux linking all of the windings on the d-axis and similarly for the q-axis are given by [32].

i) The direct-axis characterization

$$\begin{bmatrix} \lambda_d(t) \\ i_F(t) \\ i_D(t) \end{bmatrix} = \begin{bmatrix} L_{MD_0}+\ell_d & L_{MD_0}\ell_F^{-1} & L_{MD_0}\ell_D^{-1} \\ -L_{MD_0}\ell_F^{-1} & \ell_F^{-1}-L_{MD_0}\ell_F^{-2} & -L_{MD_0}\ell_F^{-1}\ell_D^{-1} \\ -L_{MD_0}\ell_D^{-1} & -L_{MD_0}\ell_F^{-1}\ell_D^{-1} & \ell_D^{-1}-L_{MD_0}\ell_D^{-1} \end{bmatrix} \begin{bmatrix} i_d(t) \\ \lambda_F(t) \\ \lambda_D(t) \end{bmatrix} \tag{10.1}$$

where

$$L_{MD_0} = [L_{AD}^{-1} + \ell_F^{-1} + \ell_D^{-1}]^{-1} = \frac{L_{MD}L_d''}{d} = L_d'' - \ell_d \tag{10.2}$$

$$L_d''^{-1} = (L_{MD_0}+\ell_D)^{-1} = \ell_D^{-1} - L_{MD}\ell_d^{-2} \tag{10.3}$$

$$L_{MD}^{-1} = L_{AD}^{-1} + \ell_d^{-1} + \ell_F^{-1} + \ell_D^{-1} \tag{10.4}$$

ii) The quadrature-axis characterization

$$\begin{bmatrix} \lambda_q(t) \\ i_Q(t) \end{bmatrix} = \begin{bmatrix} L_{MD_0} + \ell_q & L_{MQ_0}\ell_Q^{-1} \\ -L_{MQ_0}\ell_Q^{-1} & \ell_Q^{-1}-L_{MQ_0}\ell_Q^{-2} \end{bmatrix} \begin{bmatrix} i_q(t) \\ \lambda_Q(t) \end{bmatrix} \tag{10.5}$$

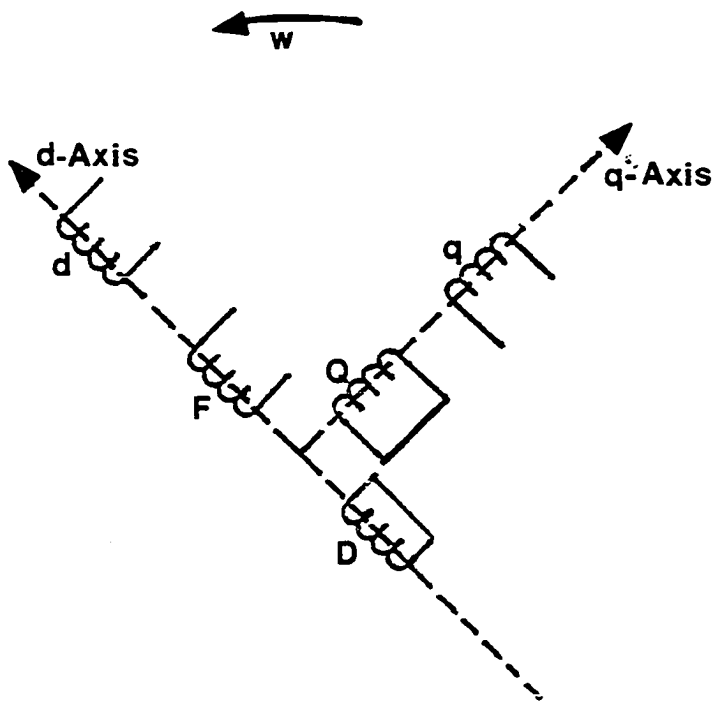

Fig. 10.1 Five winding model of a synchronous generator

where

$$L_{MQ0} = [L_{AC}^{-1} + \ell_Q^{-1}]^{-1} = \frac{L_{AQ}L_q''}{\ell_q} = L_q'' - \ell_q \tag{10.6}$$

$$L_q''^{-1} = (L_{MQ_0}+\ell_q)^{-1} \tag{10.7}$$

Equivalent circuital representation of the above characterizations as well as the graphical representation of the inductances used in the five winding model are given in Figures 10.2a and 10.2b. In Figures 10.2, upper case letters denote mutual inductances while lower case letters denote instantaneous flux linkages, instantaneous currents and leakage inductances. Knowing that all of the above have their magnitudes given in p.u. and that the rotor angular velocity ω is approximately equal to the nominal system angular velocity, $\omega_R = 1.0$, we can say that the inductances are numerically equal to reactances.

The choice of λ_F, λ_D and λ_Q as state variables is not very appropriate because of the difficulty of measuring and identifying them. Thus, a new set of state variables is selected. Instead of working with flux linkages, a set of stator equivalent voltages is defined as E_q', E_q'' and E_d''. Stator transients are neglected in the model, i.e., the transformer voltages $\frac{d}{dt}(\lambda_q)$ and $\frac{d}{dt}(\lambda_d)$ are zero. This is justified by the fact that

$$\left|\frac{d}{dt}(\lambda_d)\right| << |\omega\lambda_d| \tag{10.8}$$

and

$$\left|\frac{d}{dt}(\lambda_q)\right| << |\omega\lambda_q|$$

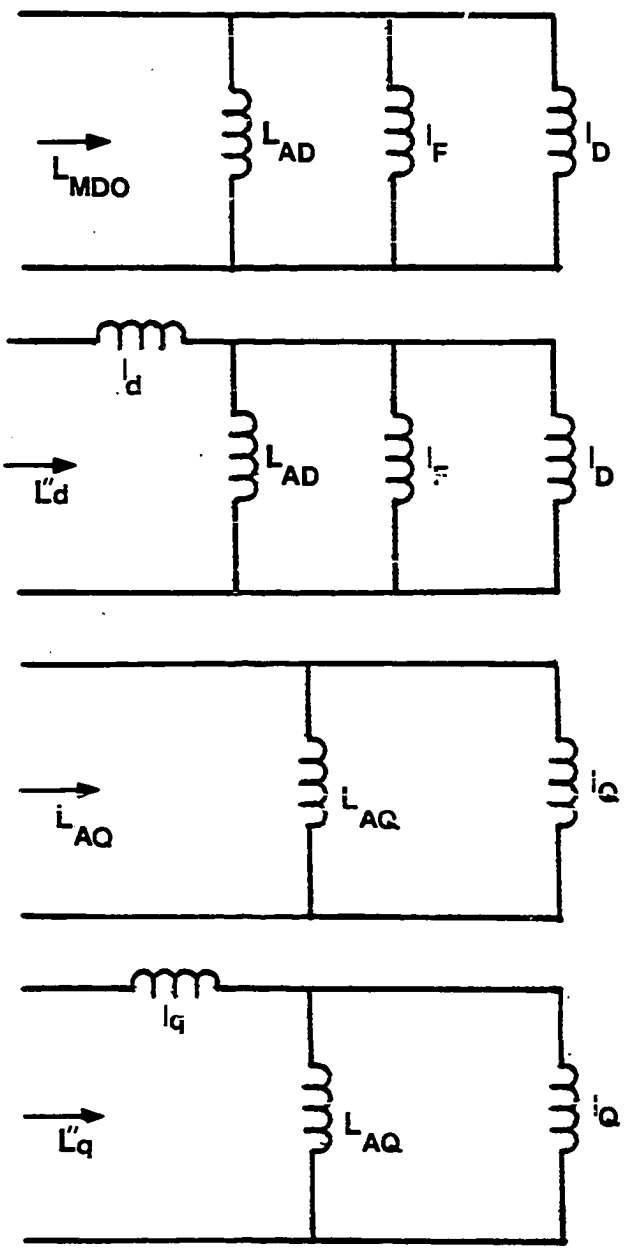

Fig. 10.2a Circuital models for computation of the inductances L_{MD_0}, L''_d, L_{AQ} and L''_q

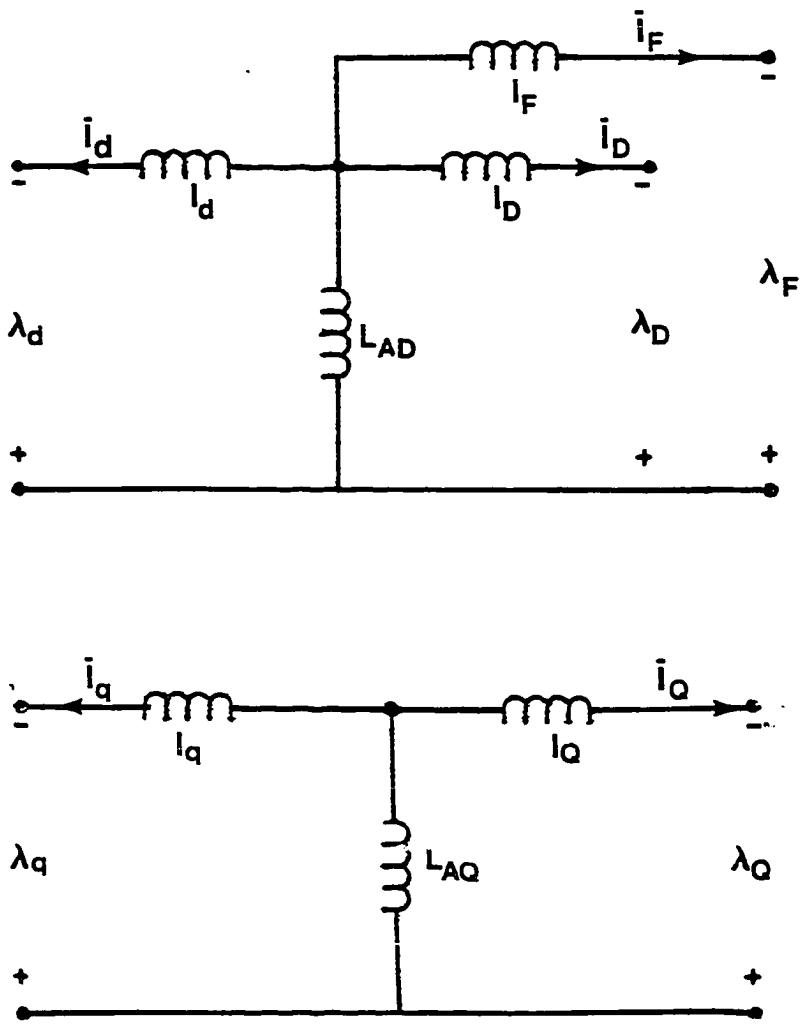

Fig. 10.2b Circuital representation of the synchronous machine hybrid model characterization

In other words, the speed voltages are much bigger than the transformer voltages. As a consequence, the equivalent stator voltages are reduced to

$$E_q' = (1/\sqrt{3})(L_{AD}/L_F)\lambda_F(t) \tag{10.9}$$

$$E_q'' = [(L_{MD}L_d''/\ell_F\ell_D)(L_F/L_{AD})]E_q'(t)+(1/\sqrt{3})(L_{MD}L_d''/\ell_d\ell_D)\lambda_D(t) \tag{10.10}$$

$$E_d'' = (-1/\sqrt{3})(L_{AQ}/L_Q)\lambda_Q(t) \tag{10.11}$$

where

$$L_F = \ell_F + L_{AD} \tag{10.12a}$$

$$L_Q = \ell_Q + L_{AQ} \tag{10.12b}$$

$$E'' = E_q'' + jE_d'' \tag{10.12c}$$

Two algebraic equations also result from the neglect of the synchronous machine stator transients. They are

$$v_d = -r_{id}(t) - \omega L_q''i_q(t) - \omega L_{MQ0}\ell_Q^{-1}\lambda_Q(t) \tag{10.13}$$

and

$$v_q = -r_q(t) + \omega L_d''i_d(t) + \omega L_{MD0}\ell_F^{-1}\lambda_F(t) + \omega L_{MD0}\ell_D^{-1}\lambda_D(t) \tag{10.14}$$

which, when divided by $\sqrt{3}$, become

$$V_d = -rI_d(t) - X_q''I_q(t) + E_d''(t) \tag{10.15}$$

and

$$V_q = -rI_q(t) - X_d''I_d(t) + E_q''(t) \tag{10.16}$$

where

$$V_d = v_d(t)/\sqrt{3} \tag{10.17a}$$

$$V_q = v_q(t)/\sqrt{3} \tag{10.17b}$$

$$I_d = i_d(t)/\sqrt{3} \tag{10.17c}$$

$$I_q = i_q(t)/\sqrt{3} \tag{10.17d}$$

Under the assumption that transient and subtransient saliency are being neglected, i.e, $X''_q = X''_d$ and $X'_d = X'_q$, and that the angular velocity ω is approximately equal to ω_R, the following set of differential equations describesthe stator equivalent rotor transients.

$$\frac{dE'_q}{dt} = -(1/T'_{d_o})\left[\frac{X_d - X_\ell}{X_d - X_\ell}\right]E'_q + (1/T'_{d_o})[(X_d - X'_d)/(X'_d - X_\ell)]E''_q$$

$$+ (1/T'_{d_o})[(X_d - X'_d)(X''_d - X_\ell)/(X'_d - X_\ell)]I_d + (1/T'_{d_o})E_{FD}$$

or

$$\frac{dE'_q}{dt} = K_1 E'_q + K_2 E''_q + K_3 I_d + (1/T_{d_o})E_{FD} \tag{10.18}$$

$$\frac{dE''_q}{dt} = (1/T_1)E'_q - (1/T_2)E''_q$$

$$+ \{(1/T'_{d_o})[(X_d - X_\ell)^2 (X_d - X'_d)/(X'_d - X_\ell)^2] + (1/T''_{d_o})(X'_d - X''_d)\}I_d$$

$$+ (1/T'_{d_o})[(X''_d - X_\ell)/X'_d - X_\ell)]E_{FD}$$

or

$$\frac{dE''_q}{dt} = (1/T_1)E'_q - (1/T_2)E''_q + K_4 I_d + K_5 E_{FD} \tag{10.19}$$

$$\frac{dE''_d}{dt} = (1/T''_{q_o})E''_d - (1/T''_{q_o})(X_q - X''_q)I_q$$

or

$$\frac{dE''_d}{dt} = (1/T''_{q_o})E''_d + K_6 I_q \tag{10.20}$$

In the above equations,

$$E_{FD}(t) = v_F(t)L_{AD}/\sqrt{3}L_F \tag{10.21}$$

$$T''_{q_o} = L_Q/r_Q \tag{10.22}$$

$$T''_{d_o} = [(\ell_D^{-1} - L_{MD_0}\ell_D^{-2})r_D]^{-1} \tag{10.23}$$

$$T_2^{-1} = \{(-1/T'_{d_o})[(X''_d-X_\ell)(X_d-X_\ell)/(X'_d-X_\ell)^2] + (1/T''_{d_o}) \tag{10.24}$$

$$T_2^{-1} = [(T'_{d_o}) - (X''_d-X_\ell)(X_d-X'_d)/T_{d_o}')(X'_d-X_\ell)^2] \tag{10.25}$$

$$T''_{d_o} = L_F/r_F \tag{10.26}$$

The equations describing the electromechanical rotor dynamics complete the set of differential equations used for representing the machine transients. They are

$$2H\frac{d\omega}{dt} = P_m - P_e \text{ (p.u.)} \tag{10.27}$$

$$\frac{d}{dt} = \omega_R(\omega-1.0) \quad \text{(electrical radians/seconds)} \tag{10.28}$$

where

$$P_e = E''_q I_q + E''_d I_d \tag{10.29}$$

and ω is the rotor angular velocity in (p.u.)

10.2 The Voltage Regulator-Exciter System Model

The addition of the voltage regulator-exciter system to the synchronous generator increases the number of differential equations and consequently the number of state variables by four. An additional algebraic equation relates the machine terminal voltage, V_t, to its (d,q) and (D,Q) components.

The equations for the exciter-voltage regulator system shown in Fig. 10.3, with saturation of the exciter being neglected, are given by

$$\frac{dV_1(t)}{dt} - (K_R/T_R)V_t - (1/T_R)V_1 \tag{10.30}$$

$$\frac{dV_3(t)}{dt} = (K_F/T_F)[1/T_E)V_R-(K_E/T_E)E_{FD}] \tag{10.31}$$

$$\frac{dV_R(t)}{dt} = -(K_A/T_A)(V_1+V_3) - (1/T_A)V_R + (K_AT_A)V_{REF} \tag{10.32}$$

$$V_{RMIN} < V_R < V_{RMAX}$$

$$\frac{dE_{FD}}{dt}(t) = (1/T_E)V_R - (K_E/T_E)E_{FD} \tag{10.33}$$

$$V_t = V_g + jV_d = (V_Q+jV_D)e^{-j\delta}$$

$$|V_t|^2 = V_q^2 + V_d^2 = V_Q^2 + V_D^2 \tag{10.34}$$

where the K's and T's denote gains and time constants respectively.

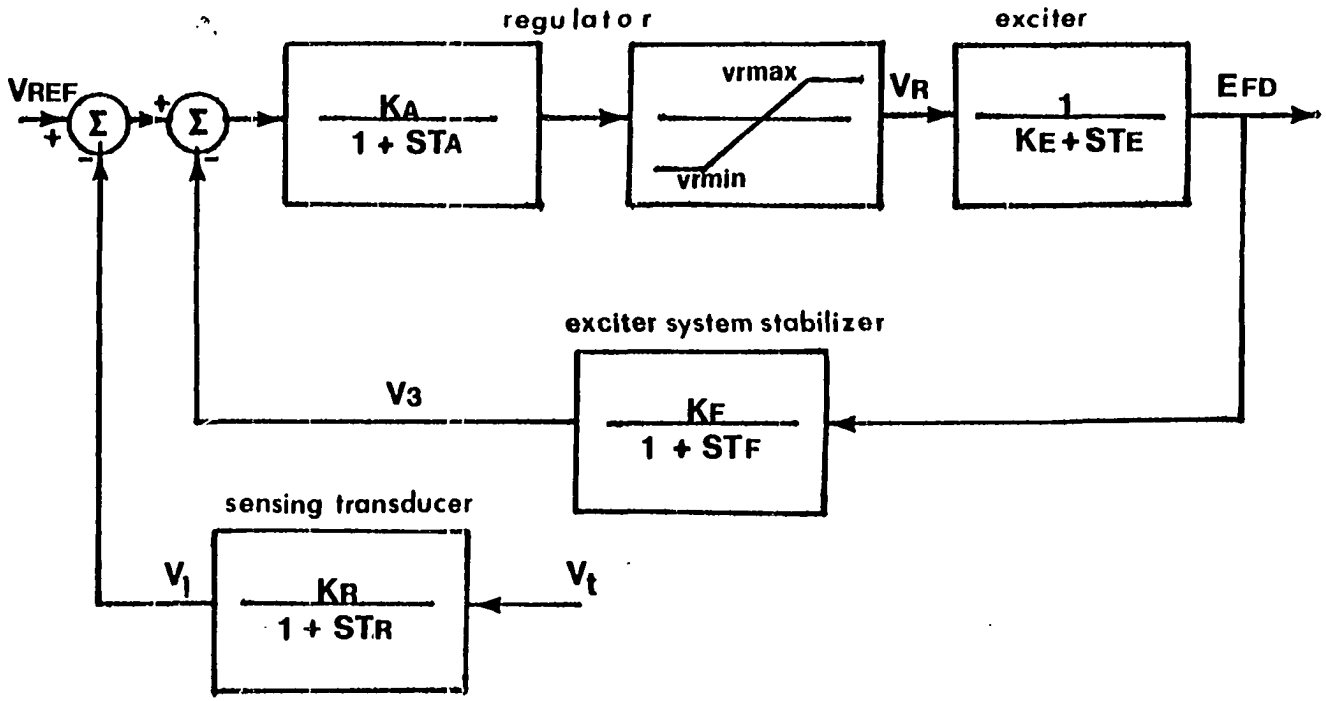

Fig. 10.3 IEEE Type I model of a voltage regulator-exciter system

10.3 The Governor-Turbine System Model

The governor-turbine system model used in this dissertation has been taken from reference [4]. A block diagram of the system is shown in Fig. 10.4. The differential equations which describe the system are

$$\frac{d\theta_1(t)}{dt} = (K'/\tau_1)(\omega-1.0) + (\tau_2 K'/2H_1\tau_1)[P_m - E''_q I_q - E''_d I_d] - (1/\tau_1)\theta_1 \tag{10.35}$$

$$\frac{d\theta_2(t)}{dt} = (1/\tau_3)\theta_1 - (1/\tau_3)\theta_2 + (1/\tau_3)P_{m_o} \tag{10.36}$$

$$\frac{dP_m(t)}{dt} = (F/\tau_3)\theta_1 + [1/\tau_5)-(F/\tau_3)]\theta_2 - (1/\tau_5)P_m + (F/\tau_3)P_{m_o} \tag{10.37}$$

where the K' is equal to $(1/Rf_R)$, with R being the governor steady-state regulation coefficient or "governor droop" in p.u. and f_R the rated system frequency in Hz. P_{m_o} is the required mechanical input during the steady-state operating condition of the system and the parameter F accounts for the p.u. shaft output ahead of the reheater for steam units or the maximum gate velocity for hydro-units.

To summarize the state variables and inputs in the model, a list specifying their location and the symbols used to identify them follows.

i) The machine model: E'_q, E''_q, E''_d, ω and δ.

ii) The voltage regulator-exciter system: V_1, V_3, V_R and E_{FD}.

iii) The governor turbine system: θ_1, θ_2 and P_m.

iv) The inputs: V_{REF} and P_{m_o}.

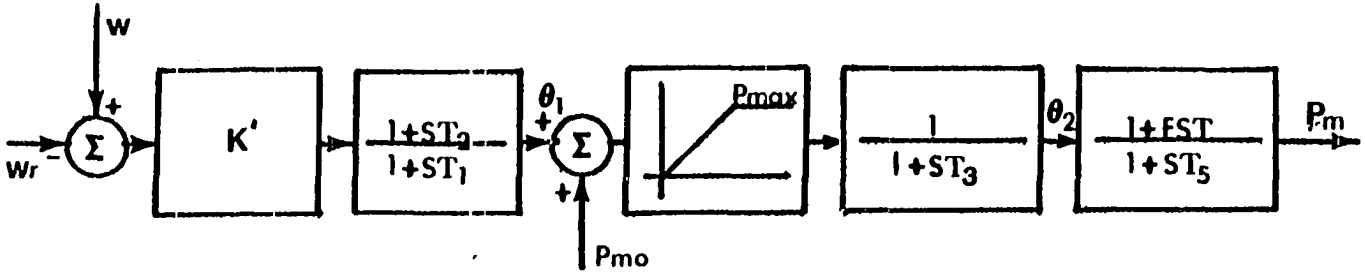

Fig. 10.4 The governor-turbine system